ADDIS ABABA INSTITUTE OF TECHNOLOGY (AAiT)

SCHOOL OF CIVIL AND ENVIROMENTAL ENGINEERING

LIFE TIME MANAGEMENT OF RAILS

BASED ON

STRUCTURAL RELIABILITY APPROACH

By: Getnet Mulatu

A thesis submitted to the school of Graduate Studies of Addis Ababa University in Partial fulfillment of the degree of Master of Science in Civil Engineering.

Advisor:

Mequanent Mulugeta (MSc.)

May, 2015

ADDIS ABABA INSTITUTE OF TECHNOLOGY (AAiT)

SCHOOL OF CIVIL AND ENVIROMENTAL ENGINEERING

LIFE TIME MANAGEMENT OF RAILS BASED ON STRUCTURAL RELIABILITY APPROACH

By

Getnet Mulatu

Approved by Board of Examiners:

Mequanent Mulugeta (MSc.)	……	……
Thesis Advisor	Signature	Date
……..……	……	…….
Internal Examiner	Signature	Date
……..……	…….	…….
External Examiner	Signature	Date
…… ……..……	…….	…….
Chairman	Signature	Date

ACKNOWLEDGEMENT

First of all, I would like to express deepest gratitude to my advisor Mr. Mequanent Mulugeta (MSc.), for his grateful motivation, guidance, support, continuous advice and constructive suggestions toward the completion of this thesis. I also thank Abrham Gebre (Dr.Ing) for giving of motivations to work on this research area as well as suggesting valuable comments to keep the research on track.

I also like to acknowledge staff of Ethiopian Railways Corporation for providing the necessary information for the input of this thesis work.

I would like to thank my family, especially W/rit Tsion Asmamaw and W/ro Wudie Zeberga, who stands on my side during the work of the paper.

Finally, I gratefully show appreciation to Ethiopian Railways Corporation, which has supported me to study at Addis Ababa Institute of technology (AAiT).

ABSTRACT

Preventing broken-rail caused derailments is a high priority for the rail industry. The current practice is to periodically inspect rails using non-destructive technologies. Determining the effective inspection frequency is a critical decision in railway infrastructure management.

This thesis discusses some applications of the modelling work to rail defect management. In particular, main applications are the determination of remedial actions and effective inspection interval on the basis of the quantitative approach as well as the adaptation of rail inspection and maintenance procedure.

The frequency of rail inspection tends to vary from one railroad to another, yet it is usually based on either time or traffic tonnage. Railroad companies have evolved their rail inspection schedules empirically based on long field experience. Rail defect management refers to the development and implementation of strategies to control the risk of rail failure. The primary method to control the risk is a rail inspection through nondestructive evaluation and is a replacement of rails based on the remedial action plan.

To demonstrate the feasibility of the above applications first, a Linear Elastic Fracture Mechanics (LEFM) analysis which can predict a crack size in a rail head, web and base is performed. Second, First Order Reliability Method (FORM) of analysis evaluates the reliability of a rail, considering some uncertainties of parameters. Third, an Event Tree (ET) analysis represents systematically all possible events and actions regarding rail defect management. Finally, a Life- cycle cost (LCC) estimation formulates the total expected cost during the service life are conducted.

Based on the analysis results, the mechanism for remedial action is developed based on critical crack size at rail head, web and base as well as rail reliability value to help infrastructure manager's decision. Then, effective number of rail inspection frequency is determined as three times a year to prevent the occurrence of rail failure by taking the required action at the right time, and extend the rail life expectancy, reduce the rail maintenance work and its cost. Finally, appropriate rail inspection and maintenance strategy model (flowchart) is adopted for Ethiopian railway industry.

***Key Words**: Rail defects, Rail inspection, Rail deterioration, reliability Analysis, fracture Mechanics, reliability index, event tree Analysis, life cycle cost.*

Notation	Definition
r	*Discount rate*
K_I	*Mode I Stress intensity factor*
$f_i(\theta)$	*Function that represents, stress dependence on θ.*
A	*Crack length in the major semi axis of ellipse*
B	*Crack length in the minor axis of ellipse*
N	*Number of load (Stress) Cycles.*
C &M	*Material specific input parameters*
ΔK	*Range of stress intensity factor*
a_i	*Initial crack size*
a_{ch}	*Critical crack size at rail head*
a_{cw}	*Critical crack size at rail web*
a_{cb}	*Critical crack size at rail base*
E_b	*Modulus of Elasticity of ballast*
K_s	*Coefficient of subgrade reaction*
K_o	*Sub grade reaction of plate test*
W_e	*Width of effective subgrade area*
K_p	*Spring coefficient of resilient pad*
K	*Spring constant of sleeper*
S	*Sleeper spacing*
P_o	*Maximum wheel-rail contact pressure*
W	*Design wheel load*
E_w	*Modulus of Elasticity of Wheel*
E_r	*Modulus of Elasticity of rail*
υ_w	*Poisson's ratios of wheel*
υ_r	*Poisson's ratios of rail*
R_1	*Principal rolling radii of wheel*

R_2	*Principal rolling radii of rail*
R_1'	*Transverse radius of curvature of wheel*
R_2'	*Transverse radius of curvature of rail*
φ	*Yaw rotation (angle between normal planes)*
W_s	*Static wheel load*
ϕ	*Dimensionless impact factor (always>1)*
P	*Hertz wheel- rail contact pressure*
Y	*Geometric correction factor*
$\Delta\sigma$	*Tensile stress range*
K_{IC}	*Fracture toughness*
D	*Distance from the origin to most probable point*
T	*Transpose function*
P_f	*Probability of failure*
β	*Hasofer-lind reliability index*
$\phi(.)$	*Cumulative function of standard normal variate*
S^m	*mean stress-range effect*
$f_s(s)$	*Probabilistic density function of stress range parameter*
N_o	*Crack initiation period*
μ	*Mean*
a_r	*Critical repair crack size*
a_d	*Critical detected crack size*
P_{det}	*Probability of detecting defects*
P_{rep}	*Probability of repairing defects*
$P_{rep/det}$	*Probability of repairing defects given a detection of defects*
X_i	*Inspection intervals*
R	*Rail segment per track- mile*
T	*Annual traffic density*

C_{insp}	*Rail defect inspection cost*
V	*Average hi-rail vehicle speed*
C_{hr}	*Inspection cost per hour*
$W_{replace}$	*Weight of replacement rail*
$L_{replace}$	*Length of replacement rail*
P_{new}	*Price of new rail*
P_{old}	*Price of scrap rail*
$C_{s,\ drepair}$	*Cost of expenses for labor, material and equipment*
T	*Tax rate*
C_{SDT}	*Train delay cost due to fixing a broken rail*
C_{DA}	*Train delay cost for multiple trains*
$S\ (K)$	*Number of broken rails per track-mile*
C_{derail}	*Train derailment related cost*
C_{bro}	*Broken rail repair cost*

LIST OF TABLES

LIST OF FIGURES

TABLE OF CONTENTS

CHAPTER 1

1.1 INTRODUCTION

1.1.1 BACKGROUND OF THE RESEARCH

Certain components in engineering systems are often subjected to cyclic loads leading to fatigue and progressive crack growth. It is essential to predict the performance of such components to facilitate risk assessment and management, inspection and maintenance scheduling, and operational decision-making. In 1978, the National Bureau of Standards and Battelle Laboratories completed an exhaustive study that estimated the total cost associated with material fracture and failure in the United States to be over $88 billion dollars per year (corresponding to almost 4% of the national GDP at the time) (R.P. Reed, J.H. Smith, and B.W. Christ,1983). The study concluded that substantial material, transportation, and capital investment costs could be saved if technology transfer, combined with research and development, succeeded in reducing the factors of uncertainty related to structural reliability. Emphasis on fracture mechanics, material properties, and improved inspection schedules/techniques were identified as potential methods of improving structural reliability while reducing material usage and replacement of critical components. Among the major industry sectors where fatigue and fracture of structural components are of critical concern is that of the railway industry.

Railway infrastructures are assets which represent a high investment. They are designed to work in a very demanding safety conditions and must display a very low occurrence of failures. Rails are the most significant and basic components of railway systems. However different factors which influence the rail degradation process gradually reduce the performance, reliability and safety of rails. Wear, fatigue, corrosion and crack generation are major contributors to rail failure. Almost 80% to 95% of all structural failures occur through a fatigue mechanism. So, fatigue is the main cause of rail degradation (failure). The failure depends on the characteristics of infrastructure, train traffic and maintenance plans used. There may exist several states of failure under which the efficiency of the system may decrease.

A failure can sometimes be catastrophic in nature. Relevant examples from the railway industry have been taken to illustrate the consequences of a failure. The German ICE train derailment on 3rd June 1998 took more than one hundred lives. The accident was caused by a fatigue fracture which started on the underside of the rim of the wheel. The derailment caused one of the carriages to swing out of line and to strike a support of a bridge, prompting its collapse (smith, 2003).

Even if failures are not catastrophic, they might cause a number of replacement and reworks leads to material wastage and additional costs, the benefit drops and the company become less competitive. There is an uncertainty involved in the occurrence of failures in a rail, which depends on its technical conditions, age and failure rate.

Therefore, reliability is an aspect of engineering uncertainty which describes the rails conditions interms of probability. Reliability analysis helps to identify the technical condition and predict the useful life of rails. The main role of reliability theory is improving system or component performance (saurahg Kumar, 2008; Takashi Kashima, 2004).

This thesis provide mechanism for effective risk assessment and management, inspection and maintenance scheduling, and future decision-making planning to reduce rail failures by the determination of mechanisms of remedial actions for rails and an effective inspection frequency which can be used effectively by inspection and maintenance personnel in the railway industry and also help in decision making when planning future inspection and maintenance intervals for different components based on structural reliability theory. To implement the approach into practice, the combination of different types of rail defects (multiple failure mode) at rail head, web and base are considered when evaluating the reliability index.

Therefore a reliability approach is required for guarantying the defined level of performance of the rails during its operation and maintenance phase.

1.1.2 STATEMENT OF THE PROBLEM

In spite of the fact that railway companies around the world have attempted to reduce the number of broken rails by making the use of various management techniques, the number have not yet reached zero and a substantial proportion of railway budget is spent on rail track inspection and maintenance.

This problem will exists in Ethiopian railway industry after operation starts due to:

- Rails deteriorate over the time due to vast movement of the people, huge import and export of goods with frequent cycle and needs maintenance to correct damage, deterioration, and cracks due to different factors which influence the rail degradation process.
- Ethiopian railway transport has no life time rail management technique developed for determination of the mechanism for remedial action of rails as well as effective rail inspection interval for the reduction of costly failure in the future as well as well-defined efficient and effective rail maintenance procedure (model).

In order to prevent rails from breaking during the service life, Ethiopian Railway Corporation will have two policy options in rail defect management. One is to improve the material, making it more

durable, the other is to increase the frequency of rail inspection. Yet it is a difficult task to develop a new material that will not develop cracks in its service life. As for the frequency of rail inspection, it is also expensive for the company to significantly increase the frequency of rail inspection. Neither option is a practical solution to the problem of rail failure.

So in this study an attempt will be made to develop life time rail management technique for rail infrastructure in Ethiopia based on structural reliability theory such as determination of remedial action plan, effective inspection interval and adaptation of rail maintenance model (procedure). It will enhance the reliability of railroad systems and reduces the possibility of costly failures in the future, reduce maintenance work and its cost, and will allow the Ethiopian Railway Corporation to save inspection and maintenance costs without increasing the risk of passengers and freight.

Even if the new railway infrastructure is under construction, recent information about future condition of rails becomes an important indicator for the operation and maintenance decision making process.

1.1.3 OBJECTIVE/AIM OF THE STUDY

1.1.3.1 GENERAL OBJECTIVE

The main objective of this study is to develop a method for effective life time rail management based on structural reliability theory. This will help to prevent the occurrence of rail failure by taking the required action at the right time, and extend the rail life expectancy, reduce the rail maintenance work and its cost.

1.1.3.2 SPECIFIC OBJECTIVE

The following are the sub objectives of the study:

- Develop *mechanism for assessment and remedial action* for different rail defects which will help in decision making when planning future inspection and maintenance intervals and determine fatigue life of rail.
- Determine an *effective and economical rail inspection interva*l to minimize costly failures in the future and reduce risk of passengers and freight.
- Adapt the *efficient and effective rail inspection and maintenance procedure (flowchart).*

1.1.4 RESEARCH METHODOLOGY

The research methodology for this study involved the following major tasks: literature review is performed to document the validation of the reliability based approach for effective rail inspection and the way to formulate reliability index. Following literature review, a four step analysis is used

for the determination of mechanism of remedial action of rails and effective rail inspection interval. The methods applied in the thesis are depicted in the following steps and flow chart fig 1.1.

- **Step 1**: **Linear elastic fracture mechanics** predicts the fatigue life of rail. A rail is modeled by beam on elastic foundation principle to determine the rail stress to predict the critical crack size. For information about rail design parameter, rails in National railway network of Ethiopia are employed.
- **Step 2: First order reliability method** create the reliability profile of rails as a reliability index: β. The reliability index of rails will determine the criteria for the mechanism of remedial action of rails.
- **Step 3: Event tree analysis** resolves all possible consequence of detecting defects and remedial action with probability.
- **Step 4: Cost Estimation** determines the effective number of inspection so as to minimize the expected total cost as well as to better predict and manage the cost of maintenance and renewal activities.
- **Finally:** Adapt the effective rail inspection maintenance flow chart procedure (model).

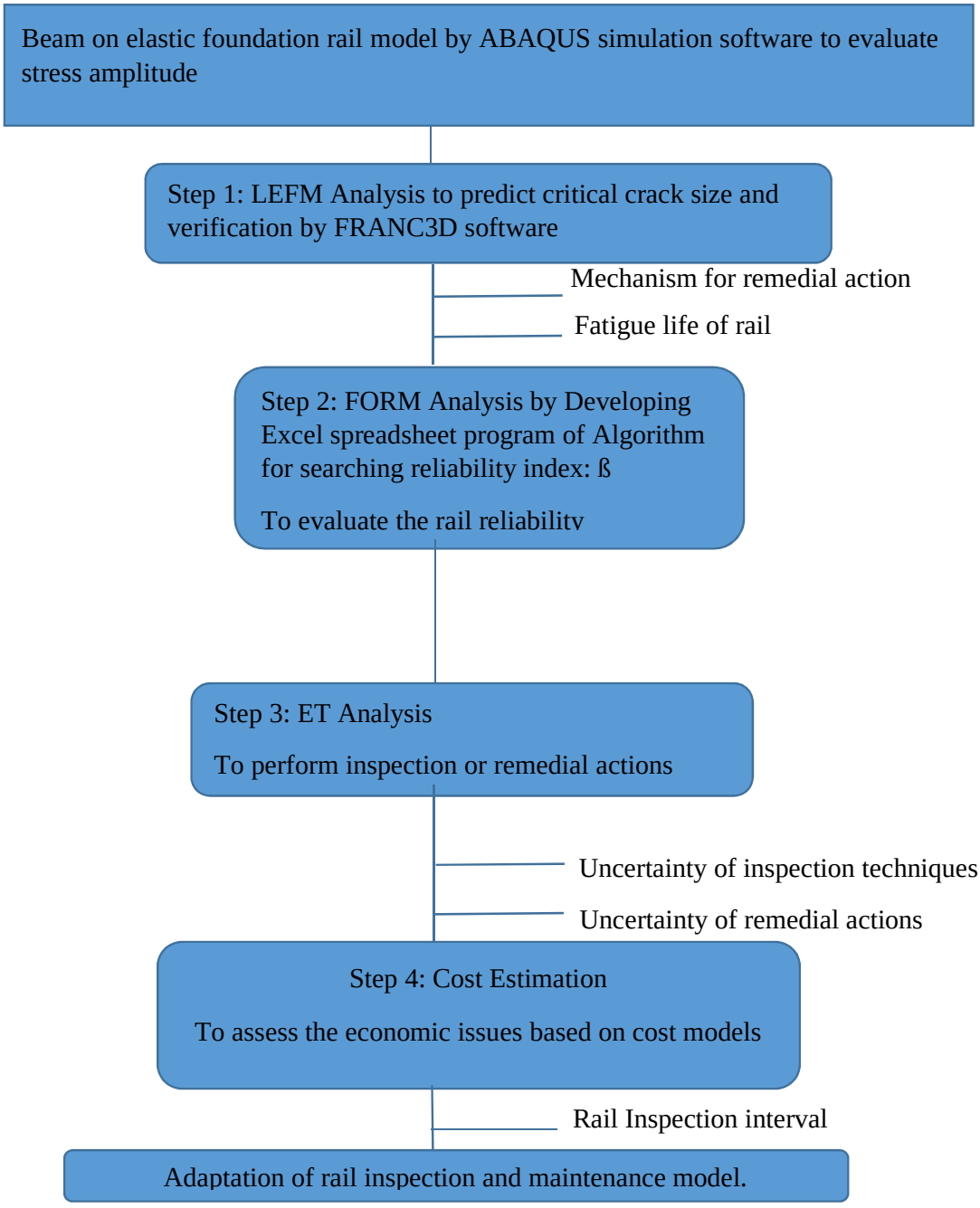

Figure 1.1: Research Methodology

CHAPTER 2

2.1 LITERATURE REVIEW

2.1.1 INTRODUCTION

Inspection and maintenance today is viewed as a value adding concept; because it contributes efficiency to the company's strategic objective in profitability and competitiveness (Al-Najjar and Kans, 2006).Achieving more efficient maintenance depends on the capability of the implemented inspection and maintenance policy to provide and employ effectively the relevant information about the factors affecting the life of rails being considered.

Inspection and maintenance of rails not only increases the life length but may also reduce the failures and degradation rates. Inspection (in the operation phase) is a maintenance activity carried out at predetermined time intervals in order to reduce the probability of failure (or the performance degradation) of the rail (Bahramin-Ghasrchami et .al, 1998). The inspection cost increases when the inspection interval is shortened (or the inspection frequency is increased), as inspection is one of the cost elements (Jardie and Tsang, 2006).For example, the rail inspection cost alone (assuming annual manual verification of detected defects) are estimated about £70 million per year for a 0.5 million Km track system in the European Union (Cannon et. al, 2003). On the other hand, the risk or loss caused by failure will increase when the inspection interval is lengthened. Therefore, appropriate scheduling of inspection activities is important for cost and risk reduction by modeling the inspection and maintenance intervals.

A wide range of maintenance models have been developed and reviewed from time to time (Sherif and smith, 1981).Complexity and increasing demands on component reliability and cost effective maintenance of rails have led to the development of more sophisticated models.However,the application of developed maintenance models using reliability or statistical analysis techniques are not common. This is due to the model mainly focusing on mathematical analysis and techniques (Dekker, 1996).

There is a need for describing an effective rail maintenance procedure, so that the risk of rail breakage and the inspection cost can be reduced Sauragh Kumar, (2008).

2.1.2 FRACTURE MECHANICS

The term "fracture mechanics" refers to a vital specialization within solid mechanics in which the presence of a crack is assumed, and quantitative relations between the crack length, the material's inherent resistance to crack growth, and the stress at which the crack propagates are defined (O. Vardar., 1988). It deals with the behavior of cracked bodies subjected to stresses and strains. These

can arise from primary applied loads or secondary self-equilibrating stress fields (e.g. residual stresses). The power of fracture mechanics really lies in the fact that local crack tip phenomena can, to a first order, be characterized by relatively easily measured global parameters, e.g. crack length and nominal global stresses (calculated in the absence of the crack), together with geometry correction factors. The crack propagation behavior is an important parameter which plays a vital role in the fatigue strength analysis of the structures (J. J. Coner Julie A. Bannantine and J. Hand Rock., 1990).

As long as the load is small enough, the structure will only deform elastically. A crack starts to propagate when the crack driving force is larger than the material resistance. If however, the structure is sensitive to cracking due to e.g. inadequate design, defects from manufacturing, handling or bad quality, materials fracture will occur. There are a number of parameters that affect the crack propagation mechanism i.e. material properties, fatigue, loading rate, environment etc.

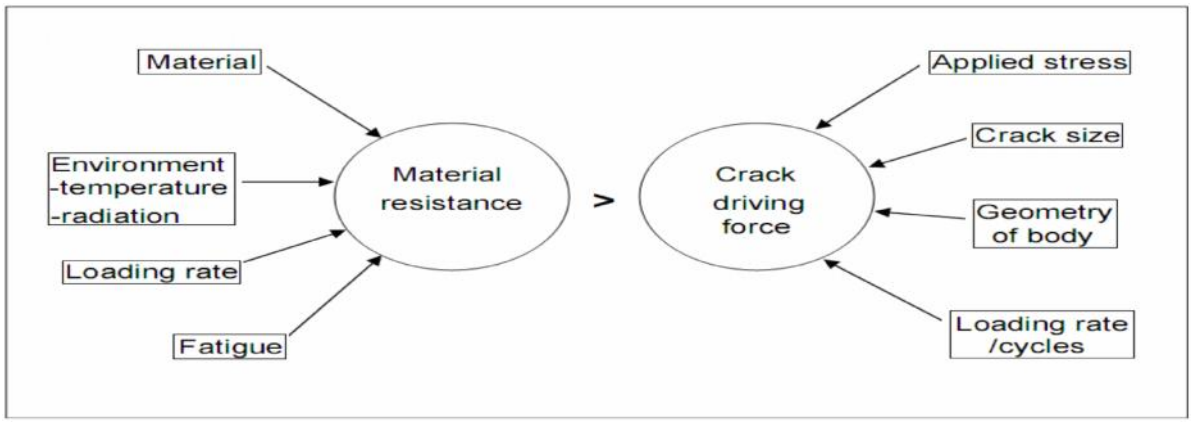

Figure 2.1: Factors influencing the crack propagation.

In short, fracture mechanics is used to answer some main questions such as: will the crack grow? Will it grow fast and unstable or slow and stable? If it grows stable at what rate does it grow? To what size can the crack grow and how many cycles or how long does it take to become an unstable crack? When fracture takes place in any structure it may lose the function it was initially designed for. Thus, the knowledge about what happens with a loaded structure with crack initiations is important in order to avoid failure.

2.1.2.1 LINEAR ELASTIC FRACTURE MECHANICS (LEFM)

For any homogeneous and isotropic material, stress surrounding the crack tip is often analyzed assuming linear elastic material behavior. The method of linear elastic fracture mechanics assumes the plastic region near crack tip is much smaller than the dimensions of the crack and the structural

member. Assuming the geometry has very small displacement and the material is elastic, homogeneous and isotropic.

Linear Elastic Fracture Mechanics (LEFM) principles are used to relate the stress magnitude and distribution near the crack tip to the remote stresses applied to the cracked component, crack size, crack shape and the material properties of the cracked component (Atkinson, B.K., 1987). The general form of the LEFM equation is given as:

$$\sigma_{ij} = \frac{K_I}{\sqrt{2\pi r}} f_{ij}(\theta) + \cdots \quad (2.1)$$

Where:

r = distance from the crack tip

KI= Mode I Stress intensity factor

f_{ij} (Θ) = function that represents the stress dependence on θ.

LEFM is based on the application of the theory of elasticity to bodies containing cracks or defects. The assumptions used in elasticity are also inherent in the theory of LEFM: small displacements and general linearity between stresses and strains.

The general form of the LEFM equations is given in equation (2.1). As seen, a singularity exists such as *r*, the distance from the crack tip, tends toward zero, the stresses go to infinity. As the yield stress is exceeded, material deforms plastically and a plastic zone is formed near the crack tip. The basis of LEFM remains valid if this region of plasticity remains small in relation to the overall dimensions of the crack and cracked body.

2.1.3 STRUCTURAL RELIABILITY THEORY

For many years it has been assumed in design of structural systems that all loads and strengths are deterministic. The strength of an element was determined in such a way that it exceeded the load with a certain margin. The ratio between the strength and the load was denoted the safety factor. This number was considered as a measure of the reliability of the structure. In codes of practice for structural systems values for loads, strengths and safety factors are prescribed.

These values are traditionally determined on the basis of experience and engineering judgment.

Characteristic values of the uncertain loads and resistances are specified and partial safety factors are applied to the loads and strengths in order to ensure that the structure is safe enough. The partial safety factors are usually based on experience or to measures of the reliability obtained by probabilistic techniques. As described above structural analysis and design have traditionally been based on deterministic methods. However, uncertainties in the loads, strengths and in the modeling of the systems require that methods based on probabilistic techniques in a number of situations have

to be used. A structure is usually required to have a satisfactory performance in the expected lifetime, i.e. it is required that it does not collapse or becomes unsafe and that it fulfills certain functional requirements.

Reliability of structural systems can be defined as the probability that the structure under consideration has a proper performance throughout its lifetime. Reliability methods are used to estimate the probability of failure. The information of the models which the reliability analyses are based on is generally not complete. Therefore the estimated reliability should be considered as a nominal measure of the reliability and not as an absolute number.

The reliability estimated as a measure of the safety of a structure can be used in a decision. A lower level of the reliability can be used as a constraint in an optimal design problem. The lower level of the reliability can be obtained by analyzing similar structures designed after current design practice or it can be determined as the reliability level giving the largest utility (benefits – costs) when solving a decision problem where all possible costs and benefits in the expected lifetime of the structure are taken into account.

CHAPTER 3

3.1 LINEAR ELASTIC FRACTURE MECHANICS ANALYSIS OF RAILS

3.1.1 RAIL STRESSES AND LOADS

Fracture in rails is a relatively complicated problem. To study fracture, different conditions such as variable and complex loading, secondary stresses, seasonal changes in environmental conditions etc. must be taken into account. Rails are subjected to primary and secondary loading components. In primary loading, the wheel load is applied from rolling contact to the rail as bending. Stresses arise from the axle static load and the dynamic motions of vehicles (pitch, bounce and rocking) cause fluctuations in the magnitudes of vertical wheel loads on the rail as trains travel over the track. The rail weight itself may also contribute bending stresses. Defects in the running surface of the rails such as joints, dips and twists as well as irregularities in the wheel such as flats and out of roundness may play a role too. Axial stresses arise from structural irregularities of the track and from the acceleration and deceleration of the train during train start and stop. The loading due to rolling contact plays a major role in the early crack extension stage. There is additional loading in lateral direction especially in curved truck sections and at switches and crossovers. These forces are also dynamically magnified with increasing speed. The main load case for rails in switches is lateral bending. Secondary loads including thermal and residual stresses are superimposed by primary loads. Axial thermal stresses, which are produced from intensive temperature fluctuations, are tensile stresses at lower temperatures; however, these stresses are compressive at higher temperatures. At temperatures about 0^0c, high tensile thermal stresses are combined with relatively low toughness values of the rail materials. So, most rail failures occur at such temperatures, Statistical analysis of rail failures have shown in different literatures that temperature has a strong influence on the failure probability. Residual stresses (tensile or compressive) in rails arise from the manufacturing process (heat treatment and roller straightening), welding at rail joints or wheel-rail contact.

The fracture of a rail as a result of the development of fatigue cracking is considered as a serious event in the rail industry as it is likely to result in vehicle derailment with a high probability of loss of life. Cracks in rails have been appearing on the head of the rail as a result of mechanical damage due to wheel /rail contact stresses, or the foot of the rail emanating from corrosion pits or bending stress and at the web of the rail. More recently, since the method of joining rails by fishplates was abandoned in favor of continuous welded rail, another source of cracking was introduced arising from various weld defects (e.g. porosity, lack of fusion, shrinkage stresses etc.). Infrastructure managers (IM) are devoting a large amount of effort to ensure that the integrity of the rail track network is

preserved by conducting regular inspections involving up to date nondestructive testing (NDT) techniques. Nevertheless, the development of cracks in rails is unavoidable. The rail damage prediction tools currently employed by the industry are based on empirical relations based on the cumulative damage sustained by the axle weight and volume of traffic passing over a rail (J. Evans, 2003). These models do not take into account the development or presence of flaws. It can be stated that decisions on replacement of a rail are not made on the basis of a fracture mechanics based flaw severity assessment (a damage tolerance approach).

This work has undertaken the study of fatigue cracks in rails using Finite element method (FEM) modeling and analytical solutions to provide a tool to rail inspectors for the quick assessment of the severity of surface breaking and embedded cracks in rails. The work does investigate crack initiation and propagation phenomena on the heads of rails, and also on cracks initiating and propagating from bending loads in the foot of the rail as a result of passing trains as well as at the web of the rail.

There are generally three modes of loading, which involve different crack surface displacements as shown below in figure 3.1. The three models are:

Mode I: Opening or tensile mode (the crack faces are pulled apart)

Mode II: Sliding or in-plane shear (the crack surfaces slide over each other)

Mode III: Tearing or anti-plane shear (the crack surfaces move parallel to the leading edge of the crack and relative to each other).

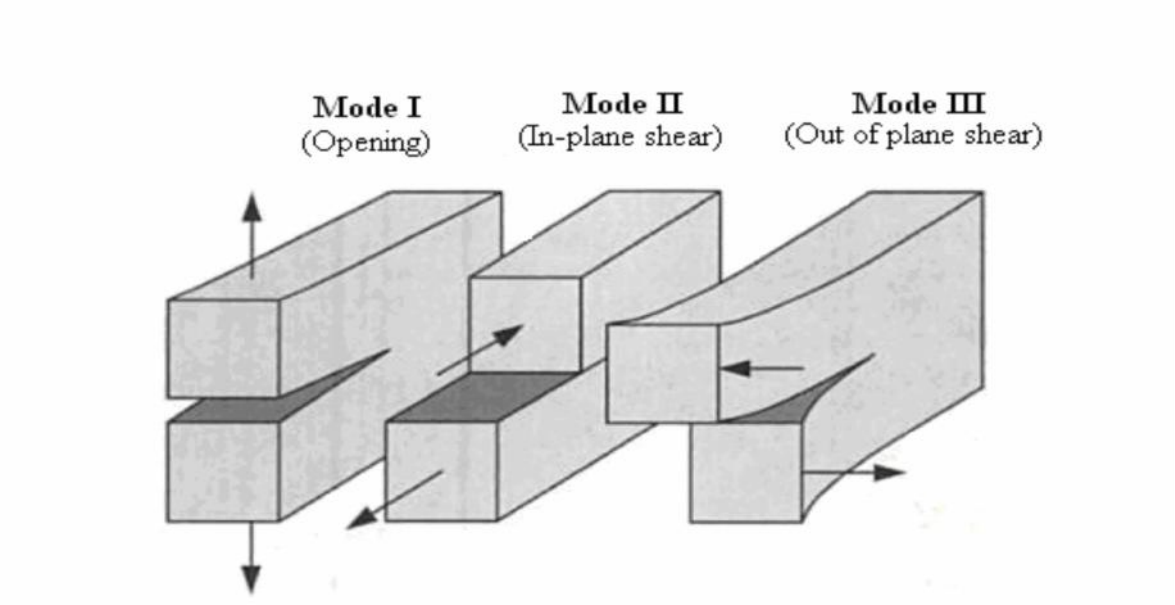

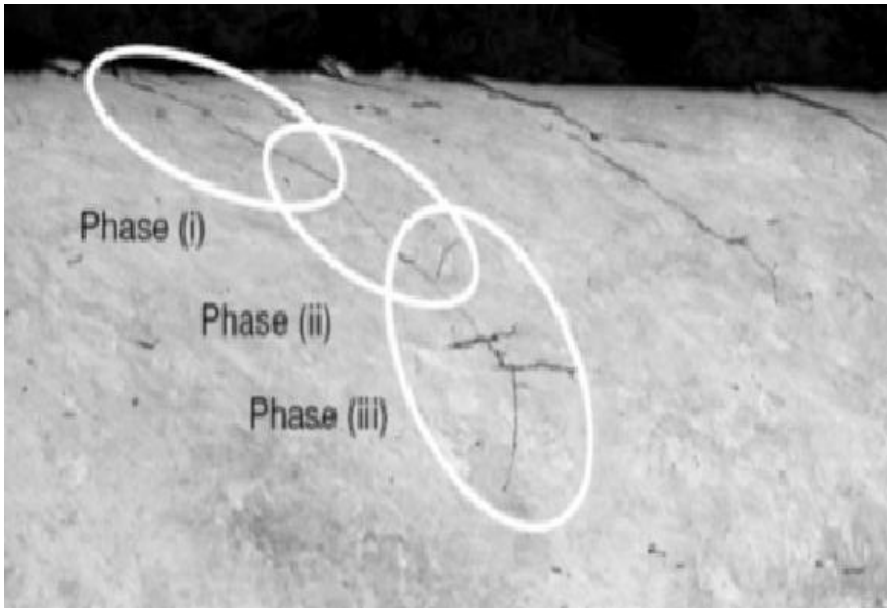

Figure 3.1: The three crack propagation modes (phases) (Anderson T.M, 1999)

N.B Mode I is the predominant loading mode in most engineering applications and also in this thesis.

3.1.2 CRACK INITIATION AND PROPAGATION FOR RAIL

Cracks may initiate at or below the surface due to high traction forces that are resulted from fast motion of vehicles over the track. Sub-surface cracks propagate towards the rail surface and behave like original surface cracks after penetration (K. L. Johnson, 1989). Crack initiation and propagation may be explained in following statement. A dark spot develops at the surface causing the crack to occur at the surface or subsurface of the rail. Subsequently, the crack grows in an inclined angle below the surface and then it branches into a horizontal and a transverse crack at a certain point. The transverse crack extends down into the rail and finally causes its fracture (M. Ishida, N. Abe, 1996). Lubricants such as water play an important role in crack extension. Indeed, lubrication slows down crack nucleation but accelerates the subsequent crack growth. Among many distinct forms of crack, the two progressive transverse defects of detail fracture and tache oval defect are known to be more important from fracture mechanics viewpoint (K. O. Edel, Theoret. Appl, 1988). The first type usually originates from a longitudinal seam or streak near the running surface on the gauge side of the railhead, but the second type originates from manufacturing defects, such as hydrogen flakes.

In the present study the first type of the crack is focused.

Fig. 3.2 Shows the geometry of a transverse internal rail defect (such as a detail fracture), modeled as an elliptical flaw embedded in the railhead and at a rail base.

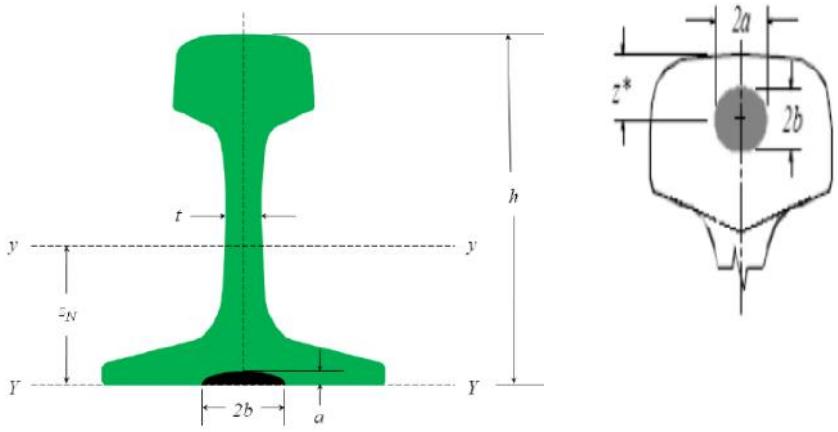

Figure 3.2. Semi-elliptical crack model

In principle, the prediction of crack growth using fracture mechanics requires the following steps:

1. Identify the relevant crack growth properties (crack growth rate as a function of the stress intensity factor, fatigue threshold, fracture toughness, etc.) for the rail.

2. Determine the initial flaw size, shape, and location.

3. Determine the stress intensity factor solution as a function of crack size, shape, geometry, and loading

4. Select a fatigue crack growth rate model and damage accumulation rule

5. Propagate fatigue crack from initial flaw size to final (critical) flaw size.

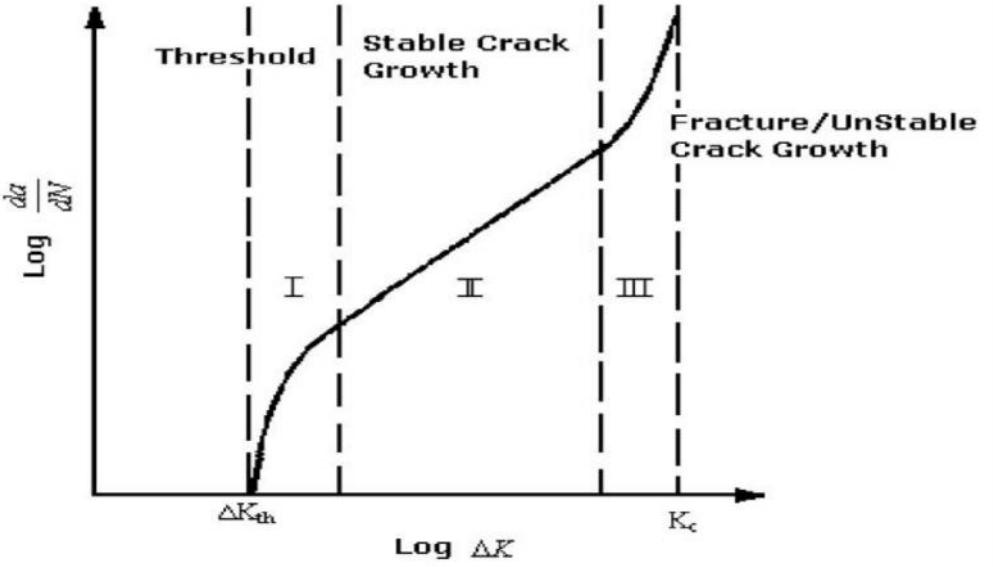

Figure 3.3 crack growth rate curve

3.1.3 CRACK GROWTH MODEL OF RAIL

In general, many fatigue life analysis have applied the Miner's damage accumulation law or some specific PDFs such as the weibull and exponential distributions, to predict the probabilistic life of a metallic material, since the models accordingly represent the characteristics of the material. However, railroad companies usually use a crack size as the inspection results. Therefore, it is hard to deal with reflecting the results of the inspections and repair strategy in their approaches because they do not provide information about crack size. A quantitative analysis for the rail reliability needs the knowledge of the crack size at arbitrary times, so a crack growth model based on linear elastic fracture mechanics is employed instead of the Miner's damage accumulation and a specific PDF model in this thesis.

3.1.3.1 SEMI-ELLIPTICAL CRACK GROWTH

Fatigue failure is initiated by an imperfection of materials or from tiny cracks inside the material. Cracks grow due to cyclic loads applied to the material. As for rail fatigue, rail defects are classified as:1)Transverse defects in the rail head;2)Longitudinal defects in the rail head;3)surface defects in the rail head;4)web defects;5)base defects;6)joint-hole defects. This study focus on the fatigue related to defects in the head, web and base area. It is believed that the head, web and base defects in rails start from surface imperfection, which is a fabrication crack in the steel Impacts of wheel and bending stress initiate growth of base separation around the tiny imperfection as well as wheel rail contact pressure initiate the growth in the rail head. Natural cracks occurring in practice are often initiated at corners and edges. They tend to grow inwards and assumed to be semi-elliptical shape. Therefore, the semi-elliptical crack model is employed to represent head and base defects of rails with the aspect ratio, a/b<1 in this thesis as shown in fig.3.2.

The crack growth model used in this study is based on the Paris and Erdogan's law (crack growth rate is an exponential function of the stress intensity factor).Paris' law (also known as the Paris-Erdogans law) relates the stress intensity factor range to sub-critical crack growth under a fatigue stress regime. As such, it is the most popular *fatigue crack growth model* used in materials science and fracture mechanics. The basic formula reads:

$$\frac{da}{dN} = C\Delta K^m \tag{3.1}$$

Where *a* is the crack length and *N* is the number of load (stress) cycles. Thus, the term on the left side, known as the *crack growth rate*, denotes the infinitesimal crack length growth per increasing

number of load (stress) cycles. On the right hand side, *C* and *m* are material constants, and ΔK is the range of the stress intensity factor.

The formula was introduced by P.C. Paris in 1961. Being a power law relationship between the crack growth rate during cyclic loading and the range of the stress intensity factor, the Paris law can be visualized as a linear graph on a log-log plot, where the x-axis is denoted by the range of the stress intensity factor and the y-axis is denoted by the crack growth rate. Paris' law can be used to quantify the residual life (in terms of load cycles) of a specimen given a particular crack size

The size of the semi-elliptical rail base crack can be expressed in terms of its area relative to the rail base area, which is equal to $3.1*e^{-5}mm^2$ for T50 rail. That is, growth is calculated in terms of crack size in percent rail base area (%BA). $A_{crack} = \frac{\pi ab}{2}$ is used to calculate the area of the semi-ellipse. The initial crack size, a_i is assumed to be 10%BA, which roughly corresponds to the smallest defect size that non-destructive testing equipment can detect. Cracks covering slightly more than half the rail base area begin to enter into the rail web (Figure Fig.3.2). Once the crack propagates into the web, its shape deviates from a semi-ellipse, and the assumption of self-similar crack growth no longer applies. Moreover, the results of the different researches suggest growth of a semi-elliptical base defect for rails range from 10 to 50% (DavidY. Jeong, 2012).In this thesis, 10%BA is employed as the elliptical crack size for the T50 rail. In this thesis, the dimension of elliptical crack is taken as 0.01mm for the major axis and 0.005mm for the minor axis respectively.

The application of Linear Elastic Fracture Mechanics to surface defects requires the knowledge of stress intensity factor. The stress intensity factor is generally a function of stress amplitude as described in the previous section. Hence, it is essential to evaluate the stress amplitude in the linear elastic fracture mechanics analysis. To determine the magnitude of stress at the rail head, web and base, finite element modeling and analysis of the railroad truck by using commercial software called ABAQUS is carried out as follows.

3.1.4 FINITE ELEMENT MODEL OF THE RAIL

The current practice in truck analysis is based on the consideration of the track as a beam on an elastic foundation developed by Winkler and Talbot.

To model the rail for national railway network of Ethiopia for the purpose of analyzing the rail stresses, the ABAQUS software was used. For the analysis implementation, the three dimensional rail of T-50 profile with 0.6m length was modeled. The cause for choosing such a length was that the two sleepers could be placed underneath the rail at the standard distances of 0.6m.

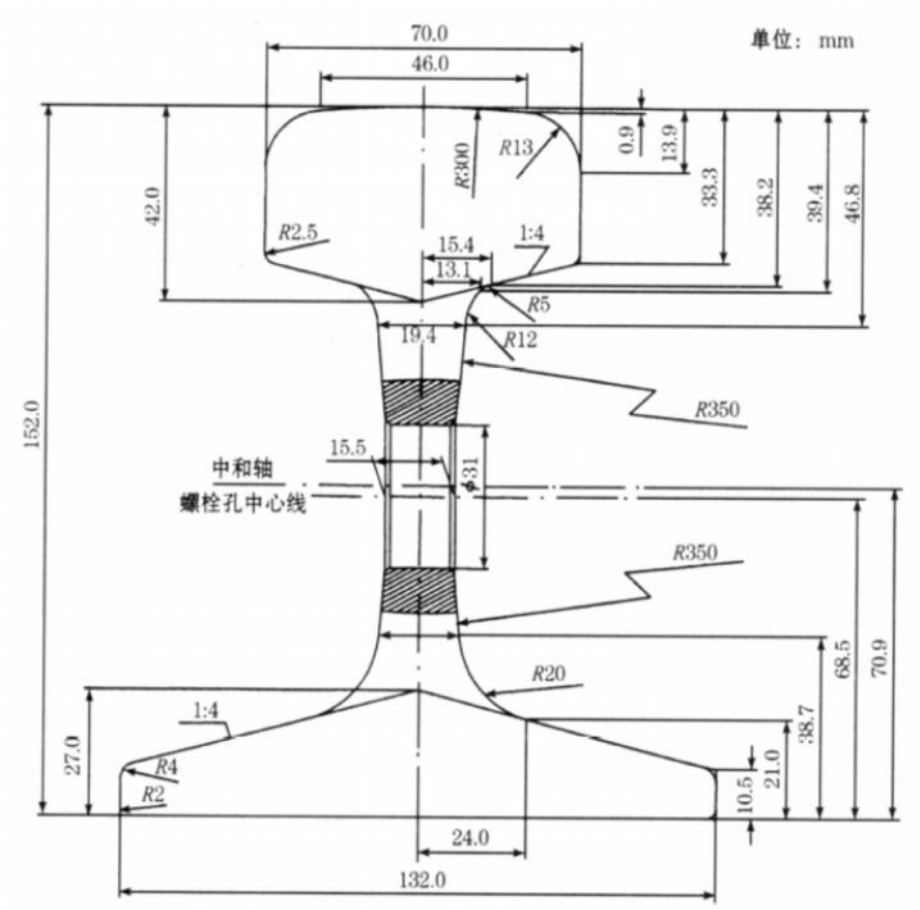

Figure 3.4 Rail profile, 50kg/m

The T50 rail model for the FEA is created with all the actual dimensions using ABAQUS as shown below:

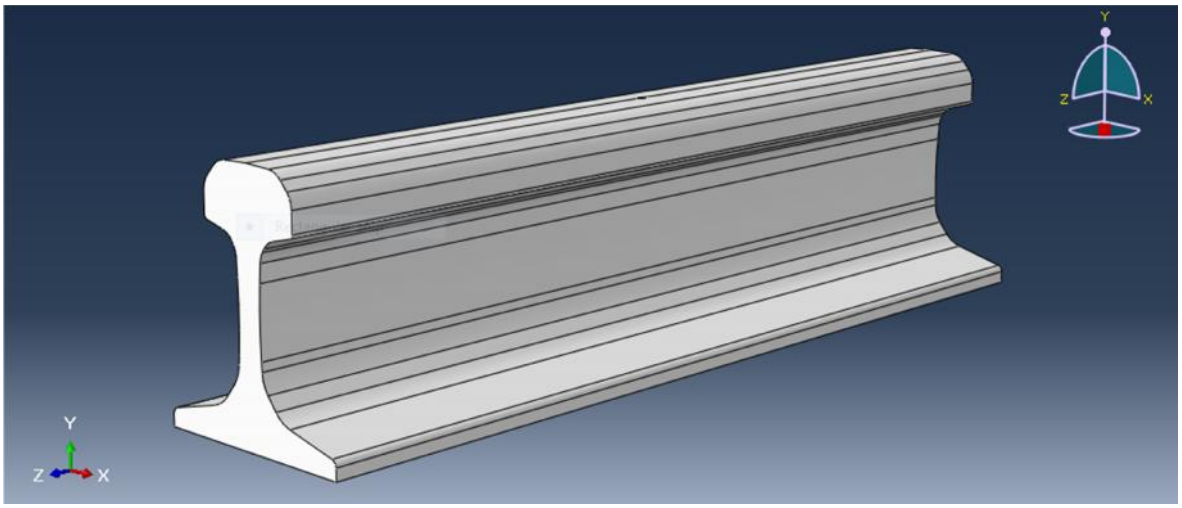

Figure 3.5 Geometric model of T50 rail created by ABAQUS

Table 3.1 Rail Material Properties

Rail Properties	Modulus of Elasticity, E (GPa)	Poisson's ration (υ)
Value	205	0.25

For the determination of stress in rail material due to the moving train, rail is modeled by Winkler's beam on elastic foundation theory, as a beam supported by soil foundation, where the soil is represented by a continuous distribution of springs along the length of the beam, as shown in Figure 3.6.

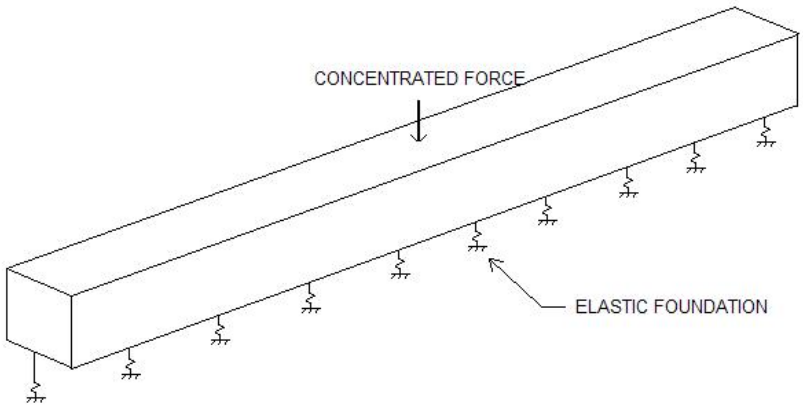

Figure 3.6: Winkler's Beam on Elastic Foundation Model

One of the most common methods for predicting the modulus of the truck support system is the pyramid method developed at bettlle Columbus laboratory (prause et al., 1974).This approach permits the use of truck parameters such as rail type, sleeper type, ballast depth, ballast type, sub grade type,

and sleeper spacing as inputs to the model as shown. The following steps were taken for the analysis of the truck stiffness based on current practice.

Ballast is considered in two layers. In each layer, the load spreads with the angle equal to the friction angle of the soil. Deformation of voids in the ballast caused by dynamic loads was taken into account for the calculation of the friction angle of the ballast materials. For this purpose, the suggestion of the schramm (1961) for consideration of 30 and 40 degree as friction angles for the top and bottom layers of ballast respectively was used here.

Using pyramid method, the ballast stiffness (Kb) was calculated by:

$$K_1 = \frac{C_1(L-B)E_b}{L_n\left(\frac{(L(C_1Z_1+B)}{B(C_1Z_1+L)}\right)} \tag{3.2}$$

and

$$K_2 = \frac{C_2(L-B)\mathrm{E}_b}{L_n\left(\frac{(C_1Z_2+L)(C_2Z_2+C_1Z_1+B)}{(C_1Z_1+B)(C_2Z_2+C_1Z_1+L)}\right.} \tag{3.3}$$

Therefore,

$$\frac{1}{K_b} = \frac{1}{K_1} + \frac{1}{K_2} \tag{3.4}$$

Where, C_1 is two times $\tan\theta_1$; C_2 is two times $\tan\theta_2$; $\theta_1$and θ_2 are angles of internal friction for the upper and lower section of the ballast, considered to be 30^0 and 40^0;

B is the sleeper width, considered to be 306.5mm;

L is the effective sleeper length under the rail seat, considered to be 900mm;

Z_1 is the depth of upper section of the ballast, considered to be 250mm;

Z_2 is the depth of lower section of ballast, considered to be 200mm;

E_b is the modulus of elasticity of ballast, considered to be 0.15KN/m2

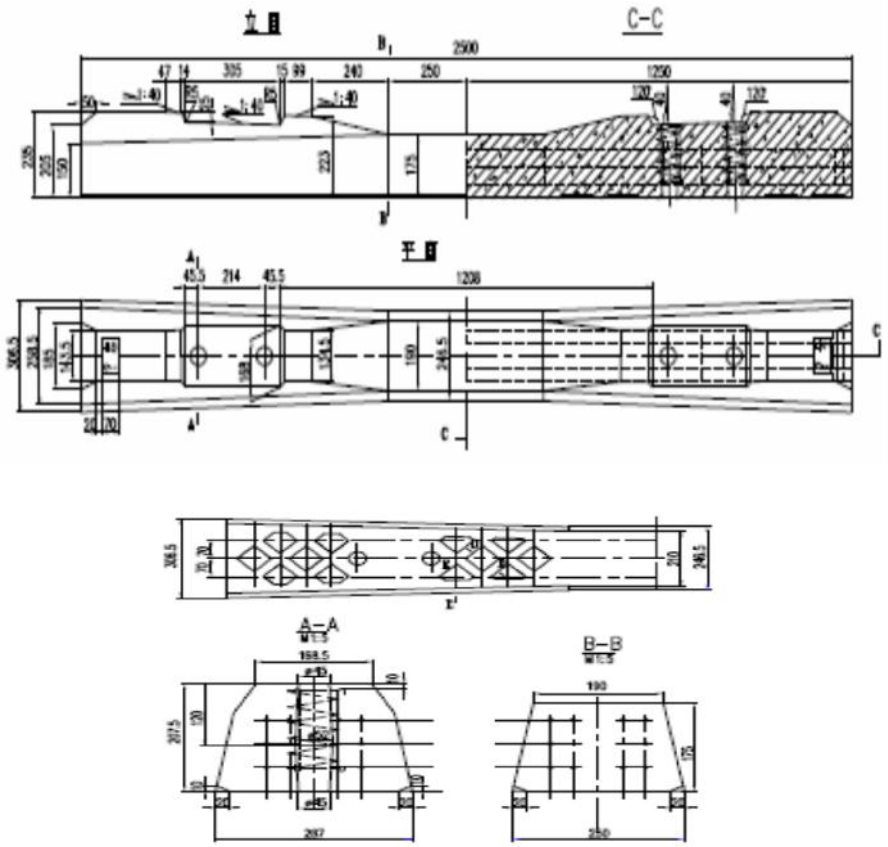

Figure 3.7 Sleeper section for national railway network of Ethiopia (Source: ERC)

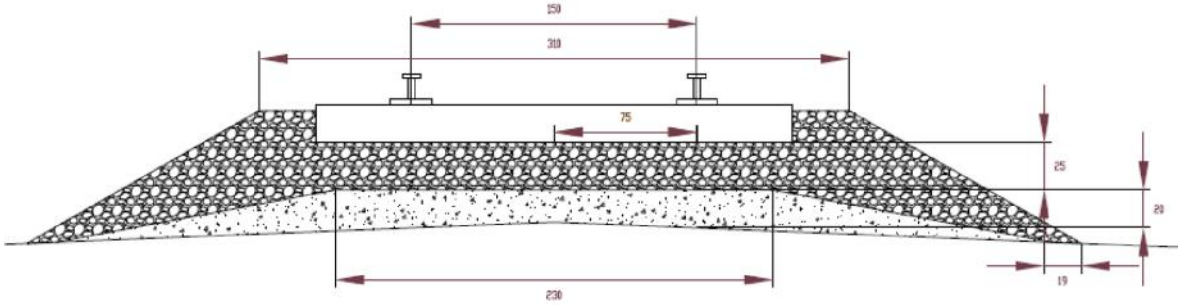

Figure 3.8Ballasted track section (Source: ERC)

$$K_1 = \frac{2*tan30\,(900-306.5)0.15}{900\left(\frac{900(2*tan30*250+306.5)}{306.5(2*tan30*250+900)}\right)} = 77.68\text{KN/m}$$

$$K_2 = \frac{2*tan40(900-306.5)0.15}{900\left(\frac{(2tan30*250+900)(2tan40*200+2tan30*250+306.5)}{(2tan30*250+306.5)(2tan40*200+2tan30*250+900)}\right)} = 136.115\text{KN/m}$$

$$\frac{1}{K_b} = \frac{1}{77.68} + \frac{1}{136.115} = 0.0202$$

Therefore, the stiffness of the ballast, K_b is obtained as 49.46KN/m.

Using the pyramid method, subgrade stiffness was calculated as follows:

$$K_{sub} = K_s(C_2Z_2 + C_1Z_1 + L)(C_2Z_2 + C_1Z_1 + B) \quad (3.5)$$

In which Ks is the coefficient of sub grade reaction for the subgrade based on experimental investigation (Terzaghi, 1955), Ks can be denoted from the measured coefficient of subgrade reaction of the plate test (K_o).

Using the concept of bulb of pressure;

$$K_s = K_o \frac{(W_e+1)^2}{4W_e^2} \quad (3.6)$$

Where

$$W_e = C_2Z_2 + C_1Z_1 + B \quad (3.7)$$

In which w_e is the width (mm) of the effective subgrade area and other parameters as defined earlier. K_o is the coefficient of subgrade reaction (KN/mm^3) for a square plate with a width of 300mm. Terzaghi (1955) recommended different values of K_o for different kinds of soils. Based on terzaghi's suggestion, K_o was considered to be 100KN/mm^3.

Therefore, W_e = 2tan40*200+2tan30*250+306.5 = 930.8mm

$$K_s = 100\frac{(930.8+1)^2}{4*930.8^2} = 25.054KN/mm3$$

$$K_{sub} = 25.054(2tan40*200 + 2tan30*250 + 900)(2tan40*200 + 2tan30*250 + 306.5) = 3.55*10^{10}\text{KN/m}$$

Considering ballast and sub grade in series, the ballast-sub grade stiffness was calculated by;

$$\frac{1}{K_{bs}} = \frac{1}{K_b} + \frac{1}{K_{sub}}\ ;\ K_{bs} = 46.45KN/m$$

To calculate the spring constant of sleeper (k), the spring constant of resilient pad (K_p, considered to be 120,000KN/m; according to simulation system model parameters commonly used in ordinary line with T50 rail in Chinese manual) and half of the spring constant of the effective ballast-sub grade foundation beneath the sleeper were considered in series. (Half of the ballast-sub grade spring constant was considered due to the continuity of the ballast and sub grade.) Therefore,

$$\frac{1}{K} = \frac{1}{K_p} + \frac{1}{\frac{K_{bs}}{2}} \tag{3.8}$$

K =23.22KN/m

Finally, overall foundation modulus was calculated as;

$$\frac{1}{k} = \frac{K}{s} \tag{3.9}$$

Where s is sleeper spacing which is 0.6m.

Therefore, overall foundation spring coefficient = 38.7KN/m per area = 8700N/m/area.

3.1.5 HERTZ CONTACT PATCH THEORY

According to Hertzian contact theory, the contact surface between two curved surfaces, such as a wheel and a rail, can be represented as an ellipse with a major semi-axis *a* and minor semi-axis *b*. The pressure exerted over this elliptical area is parabolic in two directions and is defined according to the following equation:

$$p = p_0\sqrt{1-\left(\frac{x}{a}\right)^2-\left(\frac{y}{b}\right)^2} \tag{3.10}$$

Wherep_0 is the maximum contact pressure at the initial central contact point, and the coordinates *x* and *y* refer to distances from the initial contact point along the major semi-axis and minor semi-axis, respectively. The value of p_0 is given by:

$$P_0 = \frac{3}{2}\left(\frac{W}{\pi ab}\right) \tag{3.11}$$

Where *W* is the applied normal force.

Depending on the size and orientation of the contact ellipse the positions of the contact point may be shifted in different directions based on the magnitude of x or y. However, based on the above general Hertz contact formula and assumptions, the stress due to wheel/rail contact decreases and becomes zero if it goes far away from the centerline of the rail head. Similarly, the wheel/rail contact stress is inversely proportional to the major and minor axis of the contact ellipse.

The magnitudes of *a* and *b* also depend on the applied normal force, as well as the profile and materials of the wheel and rail. They are expressed as:

$$a = m\left[\frac{3\pi W(K_1+K_2)}{4K_3}\right]^{\frac{1}{3}} \quad (3.12)$$

$$b = n\left[\frac{3\pi W(K1+K2)}{4K3}\right]^{\frac{1}{3}} \quad (3.13)$$

Where

$$K_1 = \frac{1-V_w{}^2}{\pi E_w} \quad (3.14)$$

$$K_2 = \frac{1-V_R{}^2}{\pi E_R} \quad (3.15)$$

$$K_3 = \frac{1}{2}\left(\frac{1}{R_1} + \frac{1}{R_1'} + \frac{1}{R_2} + \frac{1}{R_2'}\right) \quad (3.16)$$

Here E_w, E_r, υ_w, and υ_r are the modulus of elasticity and Poisson's ratios of wheel and rail, respectively. R_1 and R_2 are defined as the principal rolling radii of the wheel and rail, respectively. R_1' and R_2' are the transverse radii of curvature of the wheel and rail, respectively.

The coefficients *m* and *n* in Equations 3.12 and 3.13 are functions of θ.

The variable θ is defined as:

$$\theta = Cos^{-1}\left(\frac{K_4}{K_3}\right) \quad (3.17)$$

Where

$$K_4 = \frac{1}{2}\left[\left(\frac{1}{R_1} + \frac{1}{R_1'}\right)^2 + \left(\frac{1}{R_2} + \frac{1}{R_2'}\right)^2 + 2\left(\frac{1}{R_1} - \frac{1}{R_1'}\right)\left(\frac{1}{R_2} - \frac{1}{R_2'}\right)Cos2\varphi\right] \quad (3.18)$$

and φ is the angle between the normal planes that contain the curvatures $1/R_1$ and $1/R_2$ also called yaw rotation. For this thesis φ is taken as 0^0.

Table3.2Hertz coefficients

θ(deg)	**m**	**n**	θ(deg)	**m**	**n**	θ(deg)	**m**	**n**
0.5	61.4	0.1018	10	6.604	0.3112	60	1.486	0.717
1	36.89	0.1314	20	3.813	0.4125	65	1.378	0.759
1.5	27.48	0.1522	30	2.731	0.493	70	1.284	0.802
2	22.26	0.1691	35	2.397	0.530	75	1.202	0.846
3	16.5	0.1964	40	2.136	0.567	80	1.128	0.893
4	13.31	0.2188	45	1.926	0.604	85	1.061	0.944
6	9.79	0.2552	50	1.754	0.641	90	1.0	1.0
8	7.86	0.285	55	1.611	0.678			

Source: Railroad vehicle dynamics: A computational approach (2008)

To use with the computer simulations and calculations, an alternative approach to the numerical interpolation is to develop closed-from expressions for the coefficients m and n as functions of θ. The following equations were proposed by Shabana et al.

$$m = A_m tan\left(\theta - \frac{\pi}{2}\right) + \left(\frac{\pi B_m}{\theta^{C_m}}\right) + D_m \tag{3.19}$$

$$n = \frac{1}{(Atan\left(\theta - \frac{\pi}{2}\right)+1} + B_n\theta^{C_n} + D_n sin\theta_n \tag{3.20}$$

Where θ given in radians and the coefficients used for the Closed-Form Functions m and n is on the Table 3.2.

Table 3.3: Coefficients used for the Closed-Form Functions m and n (Shabana et al., 1996).

Coeff.	Value	Coeff.	Value
A_m	-1.086419052477	A_n	-0.773444080706
B_m	-0.106496432832	B_n	0.256695354565
C_m	1.350000000000	C_n	0.200000000000
D_m	1.057885958251	D_n	-0.280958376499

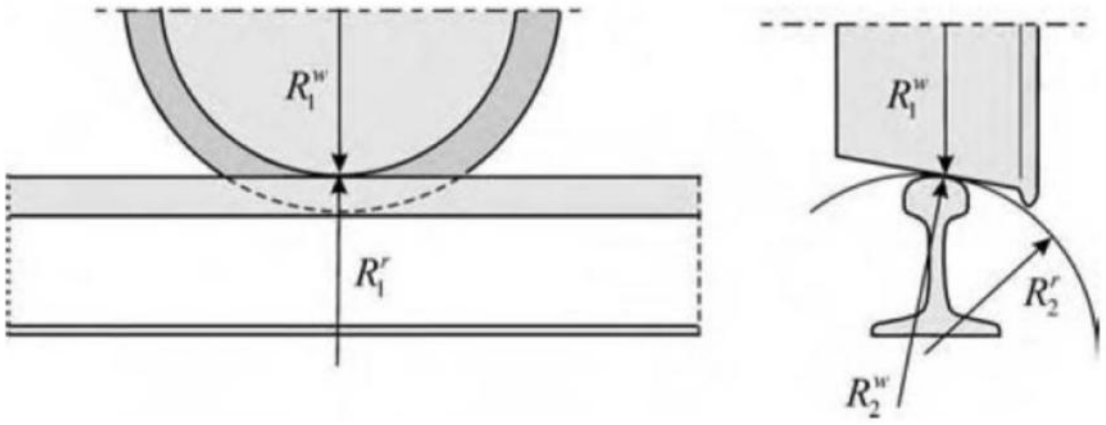

Figure 3.9wheel and rail radius of curvature

The forces imposed on the track structure could be classified as mechanical (both static and dynamic) and thermal. Esveld (2001) discussed the type of forces and their source as: (a) quasi-static loads induced by the self-weight of the vehicle and reaction forces in curves; (b) dynamic loads resulting from track irregularities; and (c) thermal loading due to temperature variations in continuous welded rail (CWR).

vertical forces are perpendicular to the plane of the rails and may be vertical wheel load or uplift force (reaction to wheel load) and are those forces result the mechanical stresses in the track [Selig and Waters, 1994 and Profillidis, 1995 cited by Ionescu, 2004]. The general method used in the determination of the design vertical wheel load according to Doyle (1980) is to empirically express it as a function of the static wheel load, i.e.

$$W = \emptyset W_s \tag{3.21}$$

Where: W=design wheel load (KN), W_s = static wheel load (KN), and $\emptyset$ = dimensionless impact factor (always >l). The nominal vehicle axle load is usually measured for the static condition, but in the design of railway track the actual stresses in the various components of the track structure and in the rolling stock must be determined from the dynamic vertical and lateral forces imposed by the design vehicle moving at designed speed [Doyle, 1980]. Dynamic impact factor is a corrective factor to compensate for dynamic as well as impact effects of wheel load resulted from wheel and rail surface irregularities [Sadeghi and Barati, 2010].

Table 3.4: Recommended relationship for dynamic coefficient factors [Doyle, 1980; Sadeghi and Barati, 2010]

Recommender	Formula
AREMA	$\emptyset = 1 + 5.21\frac{V}{D}$
DB	$\emptyset = 1 + \frac{V^2}{3*10^4}$ for V≤100 km/hr $\emptyset = 1 + \frac{4.5*V^2}{10^5} - \frac{1.5*V^3}{10^7}$, for V > 100km/hr
India	$\emptyset = 1 + \frac{V}{58.14k^{0.5}}$
South Africa	$\emptyset = 1 + 4.92\frac{V}{D}$ for narrow gage

Where: V= Vehicle speed (Km/hr); D= wheel diameter (mm); and k = track modulus (Mpa)

The axial load was chosen as 250KN.The load for each wheel was then taken to be 125KN. To determine the vertical wheel load on the rail, the dynamic impact factor expression recommended by AREMA was used and the vehicle speed for national railway network of Ethiopia was taken as 80Km/hr and the wheel diameter as 0.84m. So, the vertical wheel load is taken as W= 187,000N.

3.1.5.1 COMMON HERTZ ASSUMPTIONS:

Isotropic and homogenous material

No friction (Hertz wrote that the surfaces of both bodies had to be completely smooth).

Both bodies were considered as half-spaces with elliptical contact area

3.1.5.2 ANALYTICAL RESULTS

Table 3.5 Rail material selection

S.N	Radii of Curvature(mm)	Gauge (mm)	Axle load (N)	Chinese Standard (Kg)	Poison's Ratio	Young's Modulus (GPa)
1	$R_1^W = \infty$	1435	250,000	50	0.25	205
2	R_2^W=300					

Table 3.6 Wheel Material selection

S.N	Radii of Curvature(mm)	Gauge (mm)	Axle load (N)	Chinese Standard (Kg)	Poison's Ratio	Young's Modulus (GPa)
1	R_1^W=300	1435	250,000	64	0.25	205
2	R_2^W =∞					

On the center of rail head the contact pressure (stress) is equal to:

$$P_0 = \frac{3}{2}\left(\frac{W}{\pi ab}\right) \tag{3.22}$$

Where,

$$K_1 = \frac{1-(0.25)^2}{® * 205 * e9N/m2} = 1.456 * e-12m2/N$$

$$K2 = \frac{1-(0.25)^2}{® * 205e9N/m2} = 1.456 * e-12m2/N$$

K3= $\frac{1}{2}\left(\frac{1}{420mm}+\frac{1}{\infty}+\frac{1}{\infty}+\frac{1}{300mm}\right)$=0.00286/mm

For a straight segment the curvature of the rail is zero degree.

$$K_4 = \frac{1}{2}\left[\left(\frac{1}{420mm}+\frac{1}{\infty}\right)^2+\left(\frac{1}{300mm}+\frac{1}{\infty}\right)^2+2\left(\frac{1}{420mm}-\frac{1}{\infty}\right)\left(\frac{1}{\infty}-\frac{1}{300mm}\right)\cos 2(0)\right]$$

= 4.76*e-4/mm.

$$- = \cos^{-1}\left(\frac{K_4}{K_3}\right) = \cos^{-1}\left(\frac{4.76e-4}{0.00286}\right) = 80.4^0$$

By using linear interpolation method for hertz coefficients, the value of m and n for the chosen rail can be easily obtained as follows:

$\theta_1 = 80^0$, m1=1.128, n1=0.893; $\theta_2 = 85^0$, m_2=1.061,n_2=0.944

$$m = m1 + \frac{m2-m1}{\theta 2-\theta 1}(\theta-\theta 1) = 1.128 + \frac{1.061-1.128}{85-80}(80.4-80) = 1.123$$

$$n = n1 + \frac{n2-n1}{\theta 2-\theta 1}(\theta-\theta 1) = 0.893 + \frac{0.944-0.893}{85-80}(80.4-80) = 0.897$$

$$a=1.123\left[\frac{3® *187{,}000(2*1.456e-12m2/N)}{4*2.86/m}\right]^{1/3} = 0.0086\text{m}$$

$$b=0.897\left[\frac{3® *187{,}000(2*1.456e-12m2/N)}{4*2.86/m}\right]^{1/3} = 0.00687\text{m}$$

By using the values of a and b, the hertz stress contact pressure will be:

$$P=\frac{3}{2}\left(\frac{187{,}000}{® *0.0086*0.00687}\right)=1511.22\text{MPa}$$

To determine the size of the contact area, determination of the orientation of the shape of the contact ellipse is necessary.

$$\frac{1}{R_1{}^w}+\frac{1}{R_1{}^r}\geq\frac{1}{R_2{}^w}+\frac{1}{R_2{}^r}(3.23)$$

$$\frac{1}{420}+\frac{1}{\infty}\leq\frac{1}{\infty}+\frac{1}{300}$$

Therefore, the transverse semi axis of the contact ellipse (y direction) is less than or equal to the longitudinal semi-axis. The contact ellipse major axis a is along the length of the rail and the contact ellipse minor axis b is along the width of the rail.

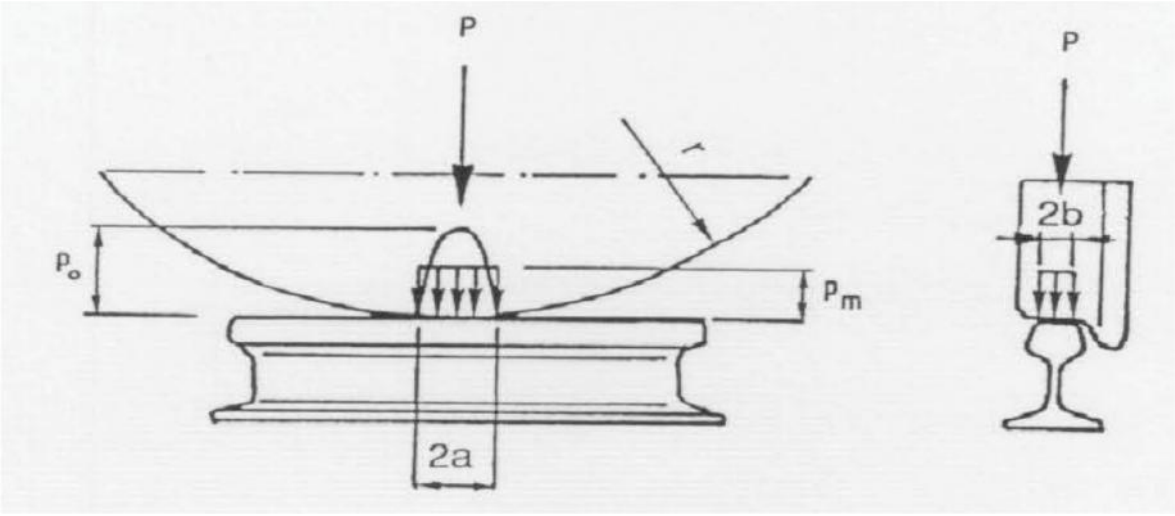

Figure 3.10 wheel rail contact pressure distribution

The result contact area was an ellipse with a contact patch area of π*a*b=1.856e^{-4}m^2.The equation for the resulting pressure distribution is

$$P = 1511.22e6N/m2\sqrt{1-\left(\frac{x}{0.0087m}\right)^2-\left(\frac{y}{0.00687m}\right)^2}$$

This parabolic distribution was applied to the finite element model, approximated as multiple uniform pressures over small areas.

Figure 3.11 wheel-rail contact patch area created by ABAQUS

Figure 3.12 loading condition of the rail created by ABAQUS

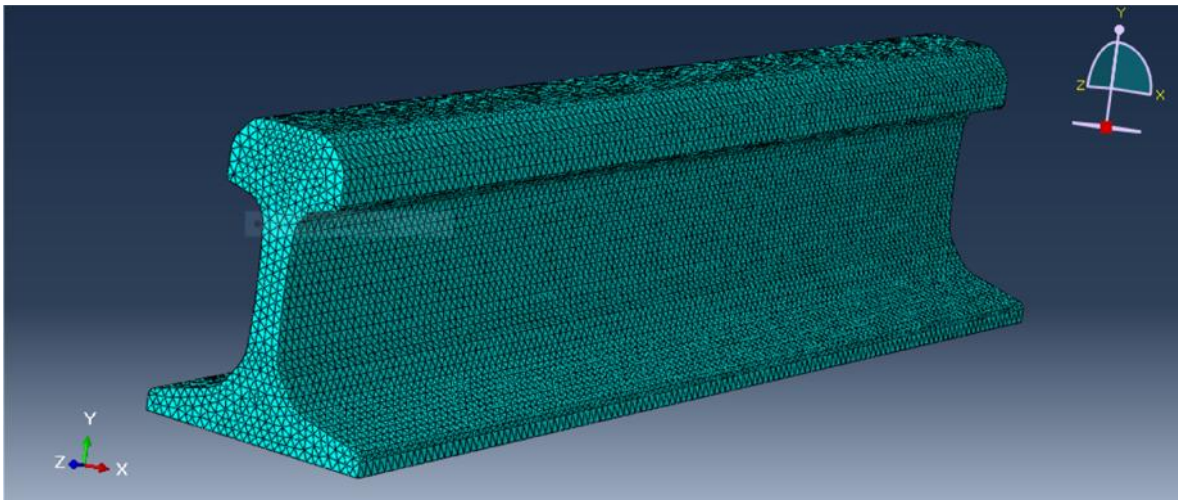

Figure 3.13 Finite Element mesh of the rail model in ABAQUS

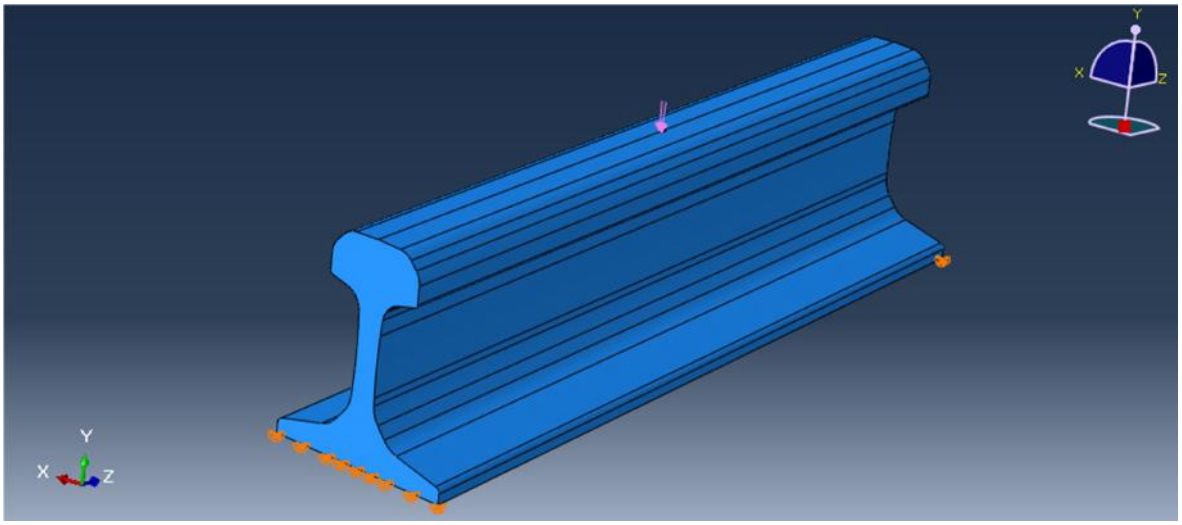

Figure 3.14 Final Model of the rail by ABAQUS

3.1.5.3 SIMULATION RESULTS

After performing the simulation in ABAQUS the results are obtained in the form of stress distributions. The results obtained from ABAQUS are described as follows;

3.1.5.3.1 STRESS DISTRIBUTION RESULTS

The stress distribution results are obtained in the form of Von-Misses stresses and a maximum value is found to be 1036MPa. The Von-Misses stress distribution obtained from ABAQUS is shown in figure 3.15.

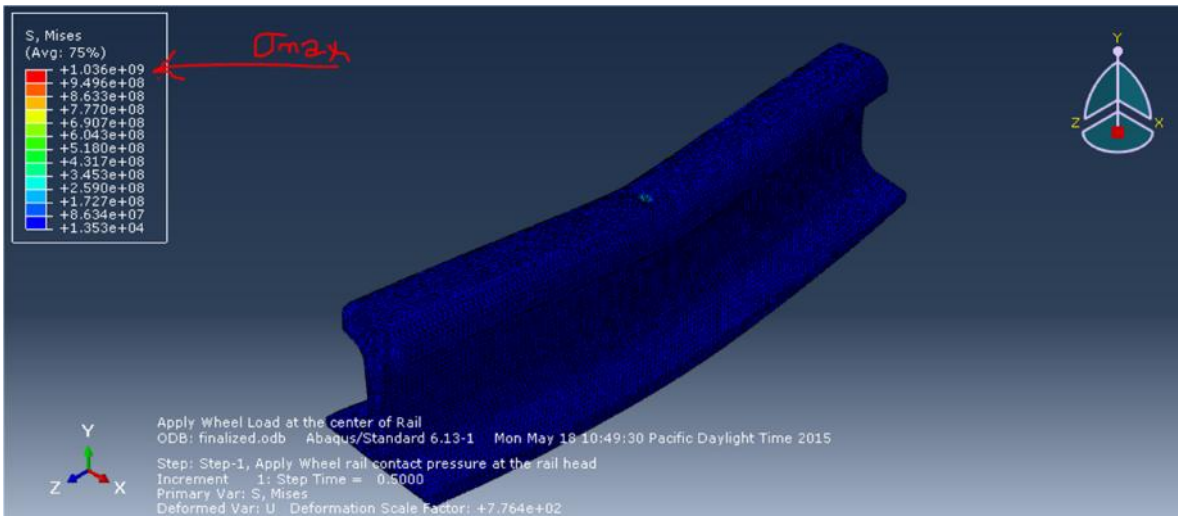

Figure 3.15 Von misses stress distribution for rail (Pa)

Therefore, the far-field stress used to compute the stress intensity factor for the rail was obtained as 1036MPa.

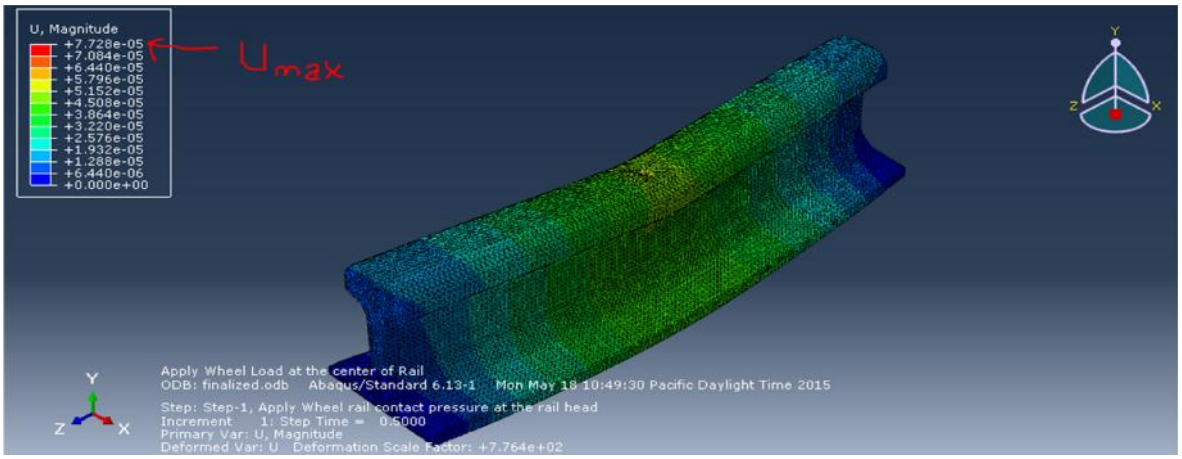

Figure 3.16 Spatial displacement at node (m)

3.1.6 DETERMINATION CRITICAL CRACK SIZE OF RAIL BY STRESS INTENSITY FACTOR APPROACH

The propagation of a crack is driven by the stress field that develops ahead of the crack tip. In fracture mechanics, the stress and strain fields can be characterized by parameters such as the stress intensity factor, *K*, under elastic conditions. The stress intensity factor (K) is used in fracture mechanics to predict stress intensity near the tip of a crack caused by a remote load or residual stresses.

As described before, the stress field near crack tips can be categorized as Mode I: opening mode, Mode II: sliding and Mode III: tearing, which each of them is characterized by a "local mode of deformation" as illustrated in Figure 3.1.

In general, stress-intensity factor depends on the stress induced on a structure, the crack size and the geometry of the crack. Such parameters describe the mechanics of the crack in terms that include the applied load and the length of the crack. The resistance of a material to fast fracture is given by the fracture toughness. Under small scale yielding conditions, to predict crack propagation life and fracture strength, accurate stress-intensity factor solutions are needed both for initial, intermediate and final crack configurations. But, because of the complexities of such problems, exact solutions are not available. Instead, investigators have had to use approximate analytical methods, experimental methods, or engineering estimates to obtain the stress-intensity factors.

According to Linear Elastic Fracture Mechanics under constant amplitude loading, stress intensity factor (ΔK) can be estimated as:

$$\Delta K = K_{max} - K_{min} = Y\Delta\sigma\sqrt{\pi a} \tag{3.24}$$

Where, Y is the geometric correction factor and Δσ is the tensile stress range, also called the far field stress range and a is the crack size.

It is noted that the use of stress intensity factor implies that the Paris and Erdogan's equation only applies to essentially elastic solution, so that the factor provides a reasonable description of a crack tip stress field for a distance up to 0.1a from the crack tip.

At any point along the boundary of the elliptical crack, the mode 1 stress intensity factor can be written as:

$$K = \frac{\sigma\sqrt{\pi a}}{\varphi}\sqrt[4]{\left(\frac{a^2}{c^2}Cos^2\theta + sin^2\theta\right)} \tag{3.25}$$

Where, σ is the far field stress, a is the crack size, Θ is the angle that defines any point around the perimeter of the elliptical crack, and φ is the elliptical integral of the second kind, given by

$$\varphi = \int_0^{\frac{\pi}{2}}\sqrt{(1 - (1 - \left(\frac{a}{c}\right)^2 sin\theta)}d\theta \tag{3.26}$$

Where, a and c are defined in fig.3.2.

An empirical expression that can describe the quantity φ of above equation for different crack depth to crack length aspect ratios, a/c, is given by;

$$\varphi^2 = 1 + 1.464\frac{a^{1.65}}{c^{1.65}} \text{ for a/c } \leq 1 \tag{3.27}$$

$\varphi^2 = 1 + 1.464\frac{c^{1.65}}{a^{1.65}}$ for a/c >1 ;(pook, 2000)

Where the crack is circular, where the aspect ratio a/c=1, the value of stress intensity factor around the crack front is a constant. From above equation, the stress intensity factor corresponding to an elliptical crack with aspect ratio a/c≤1) can be written as:

$$Ki = \frac{1.12\sigma\sqrt{\pi a}}{\varphi} = 0.806\sigma\sqrt{a}$$

Where the quantity φ = 2.464.

The finite element method was used to calculate the stress intensity factor due to the complexity of the rail geometry. Finite element codes must meet two requirements to resolve the singular stress at the crack tip. The first requirement is the element size: the new elements used to populate the crack region must be smaller than the existing mesh to calculate the stress-intensity factors accurately. However, the new elements must be large enough to address singularity at the crack tip. The second requirement is the element number: the number of elements around the crack tip influences the circumferential stress distribution. In general, the stress result is more accurate with more elements; but the results quality is compensated if the crack tip is over crowded with high aspect ratio elements. In order to meet the requirements by generating a smooth transition from the tip of the crack to the unmodified mesh, the FRANC codes insert "a rosette of crack-tip elements" that can be subdivided automatically and repeatedly into triangular and quadrilateral elements.

3.1.6.1 IMPORTANT FACTS ABOUT FRANC3D

Franc3D (Fracture Analysis Code 3 Dimensional) is available on Cornell Fracture Group web (page (http://.cfg.cornell.edu/). Franc3D is a highly interactive program for the simulation of crack growth and this software is considered to be a significant step in the development of discrete fracture analysis because of its modular software design and topological data structure.

Franc3D uses standard eight or six nodded elements with quadratic shape functions. These elements perform well for the elastic analysis and it also have the capability to incorporate the stress singularity in the solution by moving the side nodes to the quarter-point locations.

Although, Franc3D have a lot of features which provide very useful information concerning fracture mechanics and fatigue life calculations, but some of the main issues concerning Franc3D are discussed as follows.

The fracture calculations incorporated in Franc3D use three 3D LEFM concepts. The mode I SIF governs the fracture process in the LEFM context (Banks-Sills L., 1991)

3.1.6.1.1 ANALYSIS PROCEDURES USED IN FRACN3D

Franc3D uses two approaches in order to perform the simulation. The first is a direct linear equation solver for symmetric systems. The other one is a dynamic relaxation solver. Although, the linear equation solver is used in almost all cases except when nonlinear interface elements are being used.

3.1.6.1.1.1 Reading ABAQUS FE Model into FRANC3D

The simulation results from ABAQUS provide the foundation for the development of a FE model for stress intensity factor determination as well as crack propagation and fatigue strength analysis. A number of files will be created automatically as ABAQUS runs. Included in the set of files should be an *.inp* file with the job name as the prefix. This is the file that will be read by FRANC3D.

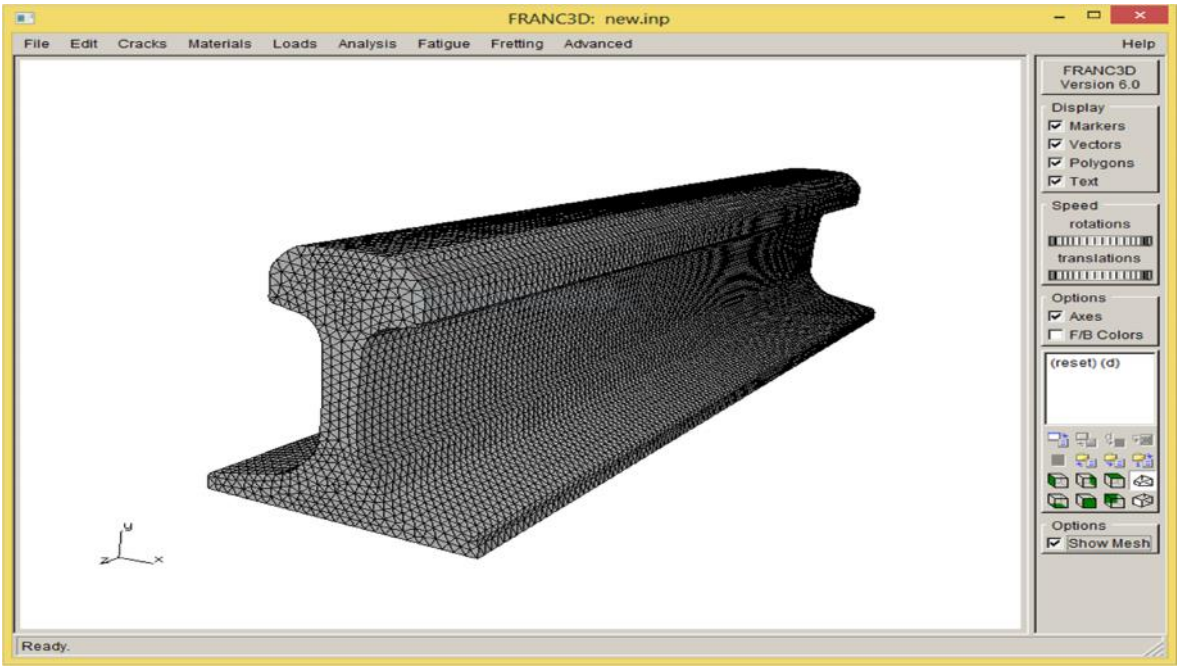

Figure 3.17 ABAQUS model converted to FRANC3D

3.1.6.1.1.2 INSERT A CRACK

As described in section 3.1.3.1, Single front elliptical cracks are defined by entering the semi-axes lengths (a and b) which are 0.01m and 0.005m respectively. Once a flaw (crack) is defined, it was inserted (translated and rotated) into the proper location relative to the unflawed body of the rail as shown below.

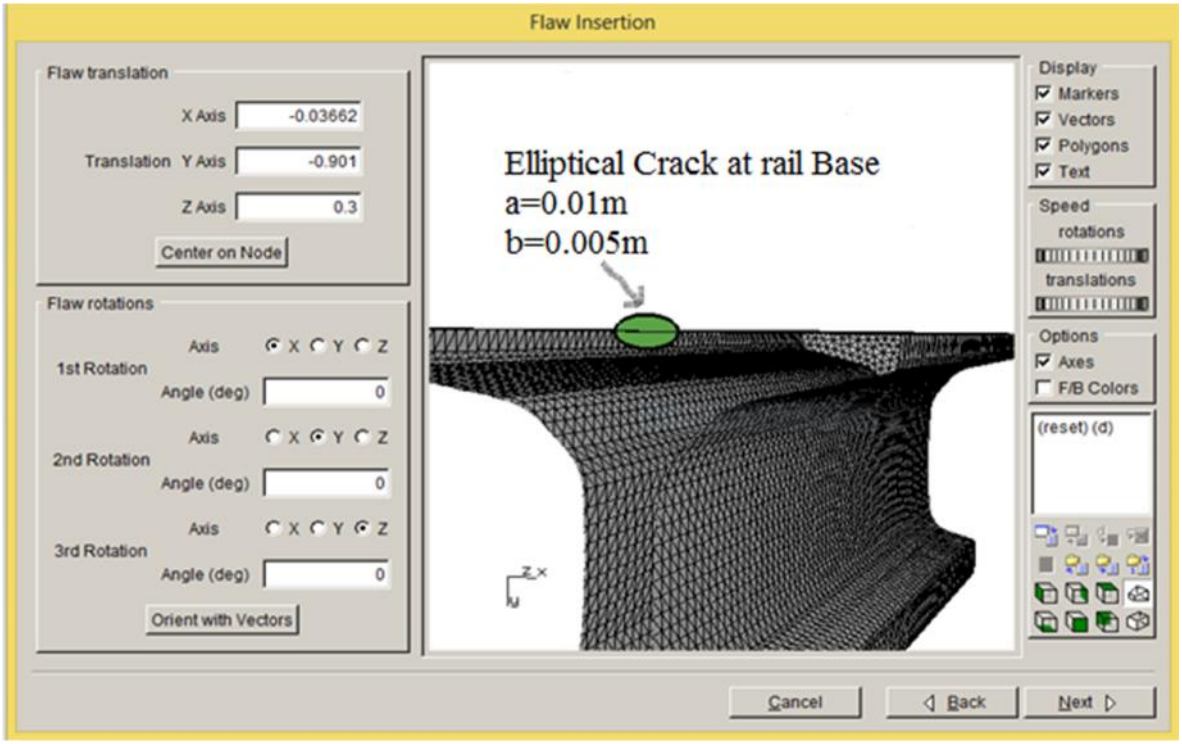

Figure 3.18 Location and orientation of elliptical crack at rail base.

For accurate stress-intensity factor computations, a pattern or "template" of elements with controlled sizes and shapes is placed about all crack fronts. The template takes the form of generalized cylindrical tubes of elements with the crack fronts serving as the axes of the cylinders. Wedge shaped elements are placed immediately adjacent to the crack fronts. These are surrounded by rings of brick elements.

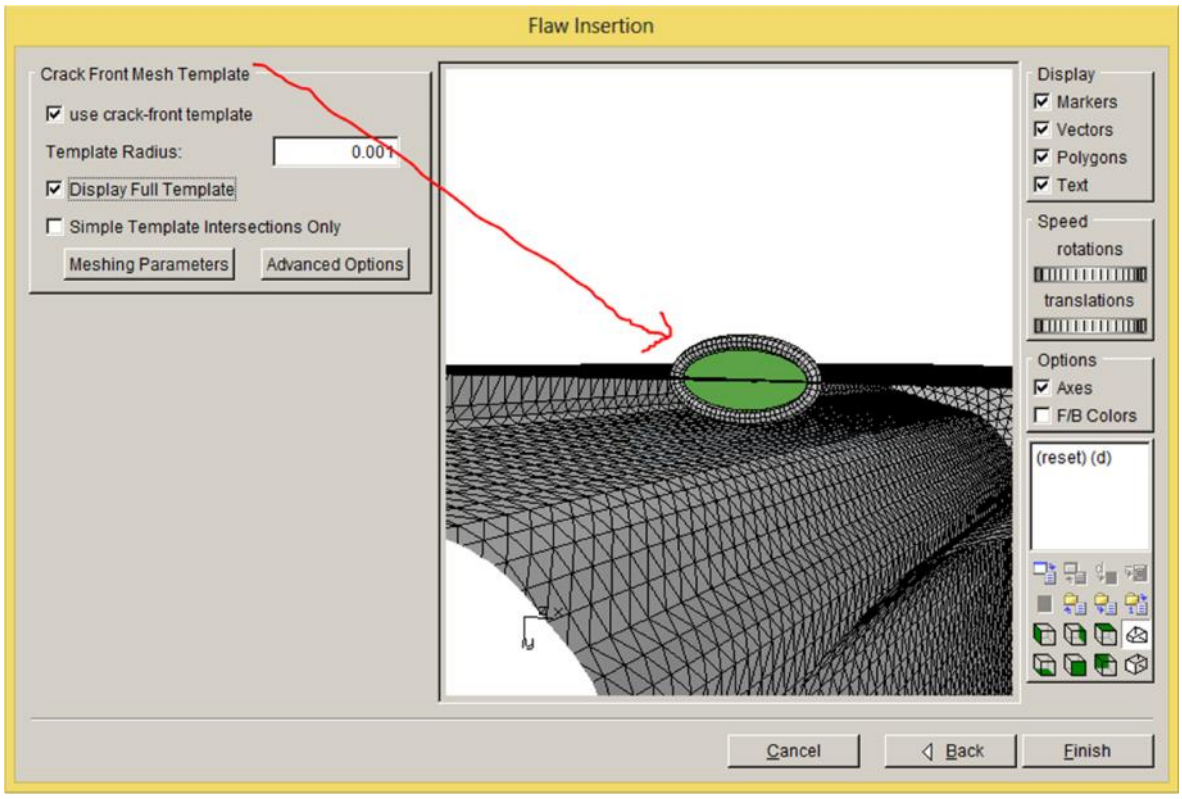

Figure 3.19 Crack front mesh template panel

3.1.6.1.1.3 CRACK INSERTION AND MESHING

After crack front mesh template panel is defined, the flaw is inserted into the rail base and the model is re-meshed. The crack geometry is inserted into the model geometry first, represented by the Doing geometric intersections status. Once the crack geometry has been inserted, trimmed, and tied to the rail model geometry, surface and then volume meshing occurs. The final mesh is smoothed to improve the element quality.

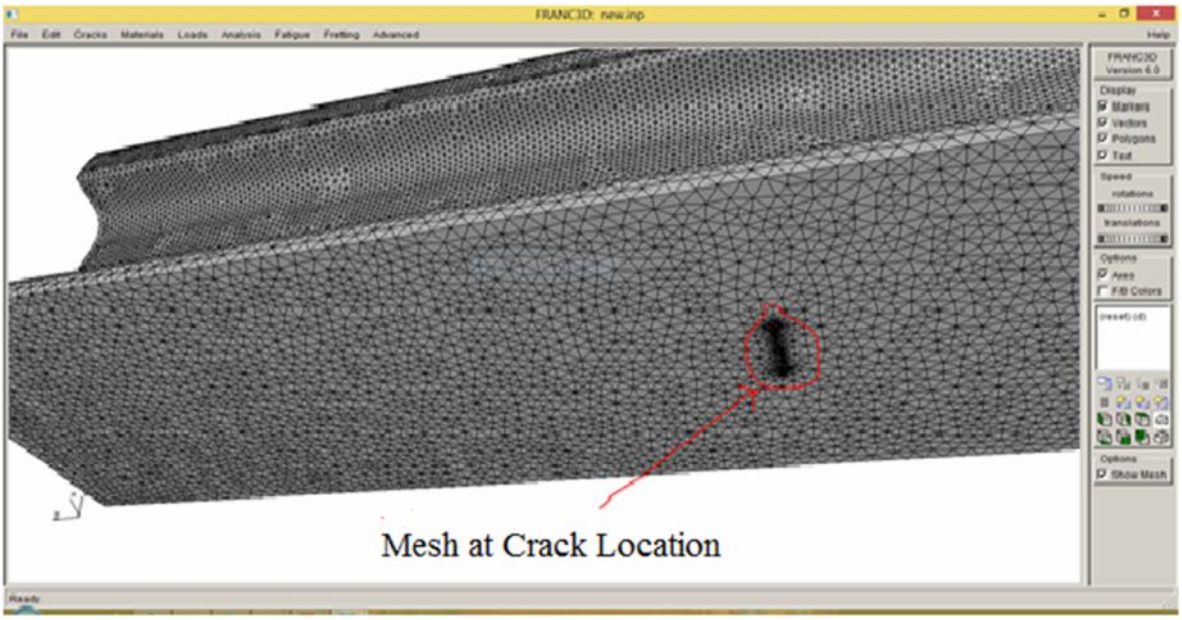

Figure 3.20 Meshed rail model with crack at rail base.

3.1.6.1.1.4 STATIC CRACK ANALYSIS

Static crack analysis is a static (single step, no crack growth) deformation analysis. This analysis is wanted to compute stress-intensity factors for this crack without performing any crack growth.

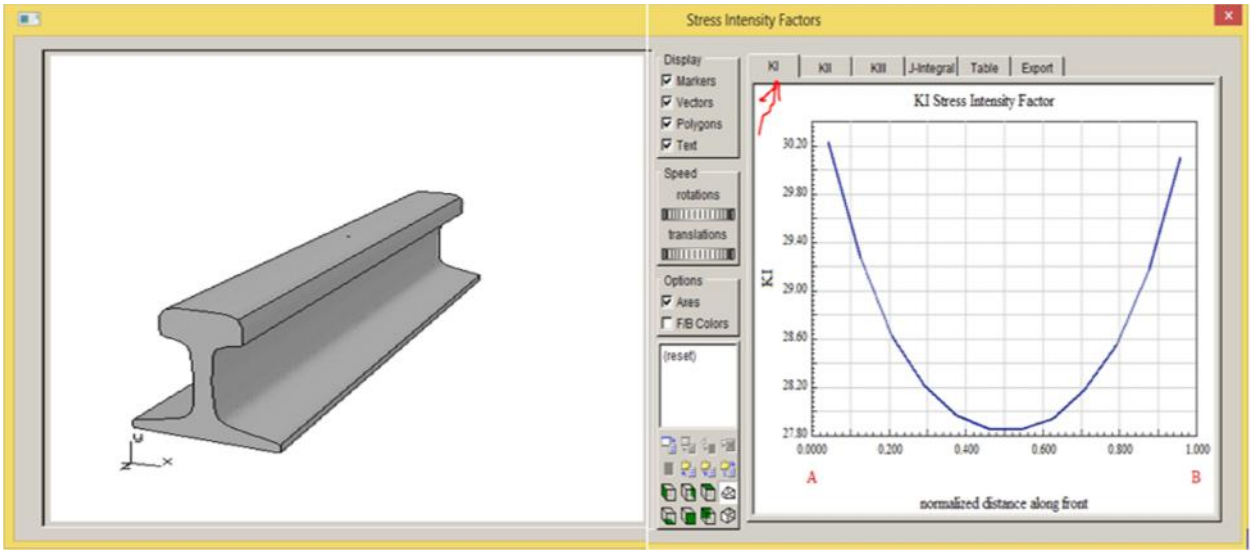

Figure 3.21 Mode I stress intensity factor with respect to normalized distance along crack front created by FRANC3D

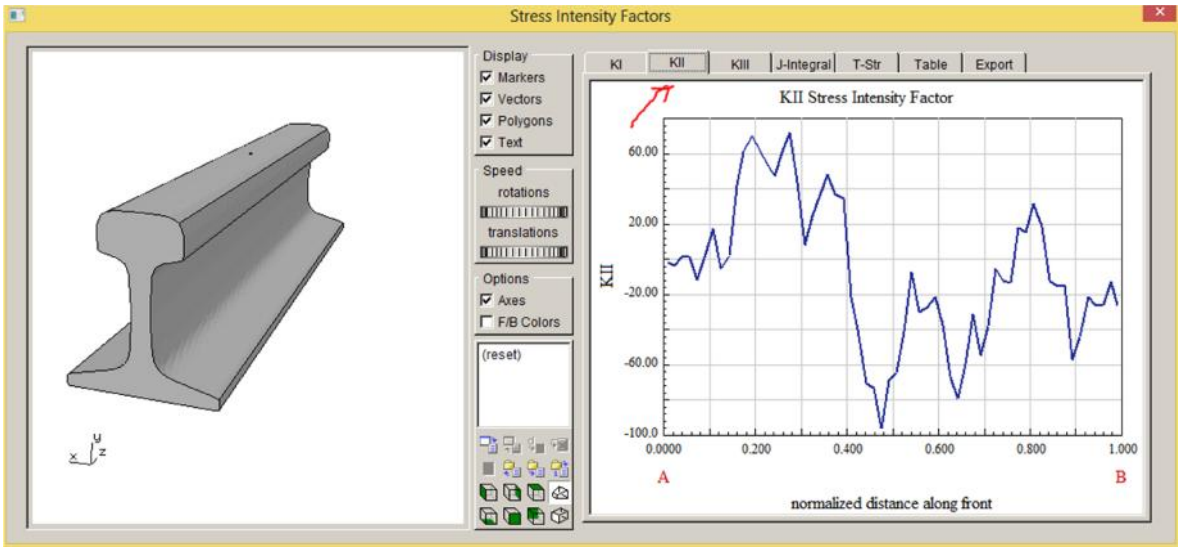

Figure 3.22 Mode II stress intensity factor with respect to normalized distance along crack front created by FRANC3D.

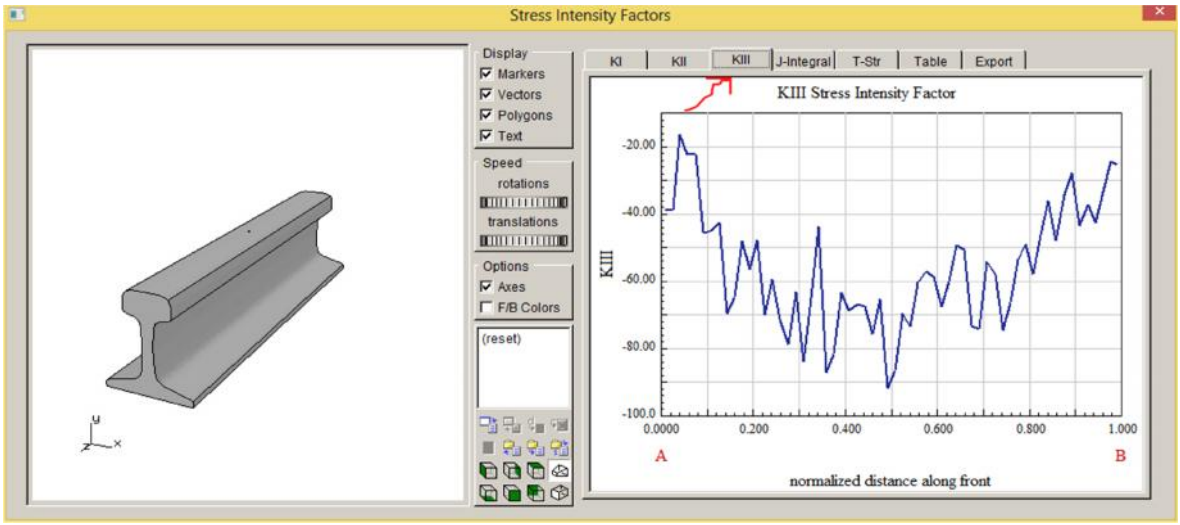

Figure 3.23 Mode III stress intensity factor with respect to normalized distance along crack front created by FRANC3D.

3.1.7 FRACTURE TOUGHNESS

In materials science, the fracture toughness K_{IC} is a property which describes the ability of a material containing a crack to resist fracture. The subscript *I* denotes mode I crack opening under a normal tensile stress perpendicular to the crack. Fracture toughness is a quantitative way of expressing the resistance of a material to brittle fracture when a crack is present. It is independent of the size and geometry of the cracked body under certain conditions. The materials with higher values of fracture toughness are more likely to undergo a ductile fracture; however, the materials with low value fracture

toughness usually undergo a brittle fracture (Anderson, T.M., 1999). The largest crack a structure can sustain under specific strength requirements can be predicted through this critical value of the SIF where the crack propagation becomes unstable. The mechanical properties and fracture toughness of rail steel is determined by static tensile experiment using MTS materials testing system of electronic discharge machining (EDM).

The national standards of the people's republic of China manual recommend the following for the fracture toughness of rail steel: 'The minimum single value of fracture toughness K_{IC} of rails shall be 26MPa√m and the minimum mean value shall be 29MPa√m'. The FRANC3D software mode 1 stress intensity factor value obtained before is much closer. So, in this thesis, a fracture toughness value of 29MPa√m is taken for the T50 rail of national railway network of Ethiopia.

Since, the fracture criterion is: $K_I=K_{IC}$, the critical crack size at the head, web and base of the T50 rail steel can be determined as follows:

CASE 1: At rail base:

$$a_c = \frac{1}{\Pi}\left(\left(\frac{K\xi}{1.12\sigma_c}\right)\right)^2 = \frac{1}{\Pi}\left(\left(\frac{29*2.464}{1.12*1036}\right)\right)^2 = 2mm$$

CASE 2: At the rail head:

$$a_c = \frac{1}{\Pi}\left(\left(\frac{K\xi}{1.12\sigma_c}\right)\right)^2 = \frac{1}{\Pi}\left(\left(\frac{29*2.464}{1.12*1511.22}\right)\right)^2 = 1mm$$

CASE 3: At the rail web

To determine the critical crack size at the web of the rail, the proportioning bending stress with respect to the maximum bending stress at the rail base is taken as follows:

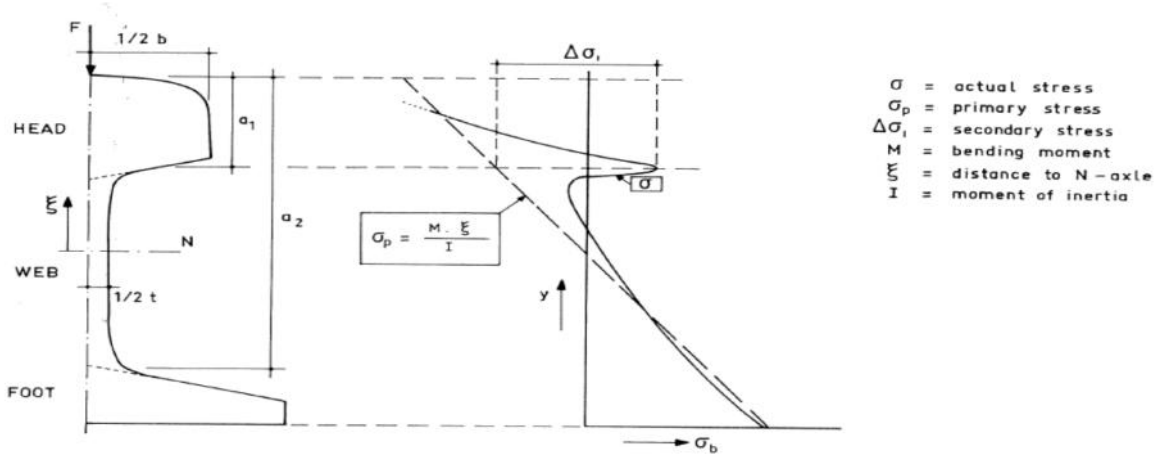

Figure 3.24 Stress as a result of flexural moment in the cross section of rail in which wheel rail contact load is applied at the center of rail.

By using the triangular proportioning of stress with respect to the centroid of rail and the bottom of the rail base, the value of bending stress was obtained as:

$$\sigma = \left(\frac{0.0387}{0.0766} * 1036\right) MPa = 523.4MP$$

Therefore,

$$a_c = \frac{1}{\Pi}\left(\left(\frac{K\xi}{1.12\sigma_c}\right)\right)^2 = \frac{1}{\Pi}\left(\left(\frac{29*2.464}{1.12*523.4}\right)\right)^2 = 5mm.$$

Table 3.7stress intensity factor versus crack size

crack size,a(mm)	SIF,KI (MPa√mm)		
	Head	Web	Base
0.0	0	0	0
0.5	861.2843	298.3001	590.4342
1.0	1218.04	421.86	835
1.5	1491.788	516.6709	1022.662
2.0	1722.569	596.6001	1180.868
2.5	1925.89	667.0192	1320.251
3.0	2109.707	730.683	1446.262
3.5	2278.744	789.2278	1562.142
4.0	2436.08	843.72	1670
4.5	2583.853	894.9002	1771.302
5.0	2723.62	943.3076	1867.117

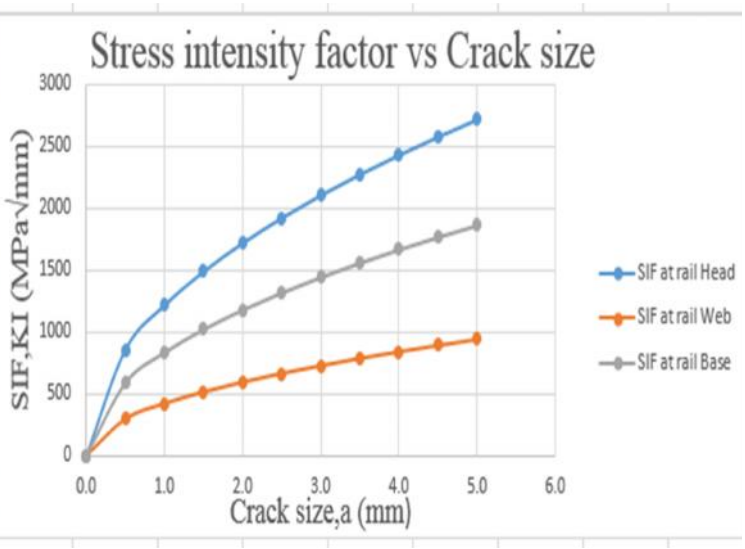

Fig.3.25 SIF vs. crack size

3.1.8 FATIGUE LIFE

It is well established that fatigue is essentially a two stage process; crack initiation and crack propagation. The crack initiation stage is governed by number of load cycles required for a fatigue crack to initiate and to become a potential stress raiser. However, crack propagation stage comprise of the loading cycles required to grow the initiated crack until the final failure of the structure is reached.

A fatigue life analysis is performed based on Paris law. As mentioned above, the Paris law states that the crack growth rate is an exponential function of the stress intensity factor, ΔK:

$$\frac{da}{dN} = C\Delta Km = C(\Delta\sigma Y\sqrt{\pi})^n \qquad (3.28)$$

Where C and m are the material specific input parameters. Generally, for metals, values of m ranges from 2.5 to 3.5 and the c values ranges from $1*10^{-9}$ to $1*10^{-11}$(N. Pugno, M. Ciavarella, 2006). So, m=3 and c= $1*10^{-11}$ are taken as the specific input parameters in this thesis for the basic understanding of the fatigue strength behavior of the rail. For calculation of fatigue life of rail, σ=1036MPa at the rail base, σ=1511.22MPa at the rail head, and σ=523.4MPa at the rail web are taken.

CASE 1: For rail base

$K_1 = (1.12\sigma\sqrt{\Pi a})/\varphi = 0.806\sigma\sqrt{a}$

$(\Delta K)_2 = 0.806*\sqrt{0.0005}*1036 = 18.67$

$(\Delta K)_4 = 0.806*\sqrt{0.001}*1036 = 26.40$

$$\frac{da}{dN} - C\Delta K^m - C(\Delta\sigma Y\sqrt{\pi a})^m$$

$(da/dN)_2 = 10^{-11}(18.67)^3 = 6{,}507.78*10^{-11}$

$(da/dN)_4 = 10^{-11}(26.4)^3 = 18{,}399.744*10^{-11}$

Mean of $(da/dN)_2$ and $(da/dN)_4 = 12{,}453.76*10^{-11}$

$dN = 0.0005/ (12{,}453.76*10^{-11}) = 4{,}014.85$

Table 3.8 Crack length vs. number of cycles for rail base

Crack length (ao) (mm)	Crack length (a) (mm)	ΔN (Cycles)	N (Cycles)
0.5	1	4,015	4,015
1	1.5	3,829.70	7,845
1.5	2	3,492.50	11,337

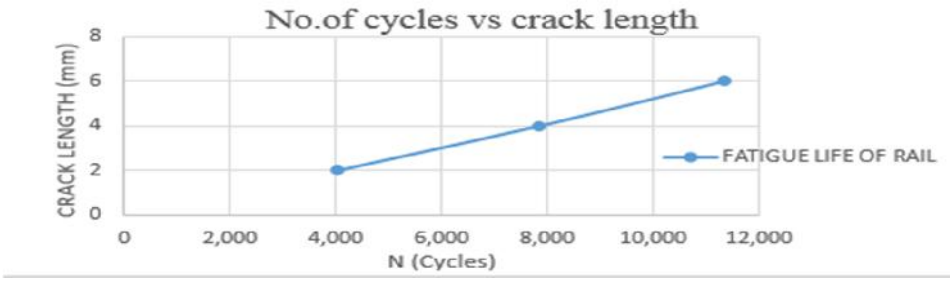

Figure 3.26 Fatigue life of rail (crack at rail base)

CASE 2: For rail head

Table3.9 Crack length vs. no. of cycles for rail head

Crack length (ao) (mm)	Crack length (a) (mm)	ΔN (Cycles)	N (Cycles)
0.2	0.4	2043.88	2,043.88
0.4	0.6	1945	3,988.88
0.6	0.8	1779	5,767.88
0.8	1	1632.12	7,400.00

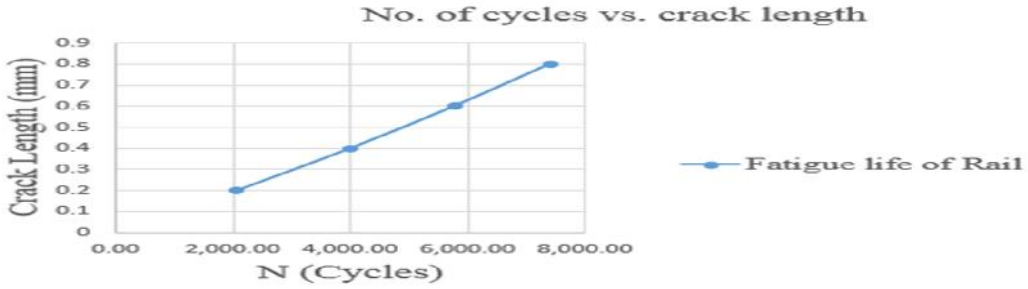

Figure 3.27 Fatigue life of rail (crack at rail head)

CASE 3: For rail web

Table 3.10 Crack length vs. Number of cycles for rail web.

Crack length (ao) (mm)	Crack length (a) (mm)	ΔN (Cycles)	N (Cycles)
1	2	21,995	21,995
2	3	20,990.00	42,985
3	4	19,151.57	62,136
4	5	17,568.90	79,705

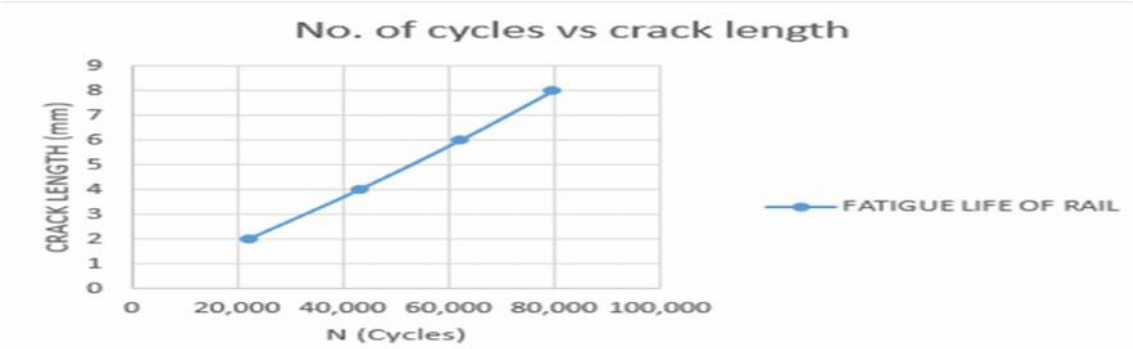

Figure 3.28 Fatigue life of rail (crack at rail web).

According to the predicted traffic volume in the feasibility study of Some National Railway Network of Ethiopia, the forecasted number of trains varies from section to section (Sebeta-Meiso section conceptual design EPC general specification).

Similarly, the annual traffic density for the National Railway Network of Ethiopia is taken as 22.67MGT (Million Gross Tones) in this thesis.

So, to determine the number of trains per day, we use the Vope center empirical formula which is as a function of annual traffic density as follows:

X (No. Of trains per day)=T/0.006312/365 = 10.

Finally, the fatigue life of rail as a function of MGT (Million Gross Tones) is obtained as follows: Assume one train passes a certain track section two times per day. So, the total number of cycles per year for loaded standard vehicle with four axles or eight wheels is 8*(10*365) =29,200 cycles/year.

29,200 Cycles = 22.67 MGT

79,705 Cycles (Maximum No. Of cycles for rail head, web and base) =?

From the above proportioning, the fatigue life of rail based on the maximum critical number of cycles for rail web is taken as **61.88MGT (Million Gross Tones).**

CHAPTER 4

4.1 STRUCTURAL RELIABILITY ANALYSIS

Reliability analysis is only one of the constituents of a decision analysis or more popularly speaking a risk analysis, namely the part which is concerned about the quantification of the probability that a considered components or system is in a state associated with adverse consequences, e.g. a state of failure, a state of damage, etc. The theoretical basis for reliability analysis is thus the theory of probability and statistics and derived disciplines such as operations research, systems engineering and quality control. Probabilistic techniques are characterized by the use of random variables to describe the various sources of uncertainty and are often referred to as reliability methods by structural engineers. These techniques are typically applied when the system under consideration is of small to moderate complexity (100-150 random variables or less) and is reasonably well understood. The objective of reliability analysis is to determine the probability of an event occurring during a specified reference period.

Classical reliability theory was developed for systems consisting of a large number of components of the same type under the same loading and for all practical matters behaving statistically independent. The probability of failure of such components can be interpreted in terms of relative failure frequencies observed from operation experience. Furthermore, due to the fact that failure of the considered type of components develops as a direct consequence of an accumulating deterioration process the main focus was directed towards the formulation of probabilistic models for the estimation of the statistical characteristics of the time until component failure. Having formulated these models the observed relative failure frequencies can be applied as basis for their calibration.

Structural reliability theory is essentially the application of probability theory to the modeling of structural failures and the prediction of success probability. In structural reliability analysis the situation is fundamentally different due to the fact that structural failures are very rare and tend to occur as a consequence of an extreme event such as e.g. an extreme loading exceeding the load carrying capacity i.e. the resistance, which possibly is reduced due to deterioration such as e.g. corrosion or fatigue. In addition to this no useful information can be collected in regard to relative failure frequencies as almost all structural components and systems are unique either due to differences in the choice of material and geometry or by differences in the loading and exposure characteristics.

4.1.1 FIRST ORDER RELIABILITY METHOD (FORM) OF ANALYSIS

First-order reliability method, (FORM), is a semi-probabilistic reliability method devised to evaluate the reliability of a system. These methods are characterized by the iterative, linear (first-order) approximation to the performance function.

Not only fatigue but also strength of materials is so sensitive that they are statistical by nature. In addition, it is intricate to evaluate meticulous probability of failure in materials applied to cycle loads in variable times. Even if estimated, the results can be much widely varied. Therefore instead of rail safety evaluated by rigorous probabilistic prediction of failure, a kind of index that is the hasofer-lind reliability index: beta assesses the reliability of rails in this thesis.

The structural reliability theory is concerned with rational treatment of uncertainties in structures and with the method for assessing the safety and serviceability in structures. A rigorous structural reliability assessment involves modeling all of the sources of uncertainty that may affect failure of the component or system. This clearly involves modeling all of the fundamental quantities entering the problem, and also the uncertainties that arise from lack of knowledge and idealized modeling. These terms are referred to as *basic random variables* and the uncertainties are usually described as a random variable vector $X=(x_1, x_2 \dots x_n)$.

The basic concept from classical structural reliability theory proposed by Cornell (1969), a random variable vector relevant to loads and resistance parameters in structures and functional relationship among them are required.

The relationship can be expressed as:

$$F = g(x_1, x_2, x_3 \dots x_n) = g(X) \tag{4.1}$$

This function is called limit state function. The failure surface which is in the limit state of the structures is called the limit state equation and it can be defined as:

$$g(X) = 0 \tag{4.2}$$

Geometrically, the limit state equation is an n-dimensional space .One side of the failure surface is the safe state, $g(X)>0$ whereas the other side of the failure surface is the failure state, $(X) <0$.

$$g(x1, x2, \dots\dots, xn) \begin{cases} > 0 & safe\ state \\ = 0 & \text{limit state} \\ < 0 & \text{failure state} \end{cases} \tag{4.3}$$

Hence, if the joint probabilistic density function of the variables, $x_1, x_2 \dots x_n$ is $f_{x1,x2,x3,\dots\dots,xn}(x_1,x_2,x_3,\dots\dots x_n)$, the probability of failure :P_f can be defined as

$$P_f = \int \dots \int_{g(x)<0} (x_1, x_2, \dots, x_n)\, d_{x1}, d_{x2}, \dots d_{xn} \quad (4.4)$$

This is rewritten for brevity by the volume integral of $f_x(x)$ over the failure region as

$$P_f = \int_{g(x)<0} f(x) dx \quad (4.5)$$

In general, solving the integrals from the above equation is a complicated process and can be done in closed form only for a simple case. Moreover, the calculation of multi-dimensional integral requires the information of the joint probabilistic density function or each probabilistic density functions of variables. For practical reasons, the information is often unavailable or too difficult to obtain sufficient data. Therefore, some alternative methods are needed in order to evaluate the probability of failure; these methods can be either analytical or numerical. Analytical methods represent the reliability as a reliability index: beta. One of them is the first order reliability method based on determining mean and variance of variables. Numerical methods evaluate directly through simulations, such as the Monte Carlo simulation, or by using reliability software's such as STRUREL or COMREL.

The concept by Cornell has an invariance problem that the results change by the way to define limit state function. Hence, Hasofer - Lind (1974) improves the concept to first order reliability method. The reliability index: beta is defined as the minimum distance from the origin to a failure surface of a space defined with the random vectors in this approach. The most probable point (MPP) of failure, the design point, or the point on the limit state that lies closest to the origin, is found in a standard normal space U for a single failure driven limit state equation. The components of U are normally distributed with zero mean and unit variance and are statically independent.

Any set of continuous random vectors can be transformed in to U using the Rosenblatt transformation discussed later in detail.

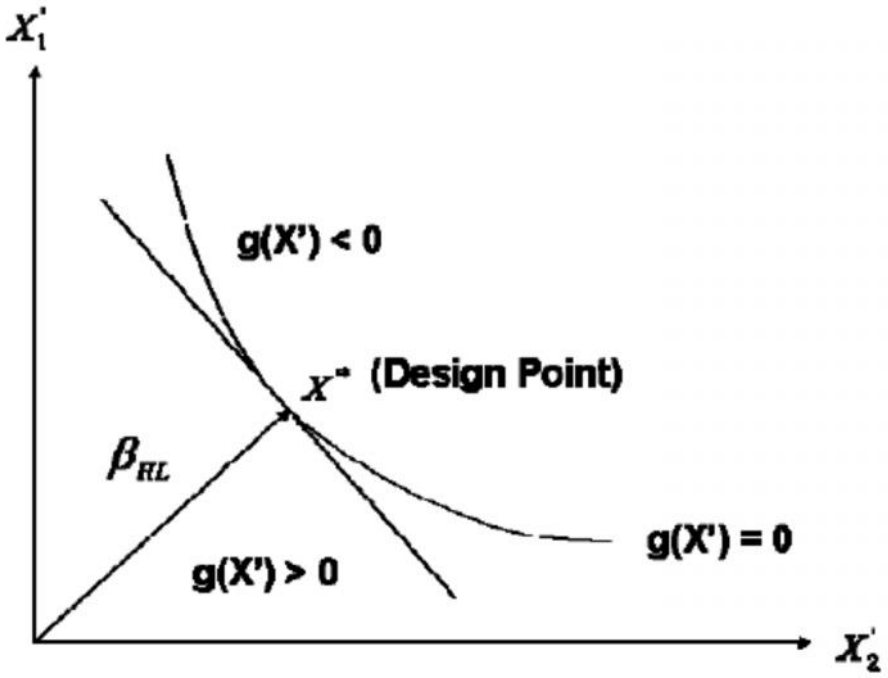

Figure 4.1: Hasofer - Lind Reliability Index: Nonlinear Performance Function

The most probable point u* also lives in the hyper surface and the location is the closest point on the limit state function to the origin in U space. The most probable point can be found by figuring out the following constrained optimization problem.

Minimize D = $\sqrt{U^T U}$ (4.6)

Where D is the distance from the origin to the most probable point, and T is the transpose notation. Although various algorithms exist to perform the most probable point search, one of them is Rackwitz-Fieesler (1978) algorithm, which is based on Newton-Raphson root solving recursive approach.

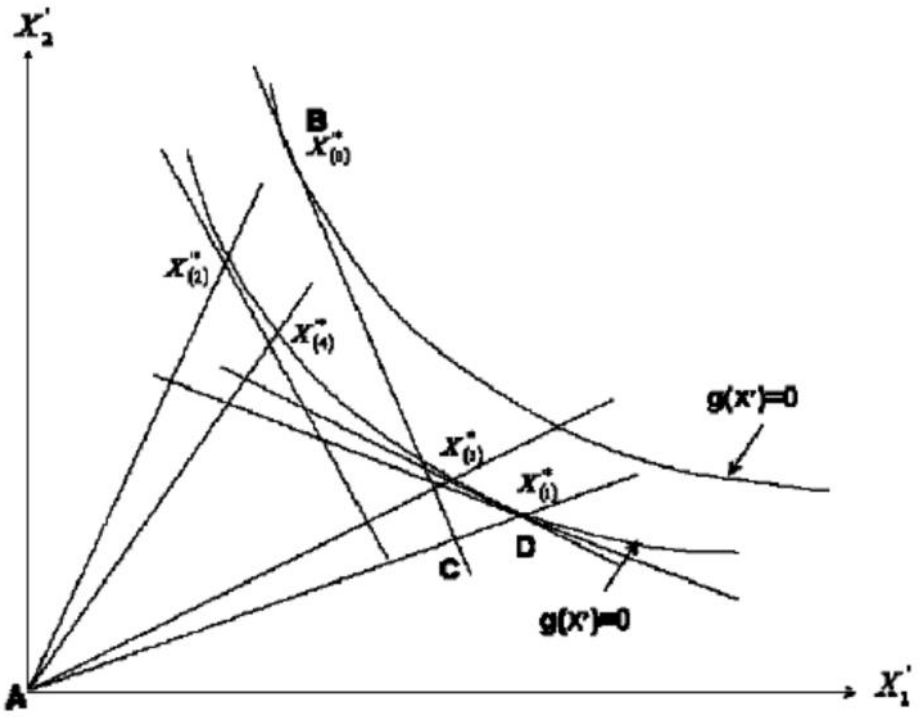

Figure 4.2 Algorithm for finding β

When the limit state equation is nonlinear, the gradient is not constant and varies from one point to another point. Hence, the most probable point has to be searched through the recursive formula. If the limit state equation is linear, first order reliability method gives the correct value regarding probability of failure.

The algorithm is repeated until convergence satisfying the following criteria:

If $g(U_k) \leq \varepsilon, stop$ (4.7)

Where ε is a small quantity (= 0.001).

After transformation by Rosenblatt transformation, the reliability index is directly related to the probability of failure (as β increases the limit state moves away from the origin and the probability of failure decreases): as described as

$P_f = \phi(-ß)$ (4.8)

Where, ϕ (.) is the cumulative function of the standard normal variant.

4.1.2 FATIGUE DAMAGE ACCUMULATION FUNCTION

Integrating equation (3.1) from a_1 to a_2 corresponding to the number of stress cycles N_1 and N_2, one obtains:

$$\int_{a1}^{a2} \frac{1}{Y\sqrt{\Pi a}} da = \int_{N2}^{N1} CS^m \, dN \tag{4.9}$$

According to Madsen (1985), a function reflecting the damage accumulation from crack size a_1 to a_2 can be defined as:

$$\Psi(a_1, a_2) = \int_{a1}^{a2} \frac{1}{Y\sqrt{\Pi a}} da \tag{4.10}$$

The damage accumulation function is related to the load accumulation by:

$$\Psi(a_1, a_2) = CS^m(N2 - N1) \tag{4.11}$$

Where, S^m is the mean stress- range effect, which is an m-order moment of the probabilistic density function of a stress amplitude parameter (Haldar 1994).

An actual rail is usually subjected to a variable amplitude load process as alluded to before. Two possibilities are the cycle-cycle counting and the mean-stress range effect method to consider the fatigue under a variable amplitude stress. The method to count step-by-step each stress occurred in a rail is not practical. The mean stress-range effect method might be appropriate to the study for the fatigue damage accumulation in rails.

The mean stress-range effect can be evaluated as:

$$S^m = \int_0^\infty S^m fs(s) ds \tag{4.12}$$

Where, $fs(s)$ is the probabilistic density function of the stress range parameter, S is assumed to follow the stationary Gaussian random process. For rails, the Rayleigh distribution would be the most appropriate for the estimation of S since the train load stress can comprise of two components: one is static and the other is dynamic stress as indicated in section 3.5.If the stress range parameter follows a Rayleigh distribution, the mean stress-range effect can be shown as follows:

$$S^m = (So\sqrt{2})^m \Gamma(\frac{m}{2} + 1) \tag{4.13}$$

Where, $\Gamma(\frac{m}{2} + 1) = \left(\frac{m}{2}\right)^{(\frac{m}{2}+\frac{1}{2})} e^{-\frac{m}{2}} \sqrt{2\Pi}$; Γ is a gamma function, and

S_o is a statistical parameter which is expressed as:

$$S_o = S\sqrt{\frac{2}{\Pi}} \tag{4.14}$$

Where, S is the mean value of S, which is 826.61 MPa, calculated in section 3.6.

$$S_o = 1036\sqrt{\frac{2}{\Pi}} = 826.61MP$$

and

Therefore, $S^m = (826.61 * \sqrt{2})^n \, \Gamma\left(\frac{m}{2}+1\right)$

$$= (1169)^n * \left(\frac{m}{2}\right)^{\left(\frac{m}{2}+\frac{1}{2}\right)} e^{-\frac{m}{2}}\sqrt{2\Pi}$$

4.1.3 RELIABILITY ANALYSIS OF RAIL BY LEFM APPROACH

Rail defects directly related to the serviceability of tracks so that the limit state of serviceability exists on a state of crack growth. When the critical crack size, ac is specified, limit state functions for rails subjected to N stress cycles can be defined as:

$$Z = g(x) = ac - a(N) \tag{4.15}$$

Where, a(N) is a crack size after a rail is subjected to N stress cycles. A crack size corresponding to the number of cycles can be obtained by the paris and Erdogan's kinetic crack growth low as discussed earlier.Once a(N) exceeds the criticall crack size, rail can be considered as failure.

Since the function Ψ(.) defined by equation(4.10) can be expressed as:

$$\Psi(ac, ao) - \Psi(aN, ao) = 0 \tag{4.16}$$

Using equation(4.10), the above limit state function (LSF) can be rewritten as:

$$\Psi(ac, ao) - CS^m(N - No) = 0 \tag{4.17}$$

$$\Psi\,(a_0, a_c) = \int_{a0}^{ac} \frac{1}{(Y\sqrt{\Pi a})^n} da \tag{4.18}$$

Where, ao is the initial crack size, and No is the crack initiation period.

The initial crack size is the crack size from which the fatigue crack will propagate. It is a lower limit for the crack size which can be a fabrication crack.The large variability in a fatigue analysis can be attributed to the uncertainity in the initial crack size,which is usually random variable.

$$g(x)=\int_{a0\,(}^{ac}\frac{1}{Y\sqrt{\pi a)^m}}da-\ CS^m(N-No) \tag{4.19}$$

$$=\int_{a0\,(}^{ac}\frac{1}{1.12\sqrt{\pi a)^m}}da-\frac{\sqrt{2\Pi}*\mathrm{C}*\mathrm{N}*(1169)^n\ *\left(\frac{m}{2}\right)^{\left(\frac{m}{2}+\frac{1}{2}\right)}}{e^{\frac{m}{2}}}$$

Therefore, $g(x)=\frac{ac^{\,1-\frac{m}{2}}-ao^{\,1-\frac{m}{2}}}{\left(1-\frac{m}{2}\right)\left(1.12\sqrt{\pi}\right)^m}-\frac{\sqrt{2\Pi}*\mathrm{C}*\mathrm{N}*(1169)^m*\left(\frac{m}{2}\right)^{\left(\frac{m}{2}+\frac{1}{2}\right)}}{e^{\frac{m}{2}}}$

Although many types of Probabilistic density functions of initial crack size in modelling the uncertainity are sugegested,in this study,it is modeled to a lognormal distribution with the mean of 0.2mm and the correlation of variance (COV) of 0.3 .The crack initiation period (No) is another aspect of crack initiation.It seems that no reasonable theory exists for the period, some models are proposed.For Simplicity, however, it is assumed that No is equal to zero in this thesis.

As determined before, the critical crack size a_c is a significant parameter in the LEFM formulation.It can be defined as the crack size causing failure of rail or the design crack size beyond which the serviceability requirements can not be satisfied. Since the fracture toughness is 29MPa√m,the kinetic crack growth law shown in equation (3.1) describes the critical crack size as:

$$a_c=\frac{1}{\Pi}\left(\left(\frac{K\xi}{1.12\sigma c}\right)\right)^2 \tag{4.20}$$

Where, σ_c is the critical far field stress.

The critical crack size has uncertainities due to the model, materials, and the enviroment so that the critical crack size is also random variables.It is assumed that the critical crack size follows a lognormal distribution.

Generally, for metals,values of m ranges from 2.5-3.5 and the C values ranges from 1e-9 to 1e-11. And based on the literature,(N. Pugno, M. Ciavarella, 2006), the values of C is 1.0E-11 and of m is 3 for the steel rail.In this thesis,the above values are taken as rail material input parameter.

Table 4.1 statistical characteristics of variables for first order reliability method of analysis

Variables	Notation	Type	Mean Value	COV
Critical crack size at head	a_{ch}	lognormal	1(mm)	0.3
Critical crack size at web	a_{cw}	lognormal	5(mm)	0.3
Critical crack size at base	a_{cb}	lognormal	2(mm)	0.3
Initial Crack size	a_o	Lognormal	0.2(mm)	0.3

4.1.3.1 ROSENBLATT TRANSFORMATION

Notation ally, **x** will refer to a vector of independent random variables, while **y** will be a vector of statistically dependent random variables. Let the joint probability and cumulative density functions of $\mathbf{y} = (y_1, y2, y3 \ldots y_n)$ be defined as: $f(\mathbf{y})$ and $F_Y(\mathbf{y})$ respectively. Define the marginal density functions and cumulative marginal distribution functions

$$f_i(y_1, y_2, \ldots, y_i) = \int_{\infty}^{-\infty} \ldots \int_{\infty}^{-\infty} f_i(y_1, y_2, \ldots, y_i, s_{i+1}, \ldots, s_n) d_{s_{i+1}} \ldots d_{s_n} \quad (4.21)$$

$$H_i(y_i/y_1, y_2, \ldots, y_{i-1}) = \frac{1}{Ki} \int_{-\infty}^{y_i} f_i(y_1, y_2, \ldots, y_{i-1}, s_i) d_{s_i} \quad (4.22)$$

Where,

$$k_i = \int_{\infty}^{-\infty} f_i(y_1, y_2, \ldots, y_{i-1}, s_i) d_{s_i}$$

and (4.23)

$$H_1(y_1) = F_1(y_1)$$

The new set of independent, standardized Gaussian random variables are then given by:

$$u = (u_1, u_2, \ldots, u_n) = \{\emptyset^{-1}[H_1(y_1)], \emptyset^{-1}[H_2(y_2/y_1)], \ldots \emptyset^{-1}[H_n(y_n/y_1, y_2, \ldots, y_n - 1)]\} \quad (4.24)$$

4.1.3.2 ADVANCED FIRST ORDER RELIABILITY METHOD ALGORITHM

In this method, point in design space is chosen to initiate the algorithm. While not necessarily the best place to start, the most common point is the vector of nominal or mean values $y^* = \{\mu_1, \mu 2 \ldots \mu_N\}$ (David Robinson, 1998).The following procedure is used for the determination of β (reliability index) in this thesis:

1. using the Rosenblatt transformation, find the vector of standardized, independent random Variables evaluated at the current design point: $u^* = u_{y_*}$

2. Calculate the Jacobian transformation matrix evaluated at the current design point:

$$J = \begin{bmatrix} \frac{\partial u_1}{\partial y_1} & \frac{\partial u_1}{\partial y_2} \cdots & \frac{\partial u_1}{\partial y_n} \\ \vdots & \frac{\partial u_2}{\partial y_2} \ddots & \vdots \\ \frac{\partial u_n}{\partial y_1} & \cdots & \frac{\partial u_n}{\partial y_n} \end{bmatrix} \quad (4.25)$$

For convenience note that:

$$\frac{\partial u_i}{\partial y_j} = \frac{\partial \emptyset^{-1}[H(y_i/y_1,\dots)]}{\partial y_j} = \frac{1}{\emptyset(u_i)} \frac{\partial H(y_i/y_1,\dots)}{\partial y_j} \quad (4.26)$$

3. Evaluate the performance function and the associated gradient at the current design point:

$$g(y^*) = g(u^*) \quad (4.27)$$

$$\nabla^* = \nabla g_{g(u^*)} = (J^{-1})^T \nabla_{g(y^*)}$$

Where the gradient is defined:

$$\nabla g(u*) = \left\{\frac{\partial g}{\partial u_1}, \frac{\partial g}{\partial u_2}, \dots \frac{\partial g}{\partial u_n}\right\}\Big|_{u^*} \quad (4.28)$$

4. Move to a new design point and calculate a new safety index:

$$u^* = \frac{1}{(\nabla^*)^T \nabla^*}[(\nabla^*)^T U^* - g(u^*)]\nabla^* \quad (reduced\ space) \quad (4.29)$$

$$\acute{y}^* = y^* + J^{-1}(\tilde{u}^* - u^*) \quad (4.30)$$

and the safety index is then:

$$|\beta| = (\tilde{u}^* u^*)^{\frac{1}{2}} \quad (4.31)$$

Or

$$\beta = \left[\frac{-\nabla*}{|\nabla*|}\right]^T \tilde{u}^* \quad (4.32)$$

5. Using the results from Step 4 as the new expansion point, repeat steps 1-4 until convergence is reached for the safety index.

6. Find the probability of failure: $Pf = \Phi(-\beta)$ (4.33)

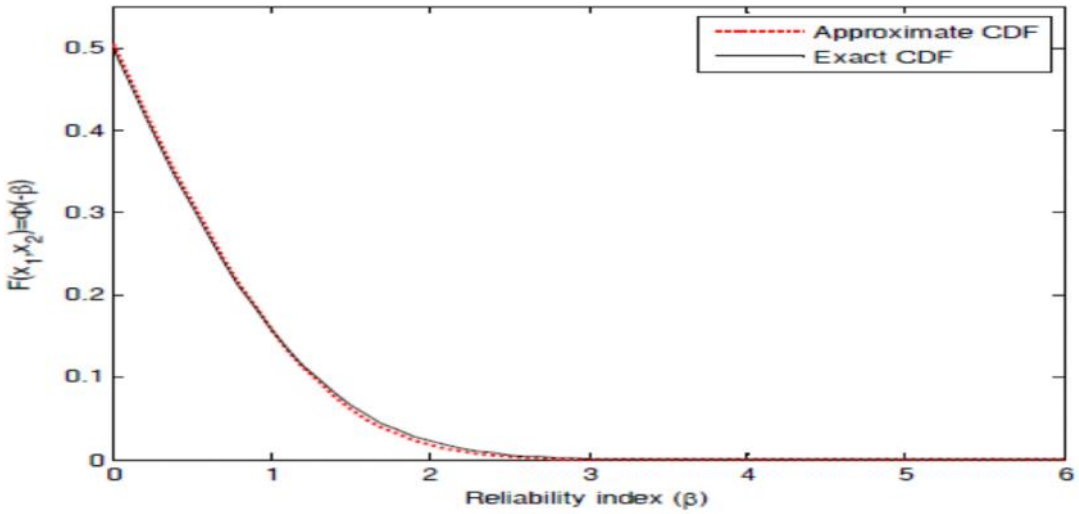

Figure 4.3 reliability index versus probability of failure.

Table4.2 Reliability index β and probability of failure P_f for log normally distributed random variables.

P_f	10^{-1}	10^{-2}	10^{-3}	10^{-4}	10^{-5}	10^{-6}	10^{-7}	10^{-8}	10^{-9}
β	1.28	2.33	3.09	3.71	4.26	4.75	5.19	5.62	5.99

4.1.3.3 RELIABILITY ANALYSIS WITH CRACK AT THE RAIL HEAD

As described before, critical crack size at the rail head is assumed to be lognormal distributed random variable with mean μ= 1mm and coefficient of variation :COV=0.3.And also initial crack size of rail is assumed to be lognormal distributed random variable with mean μ=0.2mm and coefficient of variation: COV=0.3.

The probabilistic density function of both random variables is:

$$f(y) = \frac{1}{y\xi\sqrt{2\pi}} exp\left[-\frac{1}{2}\left\{\frac{\ln(y)-\lambda}{\xi}\right\}\right] \quad (4.34)$$

Applying the Rosenblatt Transformation, vectors of standardized normal variable for lognormal distribution are:

$$u_1 = \phi^{-1}[H(y_1)] = \frac{lny1-\lambda 1}{\xi 1} \quad (4.35) \quad u_2 = \frac{\ln(y2)-\lambda-\eta(\frac{\xi 2}{\xi 1})(lny1-\lambda 1)}{\xi 2\sqrt{(1-\eta^2)}} \quad (4.36)$$

Where:

y_1 stands for initial crack size (a_o) and y_2 stands for critical crack size at rail head (a_{ch});

Using some useful relationships for the lognormal probability density function:

$$\lambda = \ln(\hat{y}) = \ln(\mu) - \frac{1}{2}\ln(1 + COV^2)$$

$\lambda_1 = \ln(0.2) - \frac{1}{2}\ln(1 + 0.3^2) = -1.653$

$\xi 1 = \sqrt{1 + COV^2} = \sqrt{1 + 0.3^2} = 0.29356$

μ_1 (mean) = $\acute{y}\sqrt{1 + COV^2}$= 0.2mm and $\bar{y}_1$ (median) = 0.192

σ_1 (standard deviation) = μ_1*COV = 0.2*0.3 =0.06

and:

$\eta 1 = \frac{\rho}{\xi 1}\left(\frac{\sigma_1}{\mu_1}\right) = \frac{0.5}{0.29356}\left(\frac{0.06}{0.2}\right) = 0.511$; assume a_o and a_{ch} are correlated positively (with coefficient of correlation $\rho = 0.5$).

$\boldsymbol{u_1} = \frac{lny_1 - \lambda_1}{\xi_1} = \frac{lny1 + 1.653}{0.29356}$**=3.4065(lny1) +5.631**

And also:

$\lambda = \ln(\hat{y}) = \ln(\mu) - \frac{1}{2}\ln(1 + COV^2)$

$\lambda_2 = \ln(1) - \frac{1}{2}\ln(1 + 0.3^2) = -0.0431$

$\xi_2 = \sqrt{1 + COV^2} = \sqrt{1 + 0.3^2} = 0.29356$

μ_2(mean) = $\acute{y}\sqrt{1 + COV^2}$= 1mm and $\bar{y}_2$ (median) = 3.4065

σ_2 (standard deviation) = μ_2*COV = 1*0.3 =0.3

and:

$\eta_2 = \frac{\rho}{\xi_2}\left(\frac{\sigma_2}{\mu_2}\right) = \frac{0.5}{0.29356}\left(\frac{0.3}{1}\right) = 0.511$; assume a_o and a_{ch} are correlated positively (with coefficient of correlation$\rho = 0.3$).

$$\boldsymbol{u_2} = \frac{\ln(y_2) - \lambda_2 - \eta_2\left(\frac{\xi_2}{\xi_1}\right)(lny_1 - \lambda_1)}{\xi_2\sqrt{(1 - \eta^2)}} = \frac{\ln(y_2) + 0.0431 - 0.511\left(\frac{0.29356}{0.23956}\right)(lny_1 + 1.653)}{0.29356\sqrt{(1 - 0.511^2)}}$$

$$= \mathbf{3.963\ln(y_2) - 2.02506\ln(y_1) - 6.72}$$

The jacobian can then be determined and evaluated at the current design point:

y* = $\{\mu_1, \mu_2\} = \{0.2, 1\}$

$$J = \begin{bmatrix} \frac{3.4065}{y1} & 0 \\ \frac{-2.02506}{y1} & \frac{3.963}{y2} \end{bmatrix} = \begin{pmatrix} 17.0325 & 0 \\ -10.1253 & 3.963 \end{pmatrix}$$

Given the original performance function:

$$g(x) = \frac{ac^{1-\frac{m}{2}} - ao^{1-\frac{m}{2}}}{\left(1-\frac{m}{2}\right)\left(1.12\sqrt{\pi}\right)^m} - \frac{\sqrt{2\Pi} * C * N * (1169)^m * \left(\frac{m}{2}\right)^{\left(\frac{m}{2}+\frac{1}{2}\right)}}{e^{\frac{m}{2}}}$$

$$= \frac{1}{3.91}\left(\frac{1}{\sqrt{a0}} - \frac{1}{\sqrt{ac}}\right) - \frac{\sqrt{2\Pi} * C * N * (1169)^m * \left(\frac{m}{2}\right)^{\left(\frac{m}{2}+\frac{1}{2}\right)}}{e^{\frac{m}{2}}}$$

g(0.2,1) = 0.168

The gradients can also be calculated and evaluated:

$$\nabla g(u*) = \left\{\frac{\partial g}{\partial u_1}, \frac{\partial g}{\partial u_2}\right\}\Big|_{u^*}$$

$$= \left\{\frac{-1}{7.82{y_1}^{3/2}}, \frac{1}{7.82{y_2}^{3/2}}\right\}^T$$

$$= \{-1.43, 0.128\}^T$$

$$\nabla^* = \nabla g_{g(u^*)} = (J^{-1})^T \nabla_{g(y^*)}$$

$$= \begin{bmatrix} 0.059 & 0 \\ 0.15 & 0.758 \end{bmatrix}^T \begin{pmatrix} -1.43 \\ 0.252 \end{pmatrix} = [-0.0844, -0.0235]$$

The new design point (in reduced space) and the associated safety index are therefore:

$$u^* = \frac{1}{(\nabla^*)^T \nabla^*}[(\nabla^*)^T U^* - g(u^*)]\nabla^*$$

$$= \frac{[(-0.0844, -0.0235)^T (0.149, 0.0844) - 0.168](-0.0844, 0.0235)}{(-0.0844, -0.0235)^T (-0.0844, -0.0235)}$$

$$= (2.1638, -1.0782)$$

$$|\beta| = (\tilde{u}^* u^*)^{\frac{1}{2}}$$

= 2.4176

and in the original design space:

$$\acute{y}^* = \{y^* + J^{-1}(\tilde{u}^* - u^*)$$

$$\acute{y}^* = (0.2,1) + \begin{pmatrix} 0.0587 & 0 \\ 0.1499 & 0.2524 \end{pmatrix}((2.1638, -1.0782) - (0.149, 0.0844)$$

$$\acute{y}^* = (0.3184, 1.0092)$$

These results are then used as input to the next iteration. Table 4.4 summarizes the input and results from iterations of the algorithm.

Since the iteration of the algorithm is very tedious for hand calculation, efficient spreadsheet algorithm is developed for the determination of exact reliability index value in this thesis as follows:

Table4.3 Summary of hohebichler-Rackwitz Iterations.

	INPUT			RESULT
ITERATION	**y***	**x***	**g(x*)**	**β**
1	(0.2,1)	(0.3184,1.0092)	0.16813	2.4176
2	(0.3184,1.0092)	(0.3716,0.9078)	0.05065	2.7778
3	(0.3716,0.9078)	(0.3610,0.8462)	0.00311	2.7891
4	(0.3610,0.8462)	(0.3581,0.8379)	-0.00036	*2.7867*
5	(0.3581,0.8379)	(0.3580,0.8376)	4.6E-07	*2.7867*
6	(0.3580,0.8376)	(0.3580,0.8375)	-7.8E-09	2.7867
7	(0.3580,0.8375)	(0.3580,0.8375)	-8.3E-11	2.7867

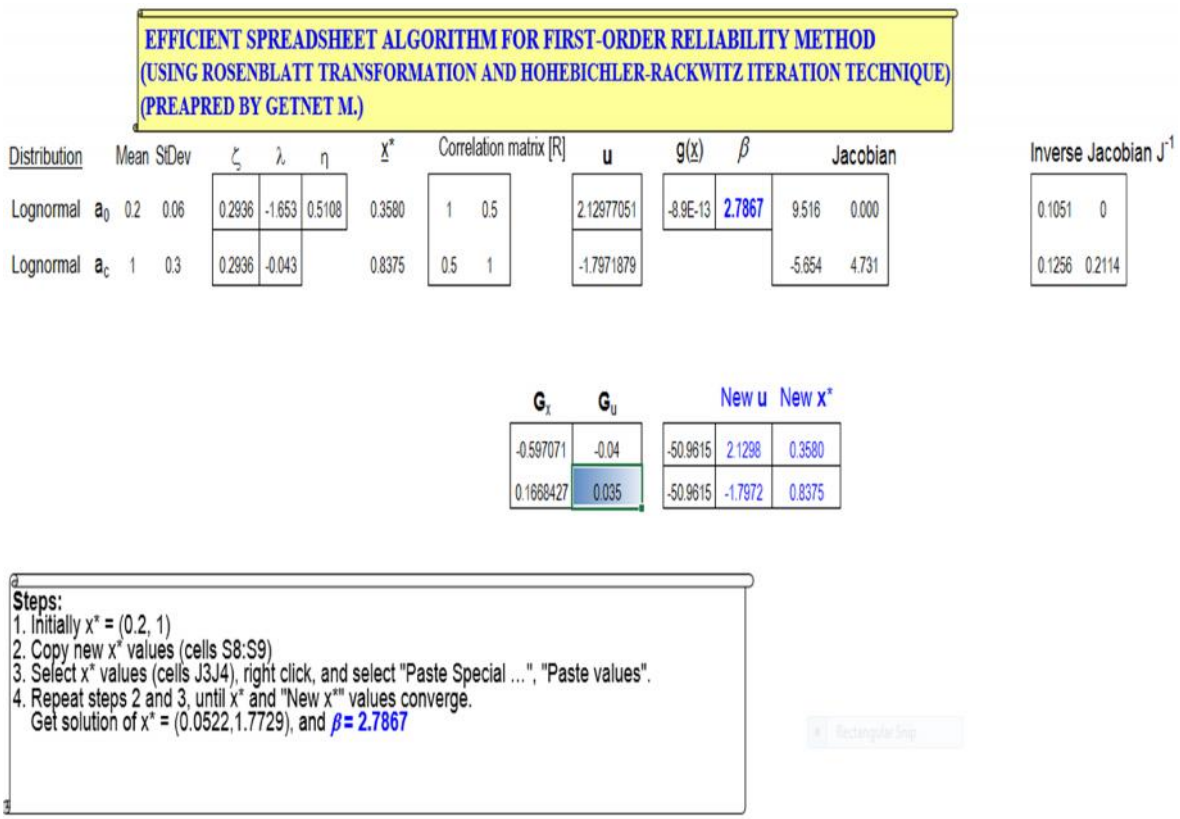

Figure 4.4 Result of hohebichler-Rackwitz Iterations of algorithm using spreadsheet program (crack at rail head).

4.1.3.4 RELIABILITY ANALYSIS OF RAIL WITH CRACK AT THE WEB

As described before, critical crack size at the rail web is assumed to be lognormal distributed random variable with mean μ= 5mm and coefficient of variation :COV=0.3.And also initial crack size of rail is assumed to be lognormal distributed random variable with mean μ=0.2mm and coefficient of variation: COV=0.3.

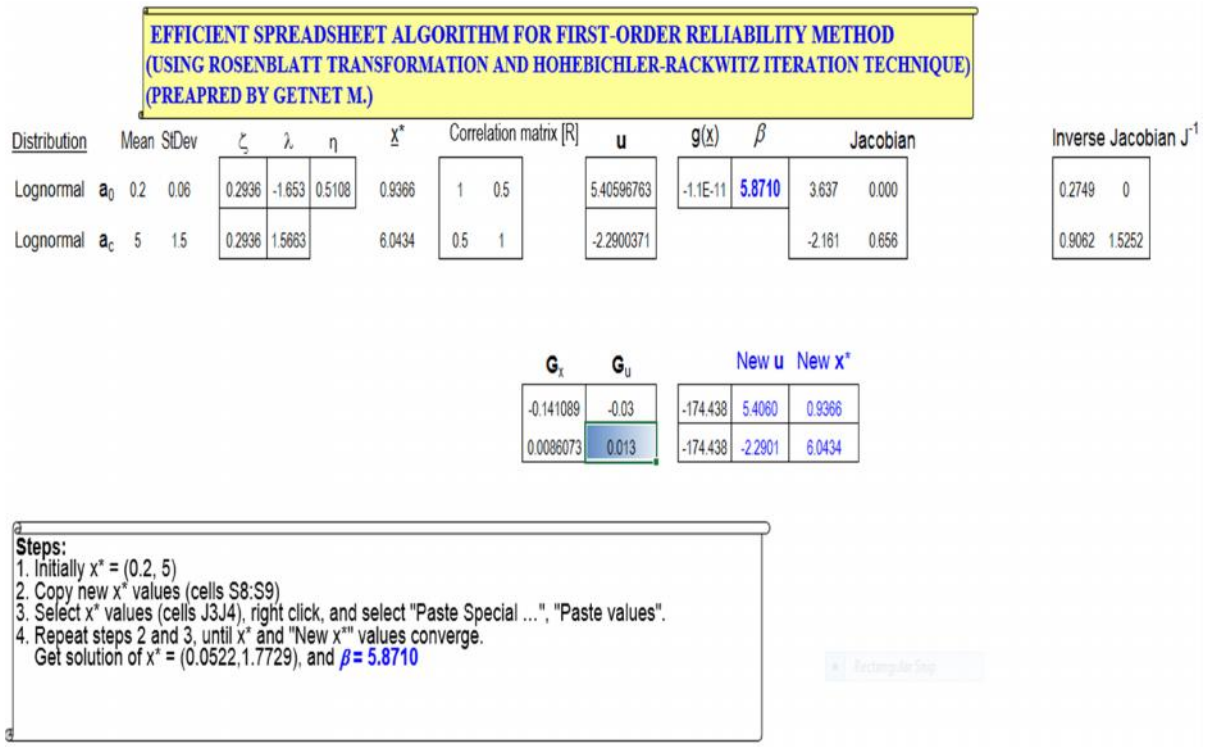

Figure 4.5 Result of hohebichler-Rackwitz Iterations of algorithm using spreadsheet program (crack at rail web).

4.1.3.5 RELIABILITY ANALYSIS WITH CRACK AT RAIL BASE

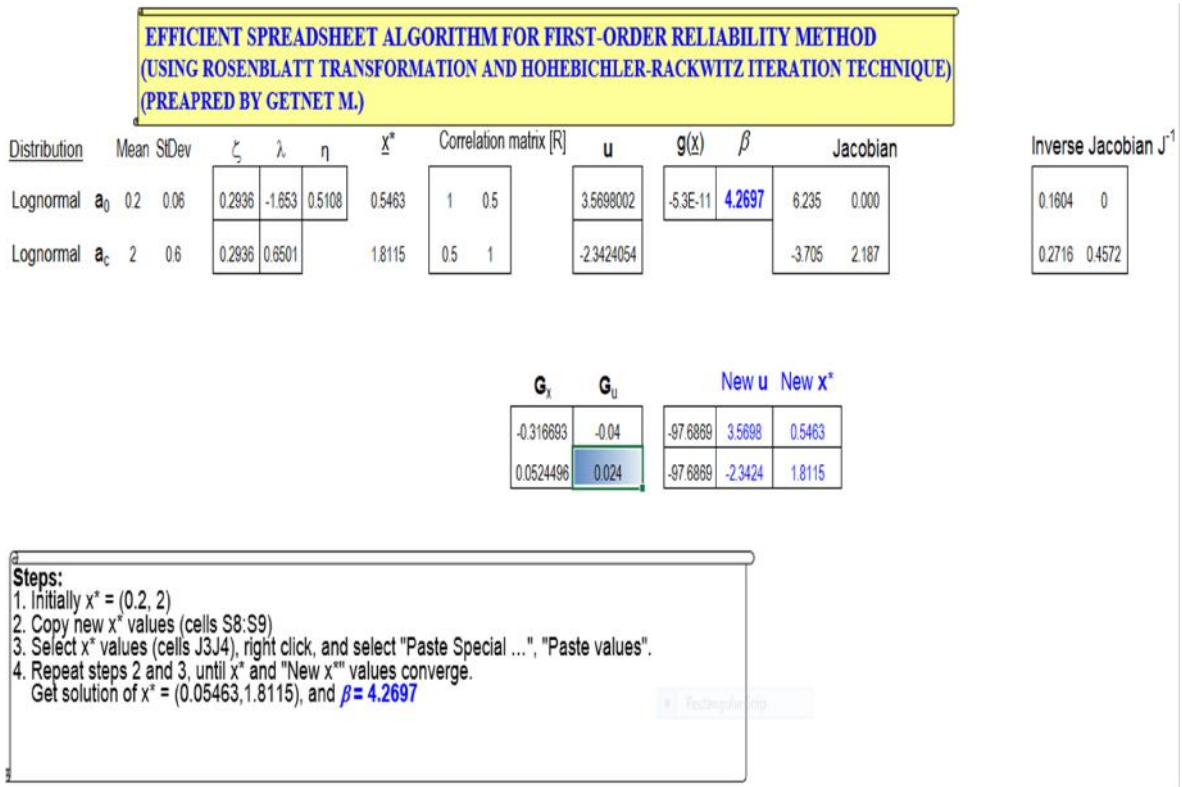

Figure 4.6 Result of hohebichler-Rackwitz Iterations of algorithm using spreadsheet program (crack at rail base.)

4.1.4 RELIABILITY EVALUATION OF RAIL DEFECTS AS SERIES SYSTEMS

The structural reliability theory can be performed both at the single failure mode and at multiple failure modes. When implementing the analysis with respect to multiple failure modes, rail defects are modeled as a series.

I	*At rail head*	*At rail web*	*At rail base*
β	2.7867	5.8710	4.2697
$\phi(-\beta)$	$4.6*10^{-3}$	$9.7*10^{-8}$	$1*10^{-5}$

Table4.4 Information concerning failure elements.

$$-\phi^{-1}(\sum_{i=1}^{m}\phi(-\beta_i)) \le \beta^s \le min_{i=1}^{m}\beta_i \quad (4.37)$$

$\beta^s \ge -\phi^{-1}(0.0046) = 2.78$

$\beta^s \le \min(2.7867, 4.2697, 5.8710) = 2.7867$

$2.78 \le \beta^s \le 2.7867$

Therefore, $\beta^s = 2.78$ and $P_f = 4.6*10^{-3}$

Finally, the reliability of rail for the provided rail type with respect to the applied stress is $R = 1-P_f = 1-0.0046 = 0.995$.

Therefore, the rail is 99.5% reliable for the applied stress and tonnage and the range of crack size for the remedial action plan of rail was decided based on this result as follows:

Table 4.5 Remedial Action plan table for rails of National railway network of Ethiopia

Types of rail defects	**Criteria (mm)**	**Remedial Action**
Vertical split head	$0<a\le0.4$ $0.4<a<1$ $1\le a$	Marking for check Maintain and Plan to replace Replace immediately
Split Web	$0\le a<2$ $2\le a<5$ $5\le a$	Marking for check Maintain and Plan to replace Replace immediately
Broken Base	$a<2$ $2\le a$	Marking for check Replace immediately

CHAPTER 5

5.1 EVENT TREE ANALYSIS

5.1.1 EVENT TREE MODEL

An event tree provides a systematic means of structuring relevant events related to an uncertain environment. It represents the direct relationship and provides a clear and precise definition among all possible events.

The event tree is used as a model to represent all possible events associated with inspection/repair actions, which are detection/repair, detection/no-repair, and no-detection in this thesis. In order to make up an event tree, a decision of above three options needs to be made after every inspection. After every new inspection, past remedial actions affect new remedial actions. Hence, if no crack is detected or the crack size can be tolerated, no-repair action would be taken. If repair work is assumed to be performed only when a crack is detected and the crack size exceeds a critical repair level, a_r, the total number of branches in an event tree is 3^N, where N is the number of inspections during the service life. Fig.5.1 shows the basic component, which consists of chance nodes and folks, of the event tree. It represents the first mutually exclusive set of chance events. At the ermines of each branch, track engineers form a new chance nodes and folks. Each probability in these chance nodes is derived from the probability of detection (POD) and the probability of repair (POR) discussed later.

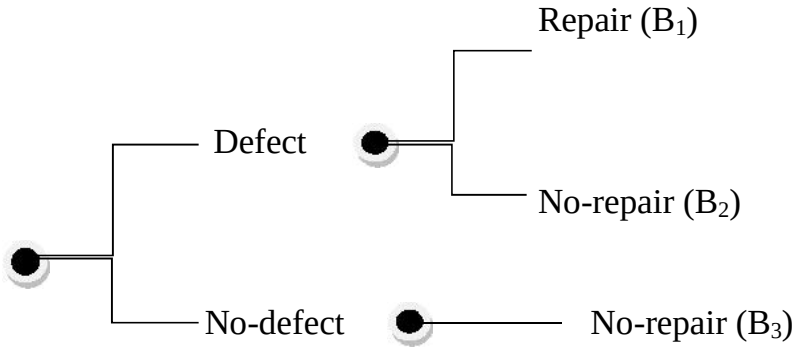

Figure 5.1 Basic components of Event Tree

The probability of the consequences, such as B_1, B_2 and B_3 shown in figure 5.1 can be calculated as follows:

$$P_r(B_1) = P_{b1} = P_{det} * P_{rep/det}$$

$$P_r(B_2) = P_{b2} = P_{det} * (1 - P_{rep/det}) \quad (5.1)$$

$$Pr(B3) = P_{b3} = (1 - P_{det}) * 1.0$$

Where, P_{det} is the probability of detecting defects; $P_{rep/det}$ is the probability of repairing defects given a detection of defects. Since the consequence of both B_2 and B_3 are the same actions, which is no repair, Figure 5.1 can be simplified as shown in figure 5.2.

The probabilities of repair and no repair shown in figure 5.2 are defined as:

P_r (repair) = $P_{det.}$*$P_{rep/det}$ (5.2)

Pr (no-repair) = P_{det}*(1-$P_{rep/det}$) + (1-P_{det})

For instance, assume that two inspections will be done during the service life. Figure 5.3 shows its event tree. Let R_1^+ indicate that a repair is done at time t_1, and let R_1^- exhibits that a repair is not done at time t_1.Similarely, an action must be taken again whether or not to repair the structure. R_2^+ displays repair and R_2^- indicates no-repair in the second action. Let P_{bi} be the probability of taking bi branch. Hence,

$P_{b1}=P_r (R_1^+)$

$P_{b2}=P_r (R_1^-)$

$P_{b3}=P_r (R_1^+ n R_2^+)$ (5.3)

$P_{b4}=P_r (R_1^+ n R_2^{-)}$

$P_{b5}=P_r (R_1^- n R_2^+)$

$P_{b6}=P_r (R_1^- n R_2^-)$

The reliability of the structure must be evaluated at time t_1, t_2 and calculate the reliability index of the structure after corresponding to the inspections.

In addition, the weighted effect of each repair of branch must be considered. Above procedures can be generalized into n time's inspections. For each branch, b: the reliability index of a rail at a time point given is multiplied by the probability of the branch, P_{bi}. The expected reliability index is equal to the sum of overall branches and defined as:

$$E[\beta(N)] = \emptyset^{-1}(\sum_{i=1}^{2^n} \emptyset(-\beta i(N)) * Pbi \quad (5.4)$$

Here, $\emptyset^{-1}(.)$ is the inverse function of a cumulative standard normal variate; n is the number of lifetime inspections.

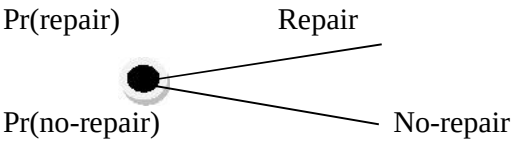

Figure 5.2 simplified basic components for ET

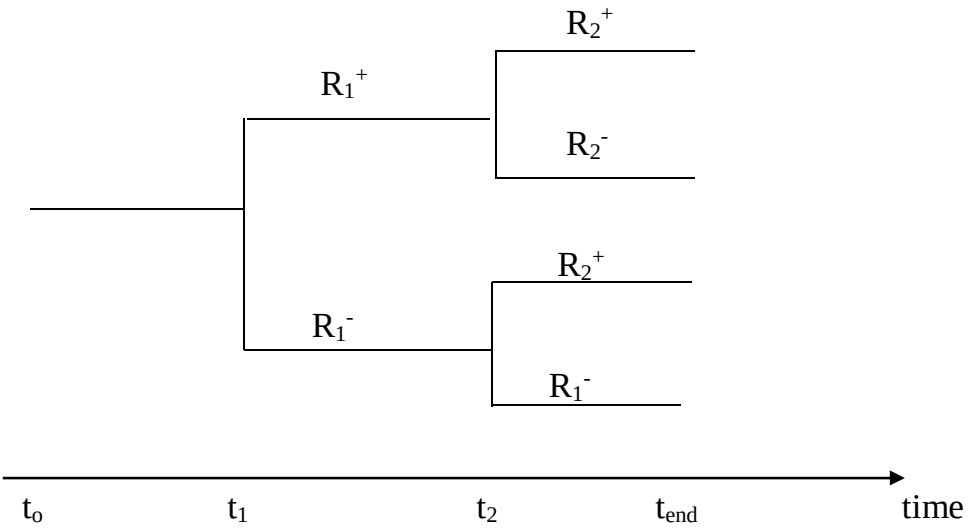

Figure 5.3Event tree for two inspections during the service life.

5.1.2 UNCERTAINITY OF DETECTION

Even if there are many rail inspection methods are available, Nondestructive testing (NDT) plays an essential role in a condition assessment in-service and repair decision-making process. Nondestructive testing (NDT) is one of rail inspection tool or technology to identify rail defects before they grow large enough to cause a broken rail. Non-destructive Testing (NDT) reliability may be defined as 'the probability of detecting a crack in a given size group under the inspection conditions and procedures specified. However, no inspection is perfect NDT outputs depend on many uncertain factors such as conditions of structures, environmental conditions during inspection, and operator skills.

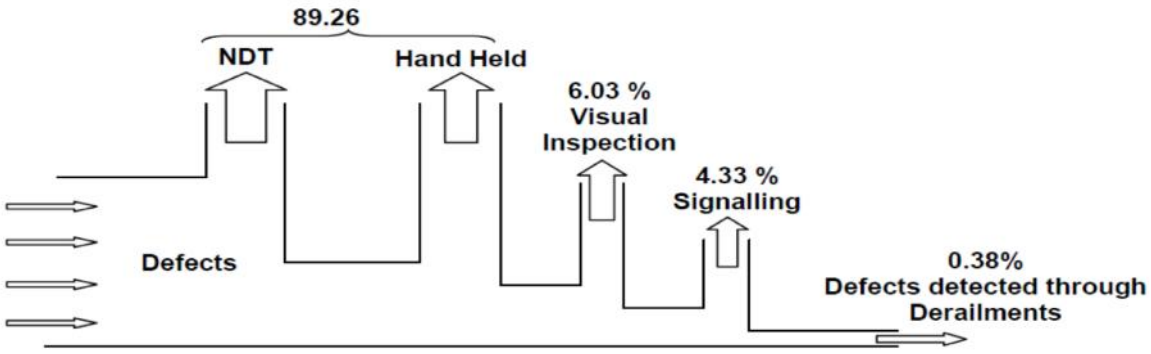

Figure5.4: Percentage of potential rail breaks detected from different inspection tools
[Adapted from Larsson, et al, 2005]

Visual Inspection *Signaling*

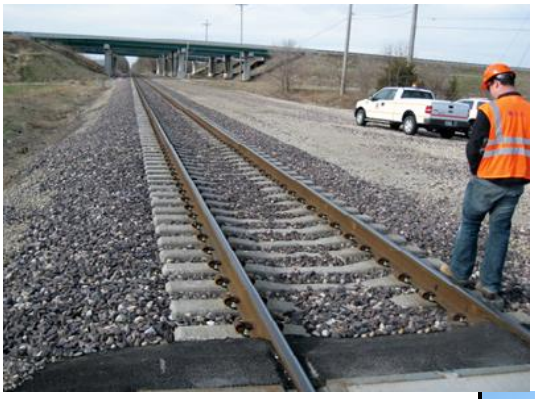

Non Destructive Testing Cars *Hand-held NDT*

Figure 5.5 Rail Inspection tools (Technology).

Neglecting these uncertainties not only results in misinformed decision-making but also leads to unnecessary remedial actions. A rational approach to evaluate the role of these sources of uncertainties is a probabilistic method.

Hence, evaluations of capability of nondestructive testing (NDT) expressed in terms of probability is essential to the event tree analysis.

The capability of an inspection technique can be defined in terms of two criteria's, detect ability and accuracy. The ability of detecting cracks, termed detect ability, depends of sizes of cracks and the resolution to the capability of a particular nondestructive testing technique adopted. It is known that there is always a critical crack size for a given nondestructive testing technique below which a crack cannot be detected. As for accuracy, errors in defects refer to measurement noises with respect to true sizes when defects are detected. The relationship between the actual and measured crack size also depends on types of cracks and attributes of a given Nondestructive testing technique. The capability of nondestructive testing is termed probability of detection (POD) in this thesis.

A probability of detection (POD) is generally expressed interms of cumulative density function (CDF). It is expected that as a crack size increases, its detectability also increases. It is assumed that detectability can be described as the mean of cumulative density function (CDF) and accuracy can be expressed as the coefficient of variation (COV) of CDF in the model.

Zheng and Ellingwood (1998) propose the Probability of detection (POD) can be modeled to an exponential distribution. Zhao and Haldar (1994) presume that POD of a crack in metal materials follows a lognormal distribution. In this thesis, the event tree analysis is performed on the assumption that POD is log normally distributed with the mean of 1mm and the COV of 0.3.

Various analyses of data from reliability experiments on NDT methods indicated that the *PoD (a)* function could be modeled closely by either the cumulative 'log-normal' distribution or the 'log-logistic' (or 'log-odds') distribution.

For no/miss data a number of different statistical distributions were originally considered for the best fit. It was found that the log-logistic distribution was the most acceptable and the *PoD (a)* function can be written as:

$$POD(a) = \frac{e^{\frac{\pi}{\sqrt{3}}\left(\frac{lna-m}{\sigma}\right)}}{1+e^{\frac{\pi}{\sqrt{3}}\left(\frac{lna-m}{\sigma}\right)}} \quad (5.5)$$

Where a is the crack size and m and σ are the median and standard deviation respectively.

For any inspection, if the actual crack size at the time of inspection is smaller than a detectable crack size when a given NDT technique, the defect is not expected to be detected (George A Georgiou, 2006). The event which is no crack is detected during the inspection when the rail has been subjected to N stress cycles, can be expressed as:

$a_d \geq a\ (N)$ (5.6)

Where, a_d is the capability at the time of inspection, a (N) is the estimated crack size at N stress cycle. The limit state function of event as no-detection during inspection can be defined as:

$$H(x) = \Psi\ (a_d - a_o) - \Psi\ (a_N - a_o) \quad (5.7)$$

$$= \Psi\ (a_d - a_o) - CS^m N$$

Where, Ψ (.) is a fatigue damage function, s^m is the mean-stress range effect defined in section 4.2 ,N is a number of stress cycle to the corresponding to the time of inspection, P_{det} can be obtained from solving this LSF based on the FORM.

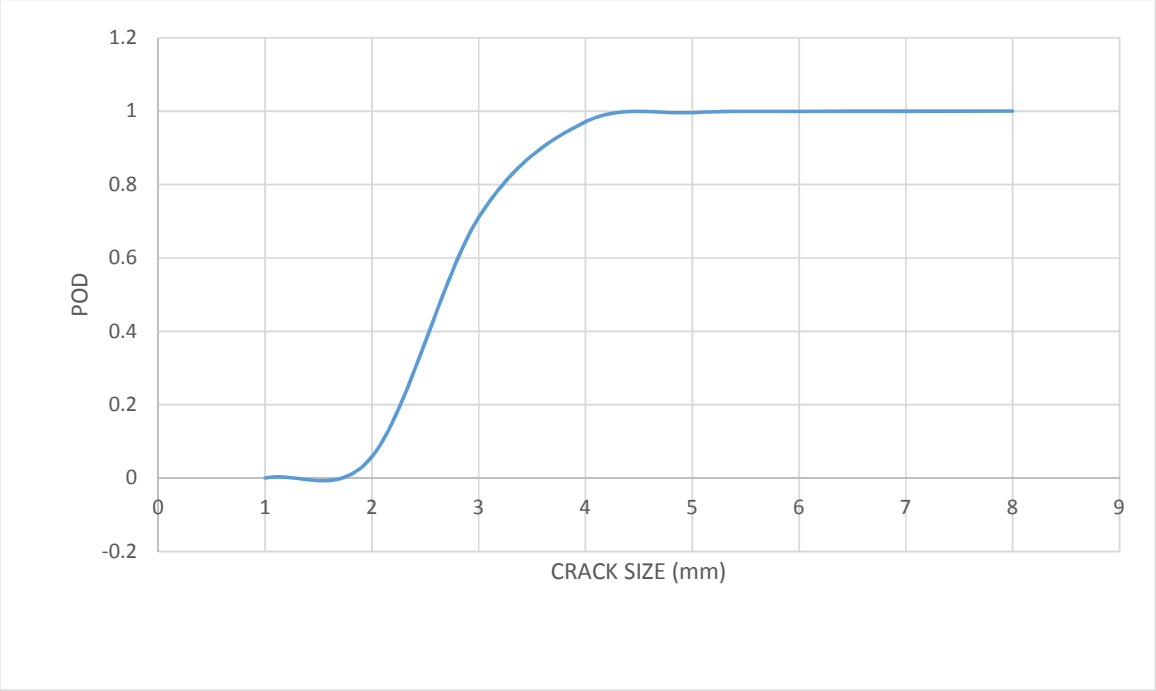

Figure 5.6 Capability of inspection.

5.1.3 UNCERTAINITY OF REPAIR

Generally speaking, railroad companies have two options to repair damaged rails, when they detect rail defects in a conventional joint rail truck. One is to replace the damaged rail; the other is to apply a joint bar. In this thesis, it is assumed that railroad companies have an only option of replacement for the simplicity of analysis. In other words, either decision of replacement or non-replacement will be made after every inspection as long as defects are detected.

In this thesis, rail remedial action is shown in table 3.7.This plan gives two opportunities regarding replacement for the track engineers. One is planning replacement policy and the other is immediate replacement policy corresponding to the critical repair level. The decision about these options can be interpreted in a probabilistic form, probability of repair (POR) that implies track engineers' actual response after inspections. It is assumed that the critical repair level, a_r follows a uniform distribution, where the maximum value of the POF is the size on which track engineers must replace the damaged rail and the maximum value of the PDF is the size on which the engineers will take some management actions. Fig.5.7 shows the CDF of a_r. An associated LSF, i(x) similar to the one employed for reliability analysis described earlier can be defined as:

$$i(x) = a_r - a(N) \quad (5.8)$$

Where, a_r is the critical repair level, a(N) is the estimated crack size at N stress cycle. The $P_{rep/det}$ can be obtained by using FORM with respect to the above LSF.

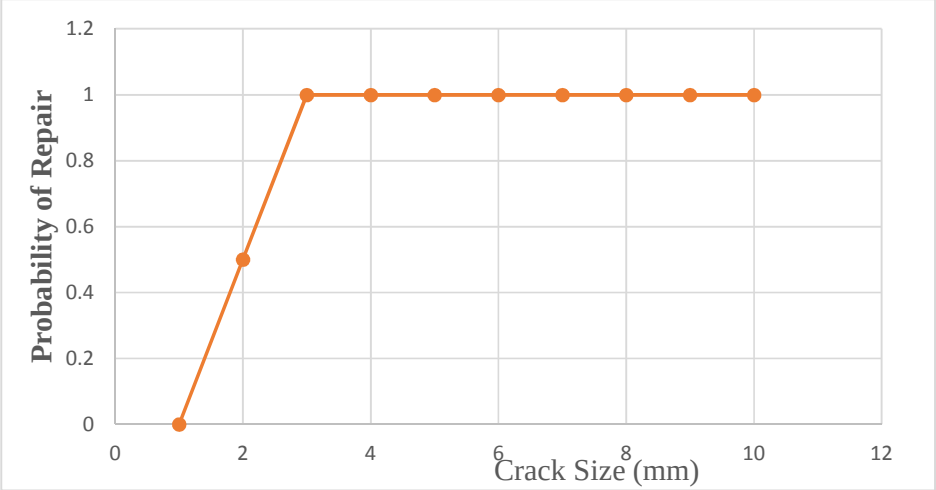

Figure 5.7Probability of repair

Therefore,

$P_r(\text{repair}) = P_{det.} * P_{rep/det}$

$P_r(\text{no-repair}) = P_{det} * (1-P_{rep/det}) + (1-P_{det})$

Location of crack for Rail	$P_{r(repair)}$	$P_{r(no-repair)}$
Head	5%	95%
Web	100%	0%
Base	50%	50%

Table 5.1 probability of failure and repair of rail.

CHAPTER 6

6.1 LIFE CYCLE COST ESTIMATION

6.1.1 LIFE CYCLE COST MODEL

A life cycle cost estimation provides an economical evaluation of all current and future costs associated with investment alternatives. It is a valuable economic analytical technique for evaluating projects which require long-term capital and maintenance expenditure over the analytical period of infrastructures, such as bridges, dams, and railroads.

It is important to note that the same service life of each alternative must be used to yield valid results when implementing life cycle cost estimation.DOT (2002) refers to this analytical service life, called analysis period as follows:

"Life cycle cost estimation uses a common period of time to assess cost difference between alternatives so that the results can be fairly compared. This time period is termed the analysis period. Allowing the analysis period to vary among alternatives would result in the comparison of alternatives with different total cost, which is not appropriate under life cycle cost estimation."

Life cycle cost estimation enables comparison of the costs of alternatives regarding inspection interval. The idea behind cost estimation is that decision related to inspection/repair intervention should consider all the costs imposed to the rail road companies incurred during the period over which the alternatives being compared. The costs regarding the rail maintenance should consists of inspection and repair costs as well as costs due to the risk of rail broken accidents using an economical technique known as discounting, these costs are converted into the present value in the life cycle cost estimation.

Inspection costs are those involved in regular inspection of rails. For a strategy involving n life time inspections, the total inspection cost, C_{INS} is expressed as:

$$C_{INS} = \sum_{i=1}^{n} \frac{C_{ins}}{(1+r)^{ti}} \tag{6.1}$$

Where, C_{ins} is each inspection cost based on the inspection technique, t_i is the time of inspection at I, and r is the discount rate.

Repair costs are those for the main structural work and include all the costs of structural assessment usually associated with repair decision making. Rail repair costs, C_{rep} can be divided into:

$$C_{rep} = C_{repa} + C_{repr} \tag{6.2}$$

Where, C_{repa} is the structural assessment costs including all the costs, such as contract cost with repair costs and reinvestigation costs to identify the precise location, and C_{repr} is the structural repair costs include all the costs of the labor, material, equipment, administration to ensure safety under construction, and quality control. The ET is used to either investigate all possible events related to repair or no-repair actions.

It is recognized that a decision to either repair or no-repair needs to be made after every inspection to establish the ET. A repair decision made after every new inspection is influenced by decisions made in the past decision. Therefore, total repair cost should be expressed as a probabilistic expected value. The costs of repair associated with each branch, b_i are:

$$C_{rep,bi} = \sum_{j=1}^{n} \frac{C_{rep}}{(1+r)^{ti}} \tag{6.3}$$

Where, $C_{rep,\,bi}$ is the costs of repair associated with the branch, b_i and t_j is the time of repair. Therefore, the total expected repair cost, C_{REP} is expressed as:

$$C_{REP} = \sum_{l=1}^{2^n} C_{rep,bi} * Pbi \tag{6.4}$$

Where, P_{bi} is the probability of taken branch, b_i.

A failure cost, derived from the risk of rail broken accident, includes all the costs resulting from a broken rail. The total failure cost is defined as a product of the cost regarding failure and lifetime probability of failure calculated by FORM.

The lifetime probability of failure is defined as:

$$P_{f,life,bi} = \max(P_{f,ti,bi}) \tag{6.5}$$

$$P_{f,life} = \sum_{i=1}^{2^n} P_{f,life,bi} * Pbi \tag{6.6}$$

Where, $P_{f,\,life,\,bi}$ is the probability of failure at branch, b_i; $P_{f,\,life}$ is the lifetime probability of failure, and n is the number of inspection during the service life.

Therefore, the total expected failure cost is expressed as:

$$C_{FAIL} = C_f * P_{f,life} \tag{6.7}$$

Where, C_{FAIL} is the total expected repair cost and C_f is failure cost.

The LCC is formulated by summing all the expected costs and expressed as:

$$LCC = C_{INS} + C_{REP} + C_{FAIL} \tag{6.8}$$

6.1.2 DETERMINATION OF ECONOMICALINSPECTION INTERVAL

As described previously, the ET analysis can provide systematically all possible events regarding rail management. However, since the number of branches in the event tree exponentially increases as the number of rail inspections increases, it is laborious to analyze the event tree as the number of inspections is more than six or seven. For instance, when the number of rail inspections is 10, the number of branches in the ET becomes $3^{10} = 59{,}049$ and an ET has 3^{15}=14,348,907 branches corresponding to 15 inspections. Therefore, some approximation methods as well as other models are needed in order to assess the each expected cost instead of the ET analysis.

6.1.2.1 NUMBER OF BROKEN RAILS PER YEAR

The U.S. Department of Transportation (U.S. DOT) Volpe Transportation Systems Center (hereinafter referred to as the "Volpe Center") developed an engineering model to estimate the number of broken rails between two successive inspections given inspection interval and rail age (Orringer et al. 1988; Orringer 1990; Jeong and Gordon 2009). The model was further enhanced and implemented by ZETA-TECH Associates, Inc. (Palese and Wright 2000). The model recommends the frequency of rail defect inspections, and its use on at least one railroad is reported to have helped them reduce broken-rail-caused derailments (Zarembski and Palese 2005).

Rail defect inspection should be scheduled such that the occurrence of broken rails is minimized. Inspection intervals are generally specified in terms of the accumulated traffic carried by a rail segment, measured in million gross tons (MGT) (Orringer et al. 1988; Orringer 1990; Zarembski and Palese 2005). The following equation presents a general model to estimate the total number of rail breaks per year between two successive rail defect inspections assuming that no complementary broken rail prevention technique (e.g., rail grinding or rail lubrication) is used.

$$MINIMIZE\left[\left(\sum_{i=2}^{k} S_{(i-1,i)}\right) + S_{(k,end)}\right] \tag{6.9}$$

Where,

$$S_{(i-1,i)} = R\,\frac{\frac{\alpha\left(0.5N_{i-1}+0.5N_i\right)^{\alpha-1}}{\beta^{\alpha}} e^{-\left[\frac{(0.5Ni-1+0.5Ni)}{\beta}\right]^{\alpha}}}{1+\frac{1}{\lambda(x_i-\theta)}}\,x_i \tag{6.10}$$

$$S_{(k,end)} = R\,\frac{\frac{\alpha\left(0.5N_k+0.5(N_o+T)\right)^{\alpha-1}}{\beta^{\alpha}} e^{-\left[\frac{(0.5Nk+0.5(No+T)}{\beta}\right]^{\alpha}}}{1+\frac{1}{\lambda\left(T-\sum_{i=1}^{k} x_i-\theta\right)}}\left(T-\sum_{I=1}^{K} x_i\right) \tag{6.11}$$

$$\sum_{i=2}^{k} X_i \le T$$

Where,

S (i-1, i) = number of broken rails per track-mile between the (i-1) th and ith inspection

S (K, end) = number of broken rails between the Kth inspection and the end of year

R = rail segments per track-mile = 61

X_i = Inspection interval (MGT) between the (i-1) th and ith inspection

T = annual traffic density (MGT) = 22.67MGT

α = Weibull shape factor, 2.94 (Davis et al. 1987), interpolating from table 6.1.

β = Weibull scale factor, 1396 (Davis et al. 1987), interpolating from table 6.1.

λ = slope of the number of rail breaks per detected rail defect (S/D) vs. inspection interval curve, 0.0108 (Orringer, 1990), interpolating from table 6.1.

θ = minimum rail defect inspection interval is assumed to be 1MGT.

N_i = rail age (cumulative tonnage on the rail) at the ith inspection, $N_i = N_{i-1} + X_i$

The minimum inspection interval is determined based on the process of rail defect formation and growth and is also dependent on inspection vehicle allocation and logistics. In this paper, the value of θ is assumed as 1. And also, the maximum tonnage between two inspections is taken as the annual traffic density. So there is at least one inspection per year. This assumption was made to illustrate the methodology but it can be adapted to account for other inspection intervals. And also the sum of inspection intervals should not exceed annual traffic density.

The parameters in the broken rail risk model (α, β, λ, θ) are related to the mechanism of rail defect formation, accuracy of rail defect inspection, and track characteristics (Orringer 1990). The following ranges were established based on published literatures:

Table 6.1 the effect of the input parameters on the expected number of broken rails within an inspection interval (Orringer 1990).

Variables	Minimum	Base	Maximum
Initial rail age (N) (MGT)	0	300	1000
Weibull shape factor (α)	2.9	3.1	5.5
Weibull scale factor (β)	1,200	2,150	3,000
Slope of the S/D v. inspection interval curve (λ)	0.010	0.014	0.021

Let as assume there are four rail inspections per year. The following figure illustrates the rail defect inspection frequencies on the hypothetical route by assuming constant inspection interval:

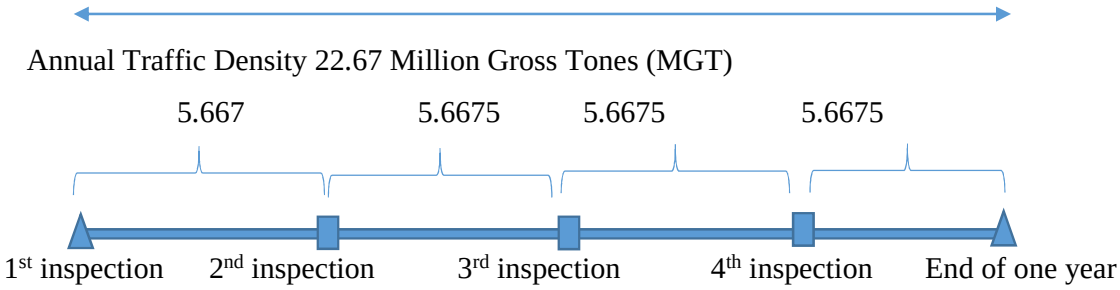

Figure 6.1 Rail defect inspection interval division per year.

$$s_{(1,2)} = 61 * \frac{\frac{2.94(0.5*61.88+0.5(61.88+5.6675))^{2.94-1}}{1396^{2.94}} e^{-\left[\frac{(0.5*61.88+0.5*(61.88+5.6675))}{1396}\right]^{2.94}}}{1+\frac{1}{0.0108(5.667-1)}} * 5.667 = 9.026*10^{-5}$$

$$s_{(2,3)} = 61 * \frac{\frac{2.94(0.5*67.55+0.5(67.55+5.6675))^{2.94-1}}{1396^{2.94}} e^{-\left[\frac{(0.5*67.55+0.5(67.55+5.6675)}{1778}\right]^{2.94}}}{1+\frac{1}{0.0108(5.6675-1)}} * 5.667 = 1.062*10^{-4}$$

$$s_{(3,4)} = 61 * \frac{\frac{2.94(0.5*73.22+0.5(73.22+5.6675))^{2.94-1}}{1396^{2.94}} e^{-\left[\frac{(0.5*73.22+0.5(73.22+5.6675)}{1396}\right]^{2.94}}}{1+\frac{1}{0.0108(5.6675-1)}} * 5.667 = 1.235*10^{-4}$$

$$s_{(4,end)} = 61 * \frac{\frac{2.94(0.5*78.89+0.5(61.88+22.67))^{2.94-1}}{1396^{2.94}} e^{-\left[\frac{(0.5*78.89+0.5(61.88+22.67)}{1396}\right]^{2.94}}}{1+\frac{1}{0.0108(22.67-3*5.6675-1)}} (22.67 - 3 * 5.6675) = 1.42*10^{-4}$$

S_{total} = 4.62*10^{-4}

Table 6.2 Annual numbers of broken rails per track mile for different inspection frequencies

Annual Number of rail defect inspections	Annual Number of broken rails per track mile (10^{-4})
1	18.1
2	9.7
3	6.4
4	4.6
5	3.5
6	2.8

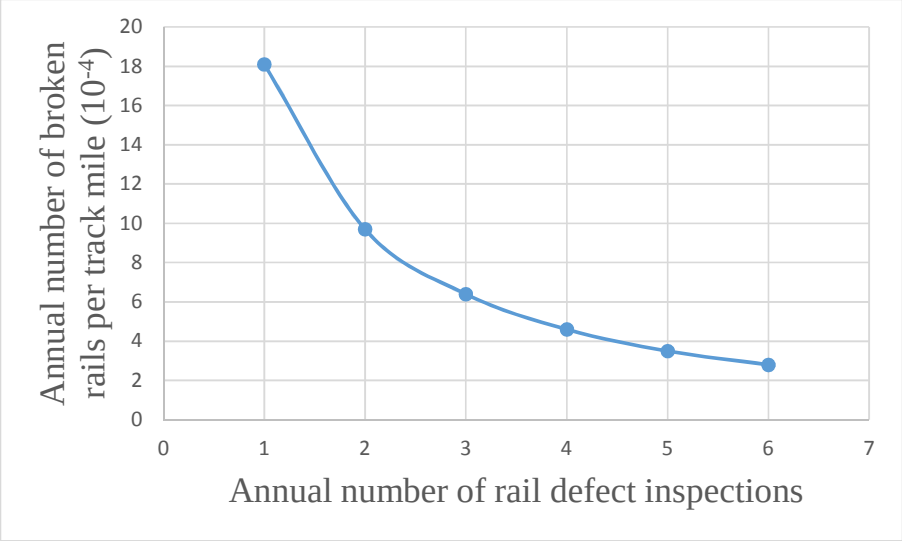

Figure 6.2: Relationship between number of broken rails and annual rail defect inspection frequency (initial rail age is 61.88 MGT and annual traffic density is 22.67 MGT)

6.1.2.2 RAIL DEFECT INSPECTION COST MODEL (INSPEC)

The rail defect inspection cost model (INSPEC) developed by the Association of American Railroads (AAR) in the late 1980s can predicts annual costs related to rail defect inspection, including derailment damage costs and costs for repairing a detected rail defects or broken rails (Davis et al. 1987). However, the data used in the model needed to be updated, in part due to changes in traffic volume, axle load, improved rail steel and better rail maintenance practices for the future. In the improved model, train delay costs (related to transportation efficiency) due to derailments or repairing rail defects were included and this model is adapted in this thesis for the national railway network of Ethiopia.

6.1.2.3 COST OF REPAIRING DETECTED RAIL DEFECTS AND BROKEN RAILS

There are three categories of costs associated with rail defect inspection and the corresponding remedial actions regarding a detected defect or broken rail: 1) rail defect inspection cost, 2) repair cost for a detected defect or a broken rail, and 3) train delay cost due to repairing a detected defect or a broken rail. Properly scheduled hi-rail defect inspection should not disrupt train operations because the hi-rail vehicle can get off the track to allow train traffic to pass. Thus the potential train delay due to inspections is generally minimal and therefore was not included in this analysis.

6.1.2.4 RAIL DEFECT INSPECTION COST

The following equation is used to estimate rail defect inspection cost:

$$C_{insp} = \frac{KL}{V} Chr \qquad (6.12)$$

Where:

C_{insp} = rail defect inspection cost ($)

L = track length (mile's)

V = average hi-rail vehicle speed (mph)

K = Annual rail defect inspection frequencies

C_{hr} = inspection cost per hour ($/hour)

Different researches from a major railroad industries indicated that the speed of inspection (V) is generally between 15 to 20 mph although the speed may be lower based on the rail condition and meteorological conditions. The average inspection cost (C_{hr}) is assumed as approximately $300 per hour per vehicle.

In this thesis, a one mile section of the truck is used for the life cycle cost estimation. Let the annual rail inspection frequency is one, the rail inspection cost is as follows:

$$C_{insp} = \frac{1mile}{20mph} * 300\$ \quad = \quad 15\$$$

Table 6.3 Rail inspection cost for different inspection frequencies

Annual Rail Inspection Frequency	1	2	3	4	5	6
Rail Inspection Cost ($)	15	30	45	60	75	90

6.1.2.5 COST FOR REPAIRING A DETECTED RAIL DEFECT

Association of American Railroads (AAR) developed the following model to estimate the cost for repairing detected defects and broken rails (Wells and Gudiness 1981) that were used with updated rail cost information. The detected defect or repair broken rail model is:

$$DDC = \left[\frac{W_{replace} * L_{replace}(P_{new} - 0.95P_{old})}{2000} + C_{drepair}\right](1 - t) \qquad (6.13)$$

Where:

DDC = total cost for repairing a detected rail defect ($)

$W_{replace}$ = weight of replacement rail, in pounds per yard = 25

$L_{replace}$ = length of replacement rail, in yards = 22.73

P_{new} = price of new rail, in dollars per ton = 1470$/ton (Source: ERC).

P_{old} = price of scrap rail, in dollars per ton = 735$/ton. (Assume 50% discount).

$C_{drepair}$ = expenses for labor, materials, equipment ($) = 15,000

t = tax rate =0.35

Based on the above model, the total cost for repairing a detected rail defect is calculated as follows:

$$= \left[\frac{25 * 22.73(1470 - 0.95 * 735)}{2000} + 15{,}000\right](1 - 0.35)$$

$$= \$\mathbf{9893}$$

The actual cost will vary depending on infrastructure and operational circumstances. Some undetected rail defects may grow large enough to cause a broken rail; however, most such breaks are identified by track inspection before an accident occurs (Dick et al 2003; Schaffer 2008).

The AAR model for repairing broken rails is similar to the one for detected rail defects (Wells and Gudiness 1981) is formulated as follows:

$$SDC = \left[\frac{W_{replace} * L_{replace}(P_{new} - 0.95P_{old})}{2000} + C_{srepair}\right](1 - t) \quad (6.14)$$

Where:

SDC = total cost for repairing a broken rail ($)

$C_{Srepair}$ = expenses for labor, materials, equipment, and termite welds for continuously welded rail ($) =20,000 and other variables as defined above.

Based on the above model, the total cost for repairing a broken rail defect can be approximated as follows:

$$SDC = \left[\frac{25 * 22.73(1470 - 0.95 * 735)}{2000} + 20{,}000\right](1 - 0.35)$$

$$= \$\mathbf{13,143}$$

6.1.2.6 TRAIN DELAY COST FOR REPAIRING A DETECTED RAIL DEFECT

The time required to repair a rail defect is dependent on its size, type, location and several other factors. Repair activities may not always delay trains because railroad dispatchers will grant maintenance-of-way personnel access to the track during intervals between trains. These uncertainties are not quantified in this paper due to data constraints, but may be accounted for in future work.

$$C_{DDT} = C_O \alpha_D exp(\beta_D x) \quad (6.15)$$

Where:

C_{DDT} = train delay cost due to fixing a detected rail defect ($)

C_0 = train delay cost per hour ($)

α_D = 1.503 (Schlake et al. 2011)

β_D = 0.0811 (Schlake et al. 2011)

x = number of trains per day (T/0.006312/365) (Schaffer 2008).

= 22.67/0.006312/365 =10.

T= annual traffic density in MGT) =22.67

Train delay cost for various traffic volume based on Dispatch simulation software for some United States railroad survey is adopted for national railway network of Ethiopia and shall be revised for the future based on real percentage ton-miles as well as exact traffic volume variation.

Table 6.4 Train delay cost based on Dispatch simulation software for various traffic volumes (Schlake et al. 2011).

	Single Track	Double Track
Average annual MGT	Delay cost ($)	Delay cost ($)
<40	460	350
40-60	590	350
60-100	1,000	360
>100	2,170	440

So, the train delay cost is taken as **$350** for National railway network of Ethiopia for double track. Based on the above model, train delay cost due to fixing a detected rail defect can be approximated as follows:

C_{DDT}= 350*1.503*exp (0.0811*10) =**$1184**

6.1.2.7 TRAIN DELAY DUE TO REPAIRING A BROKEN RAIL

$$C_{SDT} = C_O \alpha_S exp(\beta_S x) \quad (6.16)$$

Where:

C_{SDT} = train delay cost due to fixing a broken rail ($)

α_S = 3.559 (Schlake et al. 2011)

β_S = 0.0805 (Schlake et al. 2011)

Other variables are as defined above.

Therefore, C_{SDT}=350*3.559*exp (0.0805*10) = **$2787**

6.1.2.8 TRAIN DELAY COST DUE TO DERAILMENTS

In addition to infrastructure and equipment damage, a train derailment may result in train delay cost. We assumed that 24 hours are required to return the track to service after a derailment, although it may take longer time depending on the circumstances and location of the accident. Schaffer (2008) developed the following equation to estimate train delay time due to a derailment:

$$C_{DA} = Vx + \sum_{n=1}^{m}(V - nt)X \quad (6.17)$$

Where,

C_{DA} = *total train delay cost for multiple trains ($)*

V = *total delay time for service interruption (hours)*

The total delay time for service interruption is adopted from researcher's result based on the traffic volume and it shall be updated for the future.

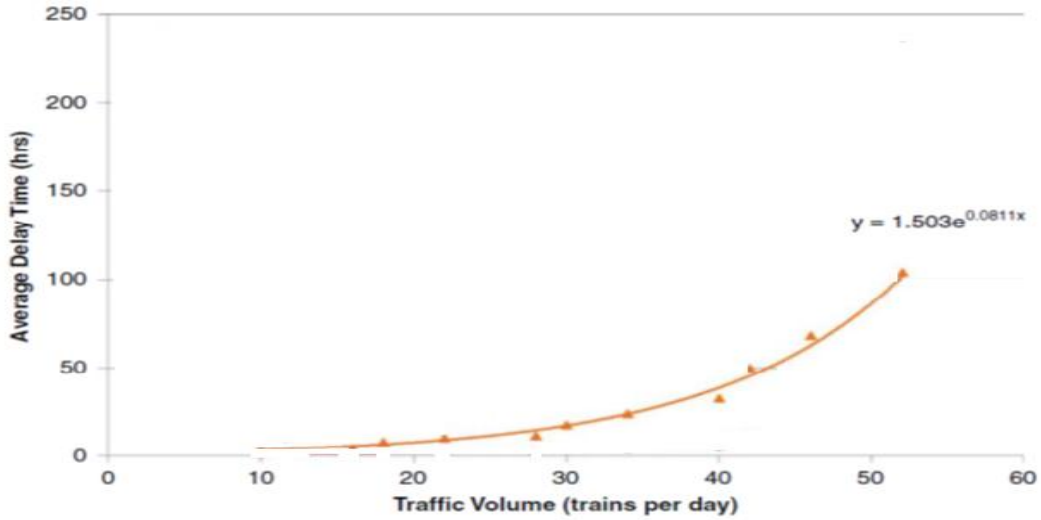

Figure 6.3Average train delay data generated from dispatch simulation software. (Schlake et.al, 2011).

Since traffic volume (trains per day) is taken as 10, the average delay time is taken as

$$V = 1.503e^{0.0811*10} = 3.40hr$$

x = cost of delay per train-hour =$350 (from table 6.4)

t = hours per train arrival = 55.33 / T (T is annual traffic density) = 55.33/22.67=2.44

n = number of following trains delayed = V / t = 2.65/2.44 =1(rounded to the nearest integer)

Therefore,

$$C_{DA} = Vx + (V - nt)x = 3.40 * 350 + (3.40 - 2.44) * 350 = \$\mathbf{1526}$$

6.1.2.9 EFFECTIVE RAIL DEFECT INSPECTION FREQUENCY

As described before, the total costs related to rail defect inspection include:

- Costs for operating inspection vehicles.
- Costs for repairing detected rail defects and the corresponding train delay cost.
- Costs for repairing broken rails and the corresponding train delay cost.

DETERMINATION OF TOTAL COST

Then the following model is adopted to minimize the total cost related to NDT rail inspection:

$$C_{total}(k) = C_{INSP} + C_{def} + C_{bro} + C_{derail} \quad (6.18)$$

$$C_{total}(K) = \frac{kL}{V}C_{ins} + \frac{S(k)L}{\lambda\left(\frac{T}{K}-\theta\right)}(DDC + C_{DDT}) + S(K)L(SDC + C_{SDT}) + S(K)L\phi(\mu DA + C_{DA})$$

Where:

C_{total} = total cost related to rail defect inspection ($) (Life cycle cost).

K = rail defect inspection frequency per year

S (K) = number of broken rails per track-mile by annual rail defect inspection frequency.

Φ = proportion of broken rails causing train derailments, 0.85% (Zarembski and Palese 2005).

DA = average track and equipment damage cost per broken-rail-caused train derailment ($3,000,000).

μ = multiplier for accounting for other related derailment costs (excluding train delay cost), 1.65 (Kalay et al. 2011) and other variables as previously defined.

The costs for repairing rail defects and the corresponding train delay cost is a multiplication of number of detected rail defects and repair & train delay cost per defect. Based on the Volpe Center model (Orringer 1990), annual number of detected rail defects is:

$$N_{def} = \frac{S(K)L}{\lambda(\frac{T}{K}-\theta)} \quad (6.19)$$

Where, N_{def} is the number of detected rail defects. S (K) is annual number of broken rails per track-mile by rail defect inspection frequency using the optimization model. L is track length in miles, T is annual traffic density, K is annual rail defect inspection frequency and λ and θ are constants related to inspection efficiency described before (Orringer 1990). Based on this information, rail defect repair and train delay cost (C_{def}) is:

$$C_{def} = \frac{S(K)L}{\lambda\left(\frac{T}{K}-\theta\right)}(DDC + C_{DDT}) \quad (6.20)$$

Let the annual rail inspection frequency is two, the cost for repairing rail defects is determined as follows:

$$C_{def} = \frac{0.00097*1}{0.0108*(\frac{22.67}{2}-1)} * (9893 + 1184) = \mathbf{\$96.26}$$

Table 6.5 Rail defect repair cost for different rail inspection frequencies

Annual rail inspection frequency	1	2	3	4	5	6
Rail defect repair cost($)	85.67	96.26	100.06	101.08	101.58	103.36

Similarly, broken rails repair and train delay cost (C_{bro}) is:

$$C_{bro} = S(K)L(SDC + C_{SDT}) \quad (6.21)$$

Let the annual rail inspection frequency is two, rail break repair cost is determined as follows:

$C_{bro} = 0.00097 * 1 * (13{,}143 + 2787) = \$\mathbf{15.45}$

Table 6.6 Rail break repair cost for different rail inspection frequency.

Annual rail inspection frequency	1	2	3	4	5	6
Rail break repair cost($)	28.83	15.45	10.19	7.33	5.58	4.46

The estimated number of broken-rail-caused train derailment is a multiplication of number of broken rails (S (K) ×L) and the proportion of broken rails causing derailments (Φ). For each train derailment, the total consequence cost includes damage cost (μ DA) and train delay cost (CDA). Train-derailment-related cost (C_{derail}) is:

$$C_{derail} = S(K)L\phi(\mu DA + C_{DA}) \quad (6.22)$$

Let the annual rail inspection frequency is two, derailment damage cost is:

$C_{derail} = 0.00097 * 1 * 0.0085 * (1.65 * 3{,}000000 + 1526) = \$40.83$

Table 6.7 Derailment damage cost for different rail inspection frequency.

Annual rail inspection frequency	1	2	3	4	5	6
Derailment damage cost ($)	76.18	40.83	26.94	19.36	14.73	11.78

The optimal annual rail inspection frequency (K^*) is determined so as to minimize total cost (C_{total}):

$$K^* = arg_k min[C_{total}(K)] \quad (6.23)$$

The total cost (including rail defect inspection, rail defect or broken rail repair, track and rolling stock damage and train delay due to derailments or repair activities) is minimized at a certain inspection frequency.

Table 6.8: Total annual total cost for different rail inspection frequencies (initial rail age is 61.88 MGT and annual traffic density is 22.67 MGT, 1-mile route).

Annual Rail Inspection Frequency	**Cost Category($)**				
	Total Cost	**Rail Inspection Cost**	**Rail Defect Repair Cost**	**Rail Break Repair Cost**	**Derailment Damage Cost**
1	205.68	15.00	85.67	28.83	76.18
2	182.54	30.00	96.26	15.45	40.83
3	182.19	45.00	100.06	10.19	26.94
4	187.77	60.00	101.08	7.33	19.36
5	196.89	75.00	101.58	5.53	14.73
6	209.6	90.00	103.36	4.46	11.78

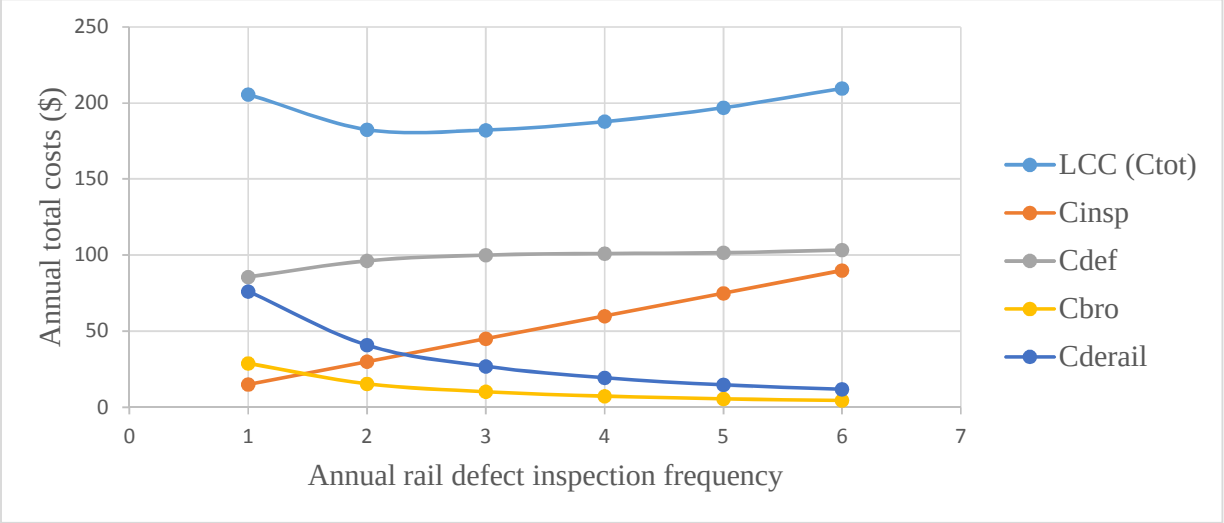

Figure 6.4Annual total cost for different rail inspection frequencies (initial rail age is 61.88 MGT and annual traffic density is 22.67 MGT, 1-mile route).

The total cost (including rail defect inspection, rail defect or broken rail repair, track and rolling stock damage and train delay due to derailments or repair activities) is minimized at a certain inspection frequency.

Table 6.8 and Fig.6.4 shows the results of the analysis for the different number of rail inspections in the LCC, using Rail defect inspection cost model (INSPEC) of AAR. It is interesting to note that the expected costs for the inspection and repair increase whereas the expected failure cost decreases, as the number of inspection increases. This indicates that the increment of the inspection can improve the reliability of rails. In this manner, there is a trade-off point at which the LCC is minimized. From figure 6.4 it is found that an effective number of rail inspections are three.

Therefore, the optimal annual rail inspection frequency that minimizes total cost is **three** per year, in other words, rail inspection should be done three times per year.

6.1.3 CONSTANT INSPECTION INTERVAL VERSUS VARYING INSPECTION INTERVAL

In practice it may be simpler to implement a constant inspection interval, an approach that is used by several U.S. railroads. Based on suggestions of different researcher's, the difference between the two approaches is not very large because the traffic between each successive inspection is less than the rail age (e.g., 11.335 MGT interval compared to 61.88 MGT initial rail age). If a constant inspection interval is simpler to implement and manage the resultant difference from the optimal solution is small. The advantage of varying inspection interval may be more substantial over larger-scale networks or multi-period planning horizons. But the National railway network of Ethiopia is not large scale network as well as to make the implementation simpler, constant inspection interval is taken in this thesis for the National Railway Network of Ethiopia.

CHAPTER 7

7.1 RAIL INSPECTION AND MAINTENANCE STRATEGY MODEL

The most rail maintenance strategies currently uses Nondestructive testing (NDT) cars, visual inspection and rail circuit detection by signals to inspect rails for identification of possible internal defects (Larsson, *et al.*, 2005). The NDT Car inspection is again verified by hand held ultrasonic equipment. Visual inspection is carried out separately by rail inspector or track staff from time to time. At the same time rail circuit detection by signals (commonly known as signaling) is also carried out. The defects detected by NDT Car and verified by hand held equipment are recorded on the spot by an inspector in the form of a report. Severe defects which the inspector thinks are of high priority are immediately recommended for unplanned maintenance. Visually inspected defects are also recorded in a report. The data recorded in this report is further analyzed by an expert. Aid of historical data and information stored in a centralized database is also taken to correlate failure patterns. Finally, a decision is made to classify these defects according to priority. Priority of defects is based on several factors, such as track geometry, traffic type, traffic density, axle load, age of rails, defect history, rail material, curvature, MGT, and consequential cost and risk with a particular defect if derailment occurs due to that defect.

The low priority defects are then recommended for planned maintenance which may be grinding, lubrication, minimal repair, rail welding or rail section rectification / replacement. The kind of planned maintenance adopted for a particular kind of defect depends on its need and severity.

The high priority defects are immediately recommended for unplanned maintenance which may be in the form of minimal repairs which is mostly carried out in winters, rail section replacement and/or welding. Minimal repair under unplanned maintenance is a temporary repair which is done in winters. The defects having minimal repair are later on repaired fully in summer. The defects detected by signaling is generally severe, often in the form of rail breaks or rail breaks in a developing stage and needs immediate attention, thus unplanned maintenance is carried out to counter these defects (Larsson, *et al*, 2005). Figure 7.1 also illustrates those areas in Banverket's maintenance strategy.

Those defects which are undetected by these three inspection tools build up operational risk in rails, some of which may eventually be detected through derailments. However, the percentage of defects leading to derailments is very small.

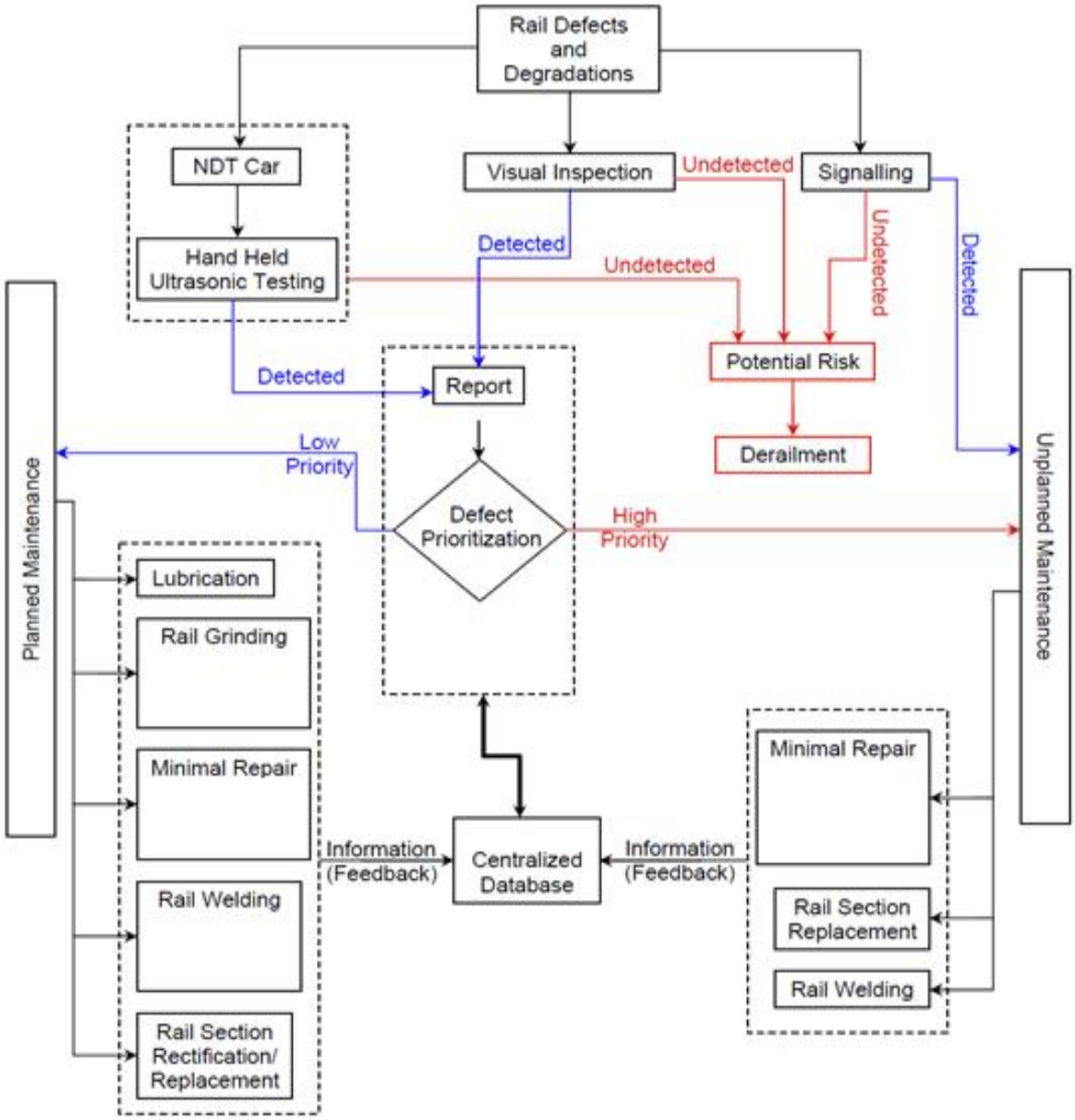

Figure 7.1 Banverket's rail inspection and maintenance strategy flowchart.

CHAPTER 8

8.1 CONCLUSION AND RECOMMENDATION

8.1.1 CONCLUSION

This thesis discusses about rail defect management. In particular, the main application is for the determination of effective and economical inspection interval on the basis of quantitative approach. The frequency of rail inspection tends to vary from one railroad to another, yet it is usually based on either time or traffic tonnage. Railroad companies have evolved their rail inspection schedules empirically, based on long field experience. Rail defect management refers to the development and implementation of strategies to control the risk of rail failure. The primary method to control the risk is a rail inspection through nondestructive evaluation and is a replacement of rails based on the remedial action plan as well as evaluation results.

To demonstrate the feasibility of the above applications, first, a Linear Elastic Fracture Mechanics (LEFM) analysis which can predict a crack size in a rail head, web and base is performed. Second, a First-Order Reliability Methods (FORM) analysis evaluates the reliability of a rail, considering some uncertainties of parameters. Third, an Event tree (ET) analysis represents systematically all possible events and actions regarding rail defect management. Finally, a Life-Cycle Cost (LCC) estimation formulates the effective inspection interval which minimize total cost are conducted.
Details, analysis and finds are explained in each section of the thesis.
Therefore, the main conclusions obtained from the research are:

1. **At every four months interval (three times a year), rail inspection should be done.**

By applying this inspection frequency, it is possible to prevent the occurrence of rail failure by taking the required action at the right time, and extend the rail life expectancy, reduce the rail maintenance work and its cost. While determining this inspection interval, there was data limitation for the actual traffic as well as some cost values. If the actual value is taken, then the number of inspection will increase.

2. Based on the present situation and determined remedial action plan for National Railway Network of Ethiopia, Infrastructure Managers (track engineers or rail inspectors) shall decide to **replace any rails that include head crack of more than 1mm, web crack of more than 5mm and base crack of more than 2mm.**
3. **Flow chart for rail inspection and maintenance management strategy** has been adopted for National Railway Network of Ethiopia. (Figure 7.1).

8.1.2 RECOMMENDATIONS FOR FUTURE WORK

This thesis demonstrates reliability based rail management. However, several issues need further development and refinement to get more accurate output.

- **Considering Environmental factors (such as Temperature, Humidity etc.) for rail stress calculation**

Because of rails extend in summer and shrink in winter due to the effect of temperature variation, thermal stress should be also taken into account to determine the total stress. As well as humidity and other environmental factors shall be taken to get most accurate total stress.

- **Considering traction and breaking force**

Load conditions under traction and breaking force in addition to under rolling wheel shall be investigated to determine crack behavior of rails.

- **Updating Crack size information**

The Linear Elastic Fracture Mechanics Analysis (LEFM) and the First order reliability Method of analysis (FORM) determine and incorporate information of crack size. In addition to the approach, whether any crack is detected or not, each inspection provides additional information about the probability distribution of the crack size. Therefore, the obtained crack size based on analytical approach shall be updated based on field data after inspection is conducted.

- **Numerical approach for calculating Life Cycle Cost (LCC)**

Each expected cost to evaluate the LCC is drawn from analytical approach specially using rail defect inspection cost model of AAR. However, a numerical approach, such as Morkov chain Monte Carlo simulation shall be attempted to raise a precision of the evaluation of the expected reliability index.

- **Updating Life Cycle Cost (LCC) analysis data's**

The data's (specially LCC analysis data's) shall be updated in part due to, changes in traffic volume, axle load, better rail maintenance practice as well as cost variation (such as inspection cost, repair cost etc.) for different durations. So, the costs shall be updated in the future by using the exact value for the National railway network of Ethiopia.

- **Input for Rail inspection manual development**

This thesis shall be input or initial tool that can be used to aid the development of better informed, more effective infrastructure management and accident prevention policies, for rail operation and maintenance decision making process and practices as well as for the development of rail defect inspection manual and track safety standard for track engineers or inspectors of national railway network of Ethiopia.

- Further research should be conducted to quantify the effect of various broken rail prevention strategies (Such as rail inspection, rail grinding and rail lubrication), alone and in combination for the development of an integrated and effective approach to train safety improvement.
- The effect of other track structures on the life of the rail shall be demonstrated to facilitate better risk assessment, management and operation decision making.

REFERENCES

1) A. A. Shabana, et al., "Numerical Procedure for the Simulation of Wheel/Rail Contact Dynamics," Journal of Dynamic Systems, Measurement, and Control, vol. 123, pp. 168-178, 2001.
2) Abraham M. Hasofer and Niles C. Lind (1974), "Exact and Invariant Second order Code Format," Journal of Engineering Mechanics, ASCE, Vol.100, No.1, pp.111-121.
3) Addis Ababa/Sebeta-Djibouti Railway Project (2012), Economic feasibility study, Addis Ababa.
4) Al-Najjar, B. and Kans, M. (2006). A model to identify Maintenance cost-effective decisions: a case study. *International Journal of Productivity and Performance Management,* 55(8), 616-637.
5) Allen C. Estes (1997),'"A system reliability approach to the life time optimization of inspection and repair of highway bridges, Ph.D. Thesis, department of Civil ,Environmental and Architectural Engineering, University of Colorado,bouler.
6) Andersen, T.M. (1999). *Short Term Maintenance Planning.* PhD Thesis. Department of Marine Engineering, Norwegian University of Technology, Trondheim, ISBN 82-471-0408-3.
7) Atkinson, B.K., Fracture Mechanics of Rock, pp. 534, Academic Press, London UK, 1987. Ch.1, 2, 4.
8) Bahramin-Ghasrchami, K., Price, J.W.H. and Mathew, J. (1998). Optimum inspection Frequency for manufacturing systems. *International Journal of Reliability Management,* 15(3), 250-258.
9) Banks-Sills L., Application of the Finite Element Method to Linear Elastic Fracture Mechanics, *ASME Applied Mechanics Reviews*, Vol. 44, No. 1 (1991), pp. 447-460.
10) Cannon, D.F., Edel, K.O., Grassie, S.L. and Sawley, K. (2003). Rail defects: an overview. *Fatigue & Fracture of Engineering Materials & Structures,* 26, 865-886.
11) Cornell Fracture Group, Cornell University, Ithaca, New York http://.cfg.cornell.edu/www.
12) Cornell C.A. (1969), "A Probability based structural code," Journal of the American concrete Institute, ACI, vol.66, No.12, pp.974-985.
13) David Robinson (1998),"A Survey of Probabilistic Methods used in Reliability, Risk and Uncertainty Analysis, Analytical Techniques 1, USA, PP.23-27.
14) David Y. Jeong, Michael E. Carolan, Hailing Yu and Benjamin Perlman, Fracture Mechanics and beam theory analysis of semi-elliptical cracks originating in the base of the rail, Cambridge, Massachusetts, USA, 2012.
15) Davis, D.D., M.J. Joerms, M.J., Orringer, and Steele, R.K. (1987). "The economic consequences of rail integrity." Report No. R-656. Association of American Railroads, Chicago, IL.

16) Dekker, R. (1996). Applications of maintenance optimization models: a review and analysis. *Reliability Engineering & System Safety*, 51(3), 229-240.

17) Department of Transportation (2002),"Life Cycle cost Analysis Primer," *http://www.fhwa.dot.gov/infrastructure/autmgmt/lcca.htm.*

18) Dick, C.T., Barkan, C.P.L., Chapman, E.R., and Stehly, M.P. (2003). "Multivariate statistical model for predicting occurrence and location of broken rails." *Transp. Res. Rec.*, 1825, 48-55.

19) Doyle, N.F., (1980). Railway track design: A review of current practice, Occasional Paper No. 35, Bureau of Transport Economics, Australia, Canberra.

20) Esveld, C. (2001). Modern Railway Track. MRT Productions, the Netherlands.

21) George A Georgiou (2006), "*Probability of Detection (POD) curves: derivation, applications and limitations*." Jacobi consulting limited research report (2006), London.

22) Henrik O. Madsen (1985), "Random Fatigue Crack Growth and Inspection," the processing of ICOSSAR'85, Vol.1, pp.475-484.

23) Ionescu D., (2004). Evaluation of the engineering behavior of railway ballast, Ph.D. thesis, University of Wollongong.

24) Jardine, A.K.S. and Tsang, A.H.C. (2006). *Maintenance, Replacement, and Reliability: Theory and Applications.* CRC Press, Taylor & Francis Group, ISBN 0-8493-3966-0.

25) Jeong, D.Y., and Gordon, G.E. (2009). "Evaluation of rail test frequencies using risk analysis." *Joint Rail Conf.*, ASME, Pueblo, Colorado, USA.

26) J. Evans. "Whole life rail model application and development for RSSB- Dynamic modeling of rolling contact fatigue", AEA Technology Rail report AEATR-VTI-2003-048 Issue 1, www.rssb.co.uk, (2003).

27) John Dalsgaard sφrenson (2004)," notes on structural reliability theory and risk analysis", Aalborg University, Denmark.

28) J. J. Coner Julie A. Bannantine and J. Hand Rock., Fundamentals of metal fatigue analysis. Printice Hall, 1990.

29) Kalay, S., French, P., and Tournay, H. (2011). "The safety impact of wagon health monitoring in North America." *Proc. of the World Congress on Railway Research*, Lille, France, 2011.

30) K. L. Johnson, "The strength of surfaces in rolling contact." Proc. Inst Mech Engng, 203, p. 151–163, 1989.

31) K. O. Edel, Theoret. Appl. Fracture Mech., 9, p. 75-82, 1988.

32) Larsson, P.O., Kumar, U. and Chattopadhyay, G. (2005) *Study of NDT Rail Inspection on Malmbanan*, Internal Research report 2005, Banverket's, JvtC, Sweden.

33) L.P. Pook (2000), "Linear Elastic Fracture Mechanics for Engineers: Theory and Applications," WIT press.

34) M. Ishida, N. Abe "Experimental study on rolling contact fatigue from the aspect of residual stress", Wear, 191, p. 65–71, 1996.

35) Ministry of Railways of the People's Republic of China (2006), National standard of the people's Republic of China, China.

36) N. Pugno, M. Ciavarella, P. Cornetti, A. Carpinteri., A generalized Paris' law for fatigue crack growth, *Journal of the Mechanics and Physics of Solids*, 54 (2006) pp. 1333–1349.

37) Orringer, O., Tang, Y.H., Gordon, J.E., Jeong, D.Y., Morris, J.M., and Perlman, A.B. (1988). *Crack propagation life of detail fractures in rails*. DOT/FRA/ORD-88/13 DOT-TSC-FRA-88-1. Federal Railroad Administration, Washington, D.C.

38) Orringer, O. (1990). *Control of rail integrity by self-adaptive scheduling of rail tests*. DOT/FRA/ORD-90/05. Federal Railroad Administration, Washington, D.C.

39) O. Vardar., Effect of single OL in FCP. *Engineering Fracture Mechanics*, V-30, n-3 (1988), pp. 329-335.

40) Palese, J.W., and Wright, T.W. (2000). "Risk Based ultrasonic rail test scheduling on Burlington Northern Santa Fe." *Proc., AREMA Annual Conference*, AREMA, Dallas, TX.

41) Prause, R.H., Meacham, H.C., (1974). Assessment of design Tools and Criteria for rail Track Structures,Vol.1, At-Grade, Battlle Columbus Laboratories, UMTA Report N0.UMTA-MA-06 National Technical Information Service, Virginia, USA.

42) P.Paris and F.Erdogan (1963), "A Critical Analysis of Crack Propagation Low," Journal of Basic Engineering, ASME, Vol.85, No.4, PP.528-534.

43) Rackwitz R. and Fieesler B. (1978), "Structural Reliability under combined Random Load Sequences," Computers and Structures, Vol.9, No.5, PP.489-494.

44) Rosenblatt M. (1952), "Remarks on a multivariate Transformation, "Annals of Mathematical Statistics, vol.23, No.3, pp.470-472.

45) Ruohua Zheng and Bruce R, Elling Wood (1998) "Pole of Non-Destructive Evaluation in Time-Dependent Reliability Analysis," Structural Safety, Vol.20, pp.325-339.

46) R.P. Reed, J.H. Smith, and B.W. Christ, "The economic effects of fracture in the United States," SP647-1, NBS, March 1983, 3.

47) Sadeghi J. and P. Barati, (2010). Evaluation of conventional methods in analysis and design of railway track system. International Journal of Civil Engineering. Vol.8,No.1

48) Sauragh Kumar (2008),"Reliability Analysis and cost modeling of degrading systems", Ph.D. thesis, Division of operation and maintenance engineering, Luliya University, Luliya, pp.1-984.

49) Schafer, D.H. (2008). "Effect of train length on railroad accidents and a quantitative analysis of factors affecting broken rails." M.S. thesis, Univ. of Illinois at Urbana-Champaign, Urbana, IL.

50) Schafer, D.H., and Barkan, C.P.L. (2008). "Relationship between train length and accident causes and rates." *Transp. Res. Rec*, 2043, 73-82.

51) Schlake W.B., Barkan, C.P.L., and Edwards, J.R. (2011). "Train delay and economic impact of in-service failures of railroad rolling stock."*Tran. Res.Rec*, 2261, 124–133.

52) Schramm, G., (1961), Permanent way Technique and Permanent way Engineering, Otto Elsner Verlargs gersellashaft Darmitadt, pp 66-70.

53) Selig E.T. and J.M. Waters, (1994). Variation of subgrade vertical stress and threshold stress with depth.

54) Sherif, Y.S. and Smith, M.L. (1981). Optimal maintenance models for systems subject to failure: a review, *Naval Research Logistics*, 28, 47-74.

55) Smith, R.A. (2003). The wheel-rail interface: some recent accidents. *Fatigue & Fracture of Engineering Materials and Structures*, 26(10), 901–907.

56) Takashi Kashima (1997),"reliability-based optimization of rail inspection", MSc. thesis, department of Civil Engineering, Massachusetts institute of technology, Bakers, pp.39.

57) Terzaghi, K, (1955), Evaluation of Coefficients of subgrade reaction, Journal of Geotechnique, pp 197-326.

58) Wells, T. R., and Gudiness, T. A. (1981). "Rail performance model: technical background and preliminary results." R-474, Association of American Railroads, Washington, D.C.

59) Zarembski, A.M., and Palese, J.W. (2005). "Characterization of Broken Rail Risk for Freight and Passenger Railway Operations." *Proc., AREMA Annual Conference*, AREMA. Chicago, IL.

60) Zhengwai Zaho, Achyntya Haldar, and Florence L. Breen Jr. (1994), "Fatigue Reliability Evaluation of steel Bridges," Journal of Structural Engineering, ASCEVol.120, No.5, PP.1608-1623.

APPENDIXES

Appendix A: Abbreviations

AAR = Association of American Railroads

BA = Base Area.

CDF = Cumulative Density Function

COV = Coefficient of Variation

DDC = Total Cost of repairing Detected rail Defect

EDM = Electronic Discharge Machine

ERC = Ethiopian Railways Corporation

ET = Event Tree

FEM = Finite Element Method

FORM = First Order Reliability Method

FRANC3D =Fracture Analysis 3 Dimensional

INSPEC = Rail Defect Inspection Cost

LCC = Life Cycle Cost

LEFM = Linear Elastic Fracture Mechanics

LSF = Limit State Function

MGT = Million Gross Tone's

MPP = Most Probable Point

NDT = Non Destructive Testing

PDF = Probabilistic Density Function

POD = Probability of Detection

POR = Probability of Repair

SDC = Total cost for repairing broken rail

SIF = Stress Intensity Factor

Appendix B: Proof of Equation 6.10

Generally,

$$\frac{S}{D} = \lambda(X - \theta) \quad (1)$$

Where:

S = rate of broken rails per track mile

D = rate of detected rail defects per track mile

X = inspection interval

λ = slope of the number of rail breaks per detected rail defect (S/D) vs. inspection interval,

θ = minimum rail defect inspection interval.

Then,

$$(S + D)X = Rf(N)X \quad (2)$$

Where:

R = rail segments per track-mile.

$$f(N) = \frac{\alpha N^{\alpha-1}}{\beta^{\alpha}} e^{-(\frac{N}{\beta})^{\alpha}} \quad (3)$$

α = Weibull shape factor

β = Weibull scale factor

N = rail age (cumulative tonnage on the rail)

From (1) to (3),

$$SX = R \frac{\frac{\alpha(N)^{\alpha-1}}{\beta^{\alpha}} e^{-\left[\frac{N}{\beta}\right]^{\alpha}}}{1+\frac{1}{\lambda(X-\theta)}} X \quad (4)$$

For the inspection interval (Ni-1, Ni), the average rail age is 0.5(Ni-1+Ni). As such, the expected number of broken rails within the inspection interval is:

$$S_{(i-1,i)} = SX_i = R \frac{\frac{\alpha(0.5N_{i-1}+0.5N_i)^{\alpha-1}}{\beta^{\alpha}} e^{-\left[\frac{(0.5Ni-1+0.5Ni)}{\beta}\right]^{\alpha}}}{1+\frac{1}{\lambda(x_i-\theta)}} X_i \quad (5)$$

Equation (6.10) is proved.